TRIBOLOGICAL BEHAVIOR OF UNFILLED AND CARBON FIBER REINFORCED POLYETHER ETHER KETONE/POLYETHER IMIDE COMPOSITES

by

Jong Hyun Yoo

Thesis Submitted to the Faculty of the

Virginia Polytechnic Institute and State University

in partial fulfillment of the requirements for the degree of

MASTER OF SCIENCE

in

Mechanical Engineering

Approved:

N. S. Eiss, Jr., Chairman

M. J. Furey

C. A. Rogers

October 1991

Blacksburg, Virginia

TRIBOLOGICAL BEHAVIOR OF UNFILLED AND CARBON FIBER REINFORCED POLYETHER ETHER KETONE/POLYETHER IMIDE COMPOSITES

by

Jong Hyun Yoo

(ABSTRACT)

The friction and wear of injection molded Poly(ether ether ketone) (PEEK) and Poly(ether imide) (PEI), PEEK/PEI blends with the weight compositions of 50/50 %, 70/30 %, and 85/15 %, with and without short carbon fibers were measured in a pin(52100 steel ball)-on-disk(polymer blend) configuration under dry friction. 50/50, 70/30, and 85/15 compositions were annealed to study the effect of crystallinity on wear test. The test variables were sliding speed and normal load.

The wear mechanism of pure PEEK matrix was plowing and as the weight percentage of PEI in the blend was increased the wear mechanism changed to the generation of small particles. The wear rates of the unfilled PEEK/PEI blends were found to be a function of not only the blend composition, but also of the normal load, sliding speed and crystallinity in complex manner. However, the coefficient of friction of the unfilled blends did not seem to significantly depend on those testing parameters. When no wear debris was produced, it was below 0.15 otherwise it was ranged from 0.2 to 0.3. The 30 weight % carbon fiber reinforced (CFR) PEEK did produced wear particles but 70/30 and 100 % PEI composites showed reduced wear rates compared to those of unfilled blends. The coefficients of friction of CFR did not seem to be changed

from those of the untreated blends except for 100% PEI. Presence of the incubation time before wear particles were produced indicated that the predominant wear mechanism was fatigue. An increase in friction correlated with the generation of wear particles and the formation of a wear groove.

ACKNOWLEDGEMENTS

"If any of you lacks wisdom, he should ask God, who gives generously to all without finding fault, and it will be given to him." *(JAMES 1:5)*

" · always giving thanks to God the Father for everything, in the name of our Lord Jesus Christ." *(EPHESIANS 5:20)*

I praise the name of our Lord Jesus Christ for helping me to finish this thesis. I would like to express my deep appreciation to Dr. Norman Eiss, Jr. for his valuable assistance throughout the course of this research. His advice, patience, and availability are sincerely appreciated. I would also like to thank the following people for the assistance and advice they have given me throughout the duration of the research:

Dr. M. J. Furey and Dr. C. A. Rogers for their service on the graduate committee; Dr. D. Baird and his students Paulo De Souza and Dr. Arindam Datta for preparation of the injection molded specimens; Dr. A. Prasad and Dr. H. Marand for their valuable advice and suggestions concerning the chemical aspects; Dale McHerron for running DSC; Bob Simonds and Dr. Dowling for running and use of the tensile tests; Chiun-Chia Kang and Kyle Thornham for their assistance on SEM; the Mechanical shop for machining the test specimens; Matthew Cerrone for running part of the pin-on-disk tests; ICI Advanced Materials Science and Technology Center for High Performance Polymeric Adhesive and Composites for providing the chopped carbon fiber reinforcements; the National Science Foundations for financial support; and finally the Tribology lab groups, Chiun-Chia Kang, Ronald Rorrer, Hamid Ghasemi, Bhawani Tripathy, Brian Weick, Rob DeTogni,and Brian McCann for their advice and help.

Special thanks are due to my family, friends, and Su-Mi Kim for their support and faith in my abilities.

TABLE OF CONTENTS

TABLE OF CONTENTS (Con't)

LIST OF FIGURES

LIST OF FIGURES (Con't)

LIST OF FIGURES (Con't)

LIST OF FIGURES (Con't)

LIST OF TABLES

LIST OF TABLES (Con't)

LIST OF TABLES (Con't)

1. INTRODUCTION

Many of thermoplastic materials replace metals because of their light weight, corrosion resistance, better fatigue performance, excellent mechanical properties, outstanding chemical resistance and ease of fabrication. This excellent property profile considerably increased the use of various thermoplastics for sliding applications such as bearing components [1-9]. Use of short fiber reinforcements further improved wear properties due to fiber's superior elastic modulus, therefore a large percentage of load is carried by the fibers [1,2].

However, heat generation of the dry sliding contacts gives rise to local decomposition, therefore limiting the serviceability of polymers in sliding applications [3,7,8,10]. Some of the heat resistant thermoplastics developed in recent years are expected to be useful under severe conditions.

Poly(ether ether ketone) (PEEK) is such a high performance, semicrystalline thermoplastic. Its relatively stiff backbone gives excellent high temperature stability. It has a glass transition temperature of 145 °C, a melting point of 335 °C, and

continuous use temperature of 200 °C [11,12]. However, when PEEK is subjected to temperatures above its glass transition temperature (T_g), its mechanical properties such as flexural strength, flexural modulus and creep resistance drastically decrease [1,13,14]. To increase the T_g of PEEK while maintaining excellent properties, researchers investigated the possibility of raising T_g by mixing with a higher T_g polymer.

Blending peek with Poly(ether imide) (PEI) which has a T_g around 220 °C [17] is a suitable choice since its blend with PEEK reveals a single, sharp T_g at all compositions and thus indicate the miscibility [14,15]. PEI is known to be a high-performance, amorphous thermoplastic. The ether linkages give good melt-flow characteristics and the aromatic imide units provide stiffness and therefore high temperature stability [13,16].

It is known that for semicrystalline thermoplastices the bulk mechanical properties are dependent on the inherent morphology of the material such as crystallinity and spherulite size [18,19]. The thermal history imparted during processing can control the morphology. Several researchers found that increasing the crystallinity increases the strength and modulus in both tensile and shear stresses, and decreases fracture toughness (G_{IC}) and elongation at break [11,18,19,20]. Lustiger, et al. [18] measured the decrease in fracture toughness values with the increase in the size of spherulite in the unidirectional long carbon fiber reinforced PEEK. Tanaka and Ueda [21] mentioned that the strength and elongation at fracture generally decreased with increasing spherulite size.

Shelling and Kaush [2] found that the increase in the crystallinity of PEEK did

not significantly change the high wear rate in both reciprocating and sliding dry friction tests although the friction coefficients decreased in the reciprocating case. Voss and Friedrich [22] observed contrary wear results. Wear measurements for the annealed PEEK and 30 wt % short glass fiber reinforced (GFR) PEEK showed that the wear rate of the annealed materials is lower than that of the unannealed. However, increased wear rates and coefficients of friction of annealed polypropylene specimens, which had higher crystallinity and larger spherulites than unannealed specimens, were reported by Tanaka and Ueda [21]. In another study, Tanaka [23] also found that a reduction in the spherulite size lowered the wear rates.

Many of researchers found that the reinforcement of short or long fibers improves the bulk mechanical properties: the addition of carbon fibers (CF) significantly improved fatigue crack resistance [24,25]. Enhancement of mechanical properties such as yield strength and modulus also contributes to the betterment of wear and friction performance [2,9,10,22,26,27]. However, under certain circumstances the reinforcement yields poor wear resistance. Examples of such situations are short glass fiber (GF) reinforced PEEK composite is sliding against steel at low speed [22,26] and when CF and GF reinforced PEEK is subjected to fretting wear [27].

Eiss [28-31] is among the many tribologists who attempted to correlate mechanical properties of polymers to their tribological behavior. The majority of his works relate to the fatigue wear mode; he found that the elastic modulus of polymers is positively correlated to the wear rates. His investigations also show that the initial abrasive wear

rate of siloxane modified epoxies varied inversely with their fracture toughness and elastic modulus.

The effects of the fiber reinforcement and morphology changed by annealing the materials can be quite different and depend on the type of wear mode, kind of fiber, volume fraction, and behavior of the matrix. Therefore, in this research the friction and wear of injection molded PEEK and PEI, PEEK/PEI blends with the compositions of 50/50, 70/30, and 85/15, with and without short carbon fibers are presented. Annealed PEEK/PEI blends are also included. Finally, an attempt to explain the tribological behavior of PEEK/PEI blends and Carbon fiber reinforcement in terms of the mechanical properties and morphology changes is made.

2. LITERATURE REVIEW

2.1 General Properties

Poly(ether ether ketone) (PEEK) is a linear aromatic polymer with the basic repeat unit shown in Fig. 1. This high temperature semi-crystalline engineering thermoplastic is commercially available under the trade name 'Victrex' PEEK® from ICI. The key properties of 'Victrex' PEEK® are :

i) A high melting temperature of 334 °C (633 °F)

ii) A continuous working temperature of 250 °C (480 °F)

iii) Tough, ductile, excellent fatigue characteristics.

iv) Low flammability, fire, smoke properties

v) Excellent chemical and solvent resistance

vi) No significant degradation below 1100 Mrad

vii) Easily processed on conventional equipment.

Typical property values are listed in Table 1.

Its excellent balanced properties have led a number of uses in oil and geothermal

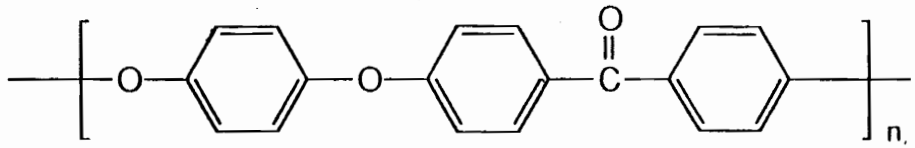

(a) PEEK® (380G)

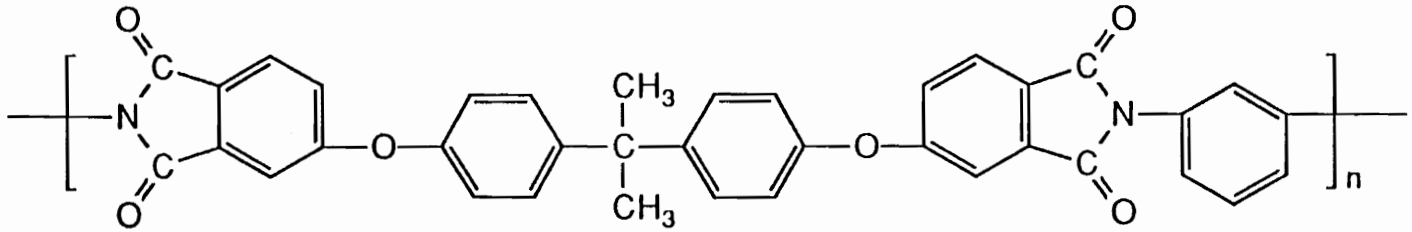

(b) ULTEM® 1000

Figure 1. Chemical structure of PEEK and PEI

TABLE 1. Typical property values of PEEK & ULTEM

PROPERTY	ASTM METHOD	UNITS (SI)	PEEK[1] 450G	ULTEM[2] 1000
PHYSICAL				
Color			Grey	Brown
Molecular Weight		gm/mole	36000	15000
Water Absorption(23°C)	D 570	%	0.5	0.25
MECHANICAL				
Tensile Strength	D 638	MPa	92	105
Tensile Elongation(yield)	D 638	%	4.9	7
Tensile Elongation(break)	D 638	%	50	60
Tensile Modulus(1% secant)	D 638	MPa	3600	3000
Flexural Strength	D 790	MPa	170	150
Flexural Modulus	D 790	MPa	3660	3300
Compressive Strength	D 695	MPa	118	150
Shear Strength		MPa	95	100
Rockwell Hardness(M)	D 785		99	109
Izod Impact,unnotched		J/m	673	1300
Izod Impact,notched		J/m	83	50
THERMAL				
Heat Distortion Temp(1.82MPa)	D 648	°C	160	200
Thermal Conductivity	C 177	W/m-°C	0.25	0.22
ELECTRICAL				
Volume Resistivity	D 257	ohm-cm	4.9E16	6.7E17
Dielectric Strength(air)	D 149	KV/cm	190	330
FLAME				
Oxygen Index	D 2863	%	35	47

[1] Data adapted from ICI Brochure [1]
[2] Data adapted from GE Brochure [16].

wells, high-pressure steam valves, aircraft and automobile engines, and chemical and nuclear plants. Also PEEK is replacing traditional metals in many bearing applications [1,13].

Poly(ether imide) (PEI) is a high performance, amorphous thermoplastic. ULTEM® is the commercial name and is available from the General Electric Company. Its general chemical structure is shown in Fig. 1. The main properties of ULTEM® are:

i) A high heat deflection temperature of up to 200 °C (392 °F)

ii) Exceptional strength and modulus

iii) Inherent flame resistance with low smoke evolution

iv) Excellent electrical properties

v) Chemical resistance to aliphatic hydrocarbons, acids, and dilute bases

vi) Transparency

vii) outstanding processibility on conventional molding equipment

Typical property values are shown in Table 1.

An excellent combination of mechanical properties and high temperature resistance with exceptional processibility offers many applications. Application areas include : under-the-hood, electrical, and heat exchange components in automobiles, connectors, switches and controls, and integrated circuit test devices in electrical and electronics, lighting, seating, wiring, and electrical hardware in aerospace field [13,16].

2.2 Miscibility of PEEK and PEI

PEEK possesses a glass transition temperature (T_g) of 143 °C, but PEEK is used as high as 200 °C in structural applications. Therefore significant creep problems are incurred at the temperatures above T_g. Blending with PEI is a part of the effort to generate advanced matrix resins. PEI generally possesses very high T_g but poor chemical resistance to organic solvents and aqueous bases, which makes it susceptible to environmental stress cracking.

Two references [14,15] report that blends of PEEK and PEI are miscible in all compositions. The quenched, amorphous blends of PEEK and PEI displayed a single, sharp T_g which obeyed the Flory-Fox equation and thus indicated miscibility. The melting points of the blends displayed little variation; however the T_g of the blend increased with PEI incorporation. The Flory-Fox equation is

$$\frac{1}{T_g} = \frac{w_1}{T_{g1}} + \frac{w_2}{T_{g2}} \qquad (1)$$

where w_1 and w_2 are the weight fractions; T_{g1} and T_{g2} are the glass transition temperatures of the component polymers respectively.

Crystallization rate (K) is retarded with the increased percentage of PEI in blend due to a decrease in nucleation density. Also, growth rate (G) of crystallites is slowed down with the increasing PEI [17].

2.3 Morphology of PEEK

The melting and crystallization behavior of PEEK is very strongly dependent on previous thermal history. Upon crystallization folded chain lamellaes of PEEK form spherulites in the bulk form. Figure 2 shows spherulite with cylindrical symmetry in a PEEK thin film. Nguyen and Ishida [24] reviewed the published studies of PEEK and its composites. The following paragraphs summarize their article.

The optimum crystallization temperature range is from 180 °C to 320 °C. The radius of spherulite ranges from 12.7 to 21.9 μm for crystallization temperatures of 240 and 287 °C, respectively. For cooling rates faster than 2000 °C/min, PEEK will be amorphous and for cooling rates faster than 700 °C/min, the spherulite growth is retarded. Annealing for 30 minute at 200 to 300 °C will yield a satisfactory degree of crystallinity.

The crystallization process can take in two ways: crystallized from the rubbery amorphous state (annealing) and crystallized from the melt. The degree of crystallinity is much smaller and the size of spherulite is smaller and thinner for the samples crystallized via annealing from the amorphous state than those of the latter.

The morphology of PEEK is strongly influenced by the presence of foreign surfaces. (i.e., As the fiber content of CF reinforced composite increases, PEEK crystallizes at higher temperatures with higher nucleation densities.) The spherulites of PEEK grow perpendicular to the fiber surface and terminate when impingement occurs either between the spherulites or between the spherulites and the fibers occurs. This

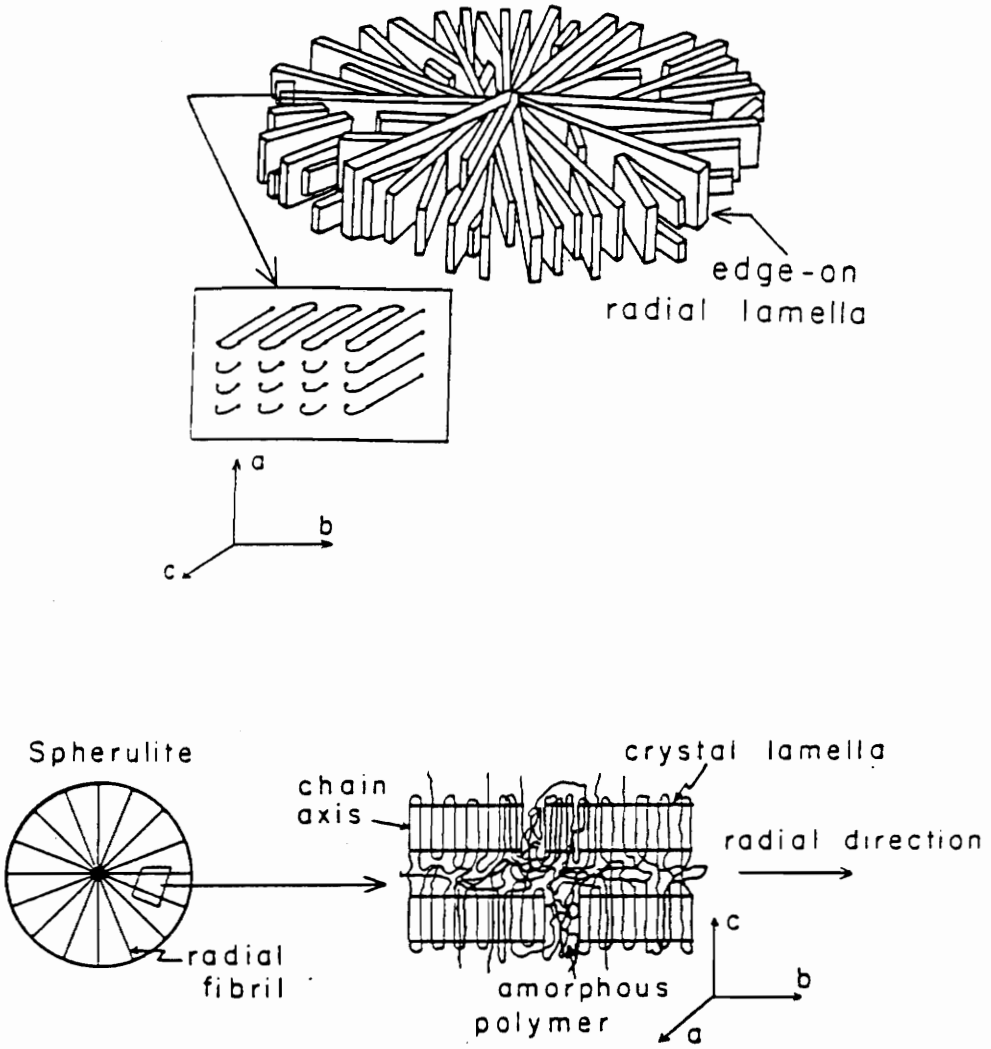

Figure 2. **Schematic representation of a spherulite with cylindrical symmetry in a PEEK thin film [24]**

columnar growth of crystals is known to be a "transcrystallinity." In highly-loaded composites with 50 to 70% fiber by volume, adjacent transcrystalline regions may impinge on each other, and their boundaries may become areas of weakness.

2.4 Morphology vs. Mechanical Properties

Tensile properties of many semicrystalline polymers have been studied and they are all strongly influenced by the heat treatments which can change the morphology. Tanaka and Ueda [21] noted that increasing the spherulite size generally decreased the strength and elongation at fracture. Harris, et al. [15] compared the mechanical properties of an injection molded PEEK/PEI blends with those of annealed blends. They observed that the increased tensile strength and modulus along with accompanying the decreased ultimate elongation and tensile impact strength when the crystallinity increased. Similar results were also found by Curtis, et al. [20]. The reduction in the ultimate elongation and in the toughness is considered to be due to a creation of regions of weakness between highly ordered spherulites.

Lustiger, et al. [18] tested unidirectional CFR PEEK composites for fracture toughness and impact delamination as measured by ultrasonic C-scan and compression strength. Higher crystallinity and larger spherulite size caused the toughness to decrease. The compression strength increased with increased crystallinity and spherulite size. In compression, the matrix materials basically provide support for the fibers. Premature

buckling can result if the matrix material is more ductile. Therefore, increased brittleness of the composite and raised compression strength are caused by increased crystallinity and spherulite size.

The radial patterns found from the fracture surface suggests that fracture occurs by crack propagating spherulite centers rather than spherulite boundaries [18]. On the contrary, Curtis, et al. [20] concluded that the crack propagates around a weakened interspherulitic boundary rather than through the spherulites.

Cebe, et al. [11] compared four differently heat processed PEEK films and related the tensile test results to the degree of crystal perfection. Slowly cooled peek films in the hot press and air cooled PEEK films did not strain harden. The crystals formed during melt crystallization act as crosslinks, and they are referred to as the lamellar crystals. Films that experience quenching showed necking development followed by strain hardening. The poorly developed crystals easily reorganize into fibrillar crystals during the hardening. The stress-strain curves indicated that the semicrystalline films require a greater stress for yield and for neck propagation than the amorphous film.

2.5 Morphology vs. Friction & Wear

The molecular and morphological structures of semicrystalline polymers should be considered the analysis of the friction and wear because of the well known fact that these structures strongly influence the physical and mechanical properties believed to be

important to polymer wear and friction.

Tanaka [23] concluded from his sliding wear experiments of various semicrystalline polymers that smaller spherulites and less bulky (smoother) molecules lower the wear rate. A later study of Tanaka and Ueda [21] reported that a defect in crystalline lamellae is a more influential factor than spherulite size in the wear of some polymers. Their experiments with the polypropylene sliding on a smooth steel surface showed that the coefficient of friction displayed a minimum at a certain diameter of spherulite. The wear rate for the untreated specimens showed a minimum at the same size of spherulite where a minimum of the friction occurred, while the coefficient of friction for the annealed specimens did not vary with spherulite size. Presumably the fracture of spherulites occurred on a smaller scale on the frictional surfaces of the annealed specimens than on the molded specimens, which caused the lower wear rate. Jones and Eiss [29] commented that the higher degree of crystallinity represses crack propagation which involves the breaking of primary bonds. It seems the increased crystallinity of the semicrystalline polymer does not always improve the wear resistance: testing conditions play a dominant role.

Voss and Friedrich [22] investigated the wear behavior of short glass- and carbon-fiber-reinforced composites of PEEK under two different types of wear. Sliding wear tests against a smooth steel surface (surface roughness, R_a = 0.06 μm) showed that the increased wear resistance with annealing while sliding against abrasive papers (mean particle size D =70 and 7 μm) did not reveal the improvement.

Schelling and Kausch [2] conducted reciprocating wear tests and continuous pin

on disc (R_a = 0.66 μm) tests of the PEEK and its composites. Even though they observed the decrease in coefficients of friction they did not see any change in the wear resistances with the annealed specimens on both wear tests.

Jones and Eiss [29] examined the chemical structure effect and found that polyimides with the most flexible chain, as indicated by the glass transition temperature, had the lowest wear rate. They also noted that a highly polar side group could increase adhesion to the contacting metal or transferred film resulting in higher tractive stresses and correspondingly higher wear rates.

2.6 Mechanical Properties vs. Friction & Wear

Wear of polycarbonate, polyvinyl chloride, ultra high molecular weight polyethylene, siloxane modified epoxies, and polyimides was investigated on a steel ball-on-polymer surface configuration by Potter and Eiss [28]. A range of cycles of polymer disk rotation was observed before a wear track initiated; thus the significant wear mode was fatigue. In the fatigue wear mode, the number of stress cycles N to failure is inversely proportional to the applied maximum tensile stress (S). The relationship is given by

$$N = \left(\frac{S_0}{S}\right)^t \qquad (2)$$

where S_0 = the tensile yield strength

t = an empirically determined constant.

The wear rates of the siloxane modified epoxies and the polyimides, indicated a positive correlation with the elastic modulus [28-31]. This correlation can be related to the equation of the maximum tensile stress (S) for a sphere sliding on a plane with friction as follows

$$S = \frac{3P}{2\pi a^2} \{ f(4+\nu)\frac{\pi}{8} + \frac{(1-2\nu)}{3} \} \quad (3)$$

where P = load

a = radius of contact based on Hertzian elastic contact

f = friction coefficient

ν = Poisson's ratio.

From the above equation, S is proportional to a^{-2}. From the Hertzian elastic contact theory, a is proportional to $E^{-1/3}$. Hence the maximum stress (S) is proportional to $E^{2/3}$. Since the wear rate is inversely proportional to the number of cycles to fatigue failure, and from Eq. 2, the number of cycles to failure is inversely related to stress, the maximum stress (S) is associated positively with the wear rate. Thus the wear rate is positively correlated with the elastic modulus raised to the power 2t/3 within a specific polymer system.

Eiss and Czichos [31] further investigated the siloxane modified epoxies in the abrasive wear mode. The modified epoxies pins were sliding on the steel surfaces (Ra

= 0.3 μm) and the initial wear rate varied inversely with elastic modulus and fracture toughness. The microroughness of the steel disk causes abrasive wear initially and the transferred epoxy smothered the steel disk surface and thus reduced wear. It is well known that the abrasive wear rate varies inversely with the energy to rupture and Eiss and Czichos results were well agreed with.

Friedrich [32] proposed an abrasive wear model as follows

$$\dot{\omega} = \dot{\omega}_{pl} + \dot{\omega}_{f} \tag{4}$$

where $\dot{\omega}$ = the abrasive wear rate

$\dot{\omega}_{pl}$ = the wear rate characterized by microplowing combined with microcuttintg

$\dot{\omega}_{f}$ = the wear rate portrayed a rate of particle removal from the worn surface after microcrack formation and local fracture.

and the microcracking component of wear rate is described as follows

$$\dot{\omega}_{f} \propto \Omega \frac{H^{\frac{1}{2}}}{G_{Ic}} \tag{5}$$

where Ω = the real probability factor for microcracking

H = the hardness

G_{Ic} = the fracture energy.

He discussed that as long as the threshold pressure (P_{crit}) above which wear particles are formed by microcracking is not reached, the microplowing is dominant wear process. Otherwise, the microcracking event is dominant wear process.

2.7 Friction & Wear of Polymers

The differences between the friction and wear of metals and polymers are caused by the low surface energy, high oxidation resistance, low hardness, low heat conductivity, and strong temperature dependence of mechanical properties of polymers relative to those of metals.

Briscoe [33] suggested the two-term model of friction : the interfacial and deformation components, which can be written as $F = F_{adh} + F_{plow}$ where F is the total frictional force, F_{adh} is the interfacial friction, and F_{plow} is the deformation friction. In the interfacial friction model, the frictional energy is dissipated within a very narrow region adjacent to the interface which experiences high rates of energy dissipation. Shear of adhesive junctions at the areas of close solid-solid contact results the frictional force F_{adh} as given by

$$F_{adh} = \tau A \qquad (6)$$

where τ = the interface shear strength (bulk shear strength)

A = the real area of contact.

In short, the interfacial friction can be referred as an adhesion friction.

The deformation friction model is associated with lower rates of energy dissipation because it involves deformation such as plowing and deformation within a large volume of material. When a rigid asperity moves over a polymer surface, the polymer is deformed. Due to the viscoelasticity of polymer, the surface does not recover the strain instantaneously. The frictional work is dissipated beneath the contact in a series of cyclic deformations. If the polymer is deformed beyond its elastic limit then plastic deformation or propagation of viscoelastic cracks occurs. The cracks propagate into the bulk of the polymer and ultimately intersect to form a debris particle. The frictional work is dissipated by generating heat in the contact area. The generation of heat affects the mechanical properties of the frictional material.

The wear process of polymer can be broken down into two classes : cohesive wear and interfacial wear [34]. The cohesive wear processes involve the dissipation of the frictional work in a large volume of material adjacent to the interface. Abrasion and fatigue wear are within this category and controlled by the cohesive strength or toughness of the polymer. In interfacial wear, the frictional work is dissipated into thinner regions and at greater energy densities. Transfer wear and chemical or corrosive wear are the two elements of interfacial wear.

Friedrich [32] analyzed the relationships between wear and material properties of

various polymers and suggested the rules for a good wear resistant polymer.

The material should possesses :

i) high hardness, H

ii) a tendency to deform plastically with high work to rupture and high resistance to cutting

iii) a low coefficient of friction

iv) a small ratio of asperity size, D, to the size of internal features, d(defects, hard filler particles)

v) a minimized ratio of: $\frac{HE}{K_{Ic}^2}$

where E = modulus

K_{Ic} = fracture toughness.

2.8 Friction & Wear of PEI Composites

PEI is an amorphous thermoplastic polyimide. Bijwe, et al. [3,7,8,35,36,37] exclusively performed the friction and wear tests of PEI matrix and its composites available from the General Electric Company. Their important properties are listed in Table 2.

Neat resins of ULTEM 1000 were slid against mild steel on a pin-on-disc

TABLE 2. Composites of PEI and important properties

Material	Composition	Tensile Moduls (N/mm^2)	Flexural Modulus (N/mm^2)	Compression Modulus (N/mm^2)	Rockwell Hardness	1/Se† $(MPa)^{-1}$	Reference
ULTEM 1000	Neat PEI	3000	3300	2900	M 109	1.58E-4	3
ULTEM 2200	20 wt% GF	6900	6900	3500	M 114	2.38E-3	8,35
ULTEM 4000	25 wt%GF + 15%PTFE + 15%(Graphite, MoS_2	7106	7106	3300	M 85	8.03E-3	7
ULTEM 4001	15 wt% PTFE	2600	2600	-	M110	1.03E-3	37

† Se is the product of tensile strength(S) and % elongation(e)

machine. When steel surface was very smooth (Ra $\leq$ 0.08 μm), the friction coefficient was very high and wear of the PEI pin was insignificant. Instead of the pin the steel disk surface was worn out; there were deep grooves in the wear track which were possibly caused by strong adhesion. For a moderately smooth surface (Ra $\approx$0.3 μm), the friction coefficient was half that for very smooth surface (Ra $\leq$ 0.08 μm) but wear was high. However, there was no film transfer on the counterface and wear debris was in the form of very fine powder. Bijwe, et al. [3] suggested that this may be due to good impact strength, hardness and reasonably good ductility. They repeated that 40 to 90 kcycles of the steel disk rotations were observed before wear initiated. This incubation time is characteristic of fatigue wear. An Increase in load decreased the friction coefficient and slightly increased the specific wear rate, K_0 ($m^3N^{-1}m^{-1}$). The specific wear rate was in the range of 10^{-13} (m^3/Nm) [3].

The same pin-on-disc machine was used at various loads, speeds and counterface roughness to test ULTEM 2200 pins. The friction coefficient reached the peak at the initial stage of sliding, decreased, and then decreased again with many fluctuations. The highest coefficient of friction was observed for the smoothest surface; smoother surface also showed more friction fluctuations. Friction and wear minima were found at the intermediate range Ra = 0.1-0.15μm. At very smooth surface (Ra $\leq$ 0.025 μm), large scale transfer of polymer on the counterface increased friction and wear. However with increased roughness, the plowing component of friction and wear increased. An Increase in load increased both friction and wear. Wear debris consisted of polymer matrix containing broken pulverized glass particles and wear powder of the metallic counterpart.

This debris may act as a third body abrasive which roughened the counterface and increased friction. Bijwe, et al. [35] deterioration of fiber-matrix adhesion and thermal degradation of the polymer due to hot spot generated by contacts between glass fibers and steel surface possibly increased the wear. Gross transfer of molten polymer from the interface of the composite was observed at a high PV value. As a result of reinforcing with short glass fiber, the specific wear rate decreased to K_0 = 4.5E-15 (m^3/Nm) and friction slightly increased [35,36].

The coefficient of friction of ULTEM 4000 also displayed a peak and increased with the increase in load. A linear increase of pin subsurface temperature and wear volume were observed as a function of sliding time. When fibers were oriented parallel to the sliding direction, the coefficient of friction and the specific wear rate were higher than that with fibers in normal direction. The average coefficient of friction was around 0.15 and the specific wear rate was 8.5 x 10^{-16} (m^3/Nm) [7].

Friction of ULTEM 4001 was lowest in the counterface Ra range 0.2 to 0.3 μm where the wear rate was high, while the friction displayed the highest value at a Ra 0.05 to 0.1 μm where the wear rate was the lowest. An Increase in load decreased the friction coefficient and the specific wear rate, even though the weight loss increased [37].

In abrasive wear (grit size = 52 μm), neat PEI has better wear resistance than its composites. Increasing the load decreased the specific wear rate in all above composites. [36].

2.9 Friction & Wear of PEEK Composites

Briscoe, et al. [38] reported that inclusion of Poly(tetra fluoro ethylene) (PTFE) reduces the friction of PEEK with small sacrifice of wear resistance. When a steel ball slid against the PEEK surface, the increases in coefficient friction with sliding distance may be due to a loss of the asperity persistence. When PEEK slid on a moderately smooth steel surface (0.3-0.4 μm c.l.a), evidence of local melting was observed. Local melting with melt transfer or fatigue tearing are the possible causes of PEEK wear.

Schelling and Kausch [2] compared the effect of reciprocating and continuous sliding motion on the friction and wear of PEEK and short carbon fiber composites. The wear process of PEEK by reciprocating dry friction may be a mixture of adhesion and abrasion because thick and irregular transferred debris was seen on the counterface. The wear mechanism of 10 wt % carbon fiber and 20 wt % of PTFE and graphite composite PEEK 450HF30 is the debonding of fibers and fracture under continuous friction, and adhesion of the matrix to the counterface under reciprocation movement. The transferred film did not stay at the interface on the polished surface (Ra = 0.03μm) and caused high wear and friction. The detailed results are shown in Table 3.

Voss and Friedrich [22] investigated the wear behavior of short fiber reinforced PEEK sliding against smooth steel (Ra = 0.06μm) and abrasive papers (mean grit sizes, D = 70 and 7 μm). In sliding wear, higher velocity produced a higher wear rate for the unfilled material. At low velocity, glass fiber reinforced (GFR) PEEK has twice the wear rate of neat PEEK while carbon fiber reinforced (CFR) PEEK has half the wear

TABLE 3. Friction and wear of PEEK 450G and PEEK 450HF30 [2]

		Reciprocating[a]			Continuous[o]		
		W(m/m)	μ	T_i(°C)	W(m/m)	μ	T_i(°C)
Ra = 0.66 μm	PEEK	2.7E-7	.39	41.5	3.3E-9	.35	51
	PEEK ANNEALED	1.97E-7	.35	40	3.95E-9	.25	49.5
	450HF30†	4.0E-7	.13	70	7.97E-11	.14	48.5
	450HF30‡	1.95E-7	.18	125	1.18E-9	.28	111
Ra = 0.03 μm	450HF30	8.2E-7	.23	76.8	5.7E-10	.22	65

Wear rate

$$w = \frac{\Delta m}{\rho A L} \quad (m/m) \tag{7}$$

where m = mass loss of the pin(kg)
ρ = density of the pin(kg/m^3)
A = apparent contact area(m^2)
L = sliding distance(m)

T_i = interfacial temperature
[a] experimental conditions : P=0.5MPa, V=1.19m/s, sliding time=70 hrs
[o] experimental conditions : P=0.5Mpa, V=0.25m/s, sliding time=70 hrs
† conducted at low interfacial temperature
‡ conducted at high interfacial temperature

rate. Measurements of the sliding counterface temperature showed that GFR was the lowest, CFR was intermediate and neat PEEK was the highest. No pronounced differences in the wear rate between the parallel and antiparallel directions was observed while the normal direction exhibited a reduction relative to the other two directions. In abrasive wear, a slight increase in the wear rate was seen. Severe fiber breakage and fiber removal were detected.

Mody, et al. [9] examined the friction and wear of PEEK and unidirectional and woven graphite fiber reinforced composites on sliding against smooth steel surface (Ra = 0.06μm). PEEK showed increased wear rate with increased sliding velocity and temperature. The wear rate of the unidirectional GFR showed somewhat contrary results to those shown previously by Voss and Friedrich [22]. The wear rates decreased when fibers were in N and P directions and increased when fibers were in AP direction, compared to the neat matrix. In the case of a two dimensional woven fiber composite, no clear dependence of fiber orientation was seen. The wear rates and the coefficient of friction of the woven fiber composite were smaller than those of the unidirectional GFR PEEK.

Cirino, et al. [39] studied the effect of orientation of continuous carbon fiber on abrasive wear. The wear rate for the N and P directions showed no difference but the AP direction showed a higher wear rate than that of the other two directions.

Cirino, et al. [26] expanded their previous study : sliding wear of continuous aramid (AF), Glass and Carbon fiber reinforced composites of PEEK against a steel ring (Rt = 0.6μm). CF and AF reduced the wear rate of PEEK matrix except for the case

of the CF in the N direction. GF reinforced PEEK showed higher wear rate than that of neat PEEK.

Jacobs, et al. [27] performed fretting wear of continuous glass, carbon and aramid fiber composites of PEEK. The wear rate was nearly symmetrical with respect to the orientation angle and showed a pronounced maximum at 45°. Only a AF reinforcement showed improvement of the fretting wear resistance, while carbon and glass fibers resulted in an increase in the wear rates.

Mody, et al. [9] discussed that an increase in sliding velocity enhances microcutting of the polymer by the steel asperities resulting in increased wear. The increase in wear rate associated with increasing temperature is caused by the degradation of the fiber-matrix interface which results in the easy removal of fibers after breakage. For the case of the continuous unidirectional fiber reinforcements, the P-oriented composites showed the lowest fiber removal because of the relative difficulty in causing fibers to fracture. In the AP-oriented case, the transverse fibers suffered an impact type of damage by the asperities which resulted in fiber fracture and fiber-matrix cracking leading to fiber removal. In the N-oriented case, wear debris trapped between the protruding stubs of the fibers and provided a cushioning effect. Cirino, et al. [26] observed that for brittle fiber reinforcements (CF & GF), pronounced wear mechanisms are fiber fracture and fiber-matrix interfacial debonding. For ductile reinforcing fibers (AF), fiber sliding wear and matrix wear are dominant process of material removal.

3. EXPERIMENTAL WORK

From the previous chapter, the morphology characteristics of PEEK strongly depend on previous thermal history and affect the mechanical and tribological behaviors of PEEK and its composite materials. Therefore the thermal history during the fabrication of samples of PEEK/PEI blends is described in this chapter. The procedures of the morphological characteristics and mechanical property tests are followed.

3.1 Sample Preparation

Brown pellets of PEI (ULTEM 1000®) and gray pellets of PEEK (Victrex PEEK 380G®) were obtained from the General Electric Company and ICI correspondingly. These two resins were vacuum dried in a Fisher Isotemp Vacuum Oven at a temperature of 150 °C for 24 hours to minimize moisture absorption, which may cause formation of voids inside a cast plaque. Once they were dried, they were mixed according to desired weight compositions and pre-blended by a Killion Extruder which melted the resins at 355-380 °C. The circular extrusions of diameter 2mm were quenched into ice water and

then chopped up into pellet forms. These pellets were once again dried out at 150 °C for 24-48 hrs inside the vacuum oven. The final blending process was completed via injection molding at 390-410 °C. The mold temperature was between 90 to 105 °C which was below the T_g of PEEK, 145 °C, and the cooling time was 60 seconds which yielded a cooling rate of approximately 300 °C/min. The resins were molded into plaques with the geometry shown in Fig. 3. Most of plaques were transparent except for the 100 % PEEK and the half of the plaque closest to the manifold of the 85/15 blends of PEEK and PEI which were opaque indicating some degree of the crystallinity.

The 50/50, 70/30 and 85/15 blends of PEEK and PEI were annealed in the oven for 24 hrs at 205 °C to achieve the maximum crystallinity so that the crystallinity effects on friction and wear could be studied. The annealed plaques warped possibly due to residual stresses generated from an uneven cooling process during injection molding. In order to make them useful for the friction and wear test, they were flattened out by compressing in the Pasadena Hydraulics compression molding at 205 °C and 267 kPa for 5 min followed by quenching into ice water while being clamped.

PEEK and PEI resins filled with 30 wt % of short carbon fibers were supplied from ICI in pelletized form. They were dried at 150 °C at the vacuum oven and then fabricated into plaques by injection molding using the same temperature and time parameters as used for the unreinforced blends. It was not possible to injection mold a complete plaque with the carbon fiber reinforced (CFR) composites of PEEK because the melted CFR PEEK only half filled the mold. The most likely cause for the partial fill of the mold is the high viscosity of PEEK and the high tendency to crystallinize due to

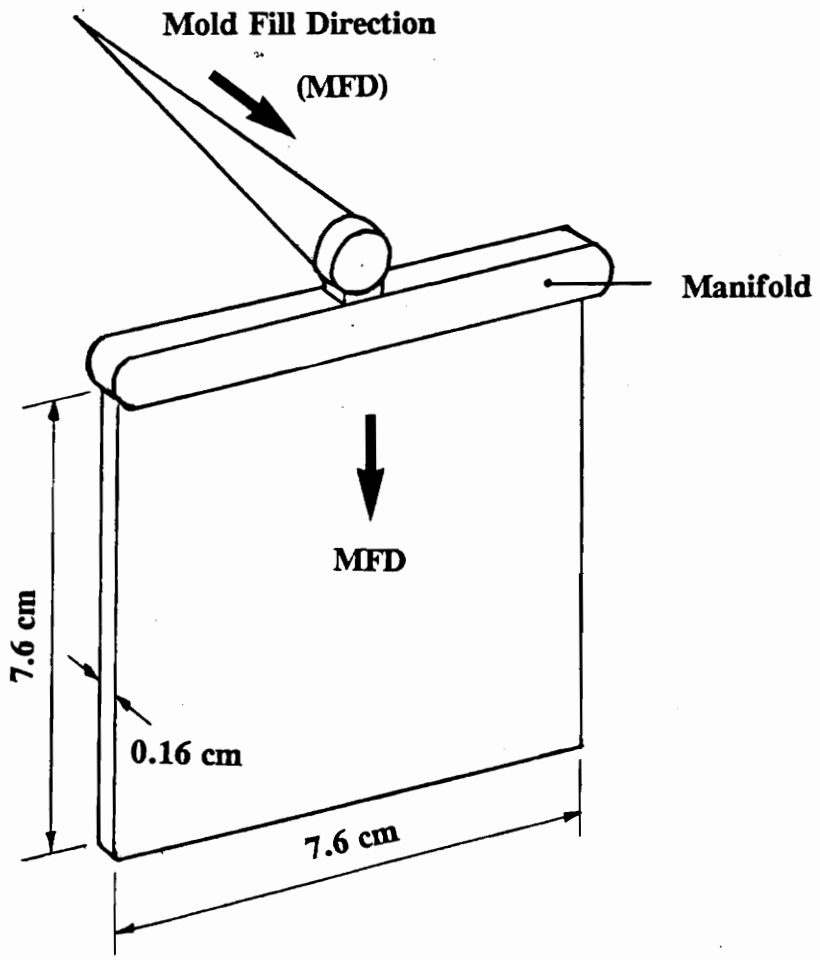

Figure 3. Injection molded plaque geometry

an increase in nucleation density sites that were provided by the presence of short carbon fibers [40].

3.2 Morphology Testing

The glass transition temperature T_g and the degree of crystallinity of two samples for each composition were determined using a Seiko 1 Differential Scanning Calorimetry (DSC) 210. A 6 to 13 mg sample was cut from the plaque and placed into a sample pan which was placed on a thermocouple. An empty aluminum pan was also placed on the thermocouple as a reference to monitor the amount of heat flow into the sample while they were heated. All experiments in the DSC were performed at a heating rate of 10 °C/min in nitrogen atmosphere to prevent oxidation of the specimen.

Since the crystallinity may vary across the thickness of the plaque because of different cooling rates, the crystallinity was measured for a sample from the entire crossection area and a sample from only the surface for the upper part of 85/15 blends. The latter samples were approximately 0.13 mm thick. Statistic analysis of the results indicated no difference in their mean crystallinity at a 99 % confidence level. Therefore, an uniform crystallinity across the plate was assumed. For the DSC test of the CFR blends, samples were shaved off the edge of the plaque and compared with the unreinforced blend.

The relative crystallinity of PEEK was obtained by measuring the area under each

exotherm and endotherm which depends on a somewhat arbitrarily chosen baseline. Blundell, et al. [41] presented two methods for the routine measurements of the crystallinity of Poly(ethylene terephthalate) (PET) and Polyethylene (PE): the total enthalpy method and peak area method. For the polymer that does not have sharp and well defined melting peaks, they suggested some adjustment of the baseline for the peak area method. The details will be found in reference [41].

The crystallinity measurement for this experiment was performed using the peak area method and some adjustments were made because of unclear melting peaks. Fig.4 illustrates an example of DSC trace to account for the gradual ending of the exothermic crystallization process between T_1 and T_3, the baseline was not drawn in straight between points at T_1 and T_2. A point of inflection at T_3 was selected and lines were drawn from T_1 to T_3 and from T_3 to T_2 (see Fig. 4.)

The relative crystallinity of PEEK in a sample was determined from the expression

$$\chi_c = \frac{H_{endo} - H_{exo}}{\Delta H_f \, \omega_{PEEK}} \times 100 \qquad (8)$$

where χ_c = the weight fraction crystallinity

H_{endo} = the area under the endothermic melting peak

H_{exo} = the area under the exothermic crystallization peak

ΔH_f = the heat of fusion for fully crystalline PEEK, 130 J/g [19,40,42]

ω_{PEEK} = the weight fraction of the PEEK in the sample.

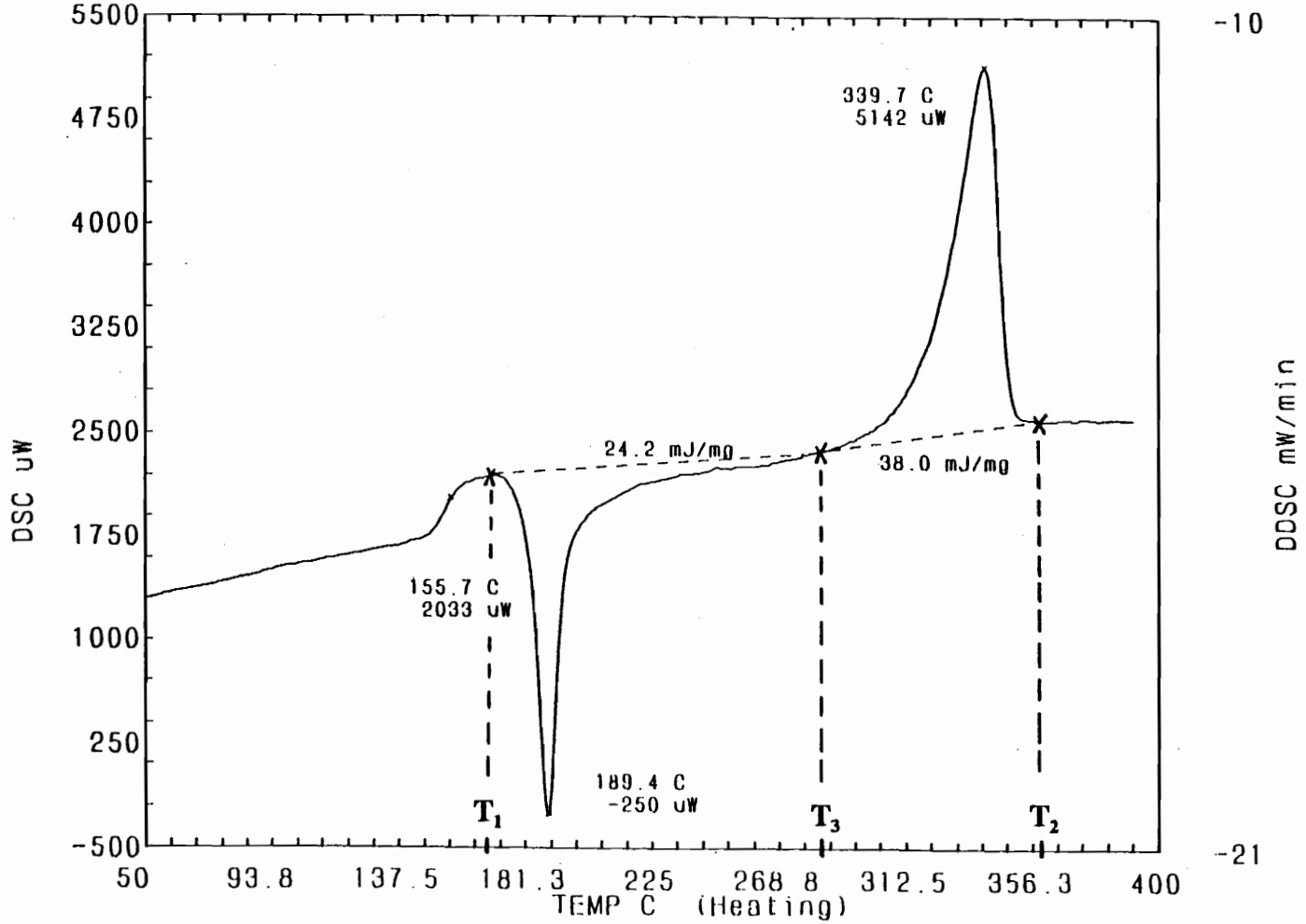

Figure 4. **Plot of DSC trace for 85/15 blend of PEEK and PEI illustrating the adjusted base line for the peak area method**

3.3 Tensile and Fracture Testing

Fracture toughness tests of pure PEEK and PEI were carried out under Mode I (tension) loading using compact specimens (see Appendix A for geometry). The tests were done using an Instron machine at a cross-head speed of 2.54 mm/min (= 0.1 in/min) at room temperature. The load-displacement curve was plotted with aid of an extensometer and the stress intensity was calculated to determine plane strain or plane stress. For the 100% PEI test, the specimen buckled and shortly after fractured. The stress state of pure PEI test was the plane stress. As shown in Appendix A, the linear elastic fracture mechanics (LEFM) would not apply due to its thin thickness (t=1.6 mm, 1/16 in) therefore fracture tests were not performed for any other blend. The details of the fracture toughness testing procedure, and geometry of the compact specimen are presented in Appendix A. The fracture toughness test was not fully carried out for the 100% PEEK specimen due to severe buckling without fracture failure. The buckling was caused by the ductility of the PEEK.

The dog-bone shaped tensile specimens shown in Fig. 5 were machined out of the molded plaque and utilized to obtain mechanical properties of 100% PEEK, 100% PEI and 50/50 blend. The samples were tested in the Instron testing machine at a cross-head speed of 0.5 mm/min (0.02 in/min.) The procedure and a typical load-displacement curve are presented in Appendix B. The extensometer which has 12.7 mm gage length was only used at the beginning of the each test because it is limited to 15% elongation. The load-displacement curve was plotted until the specimen broke. The measurement of

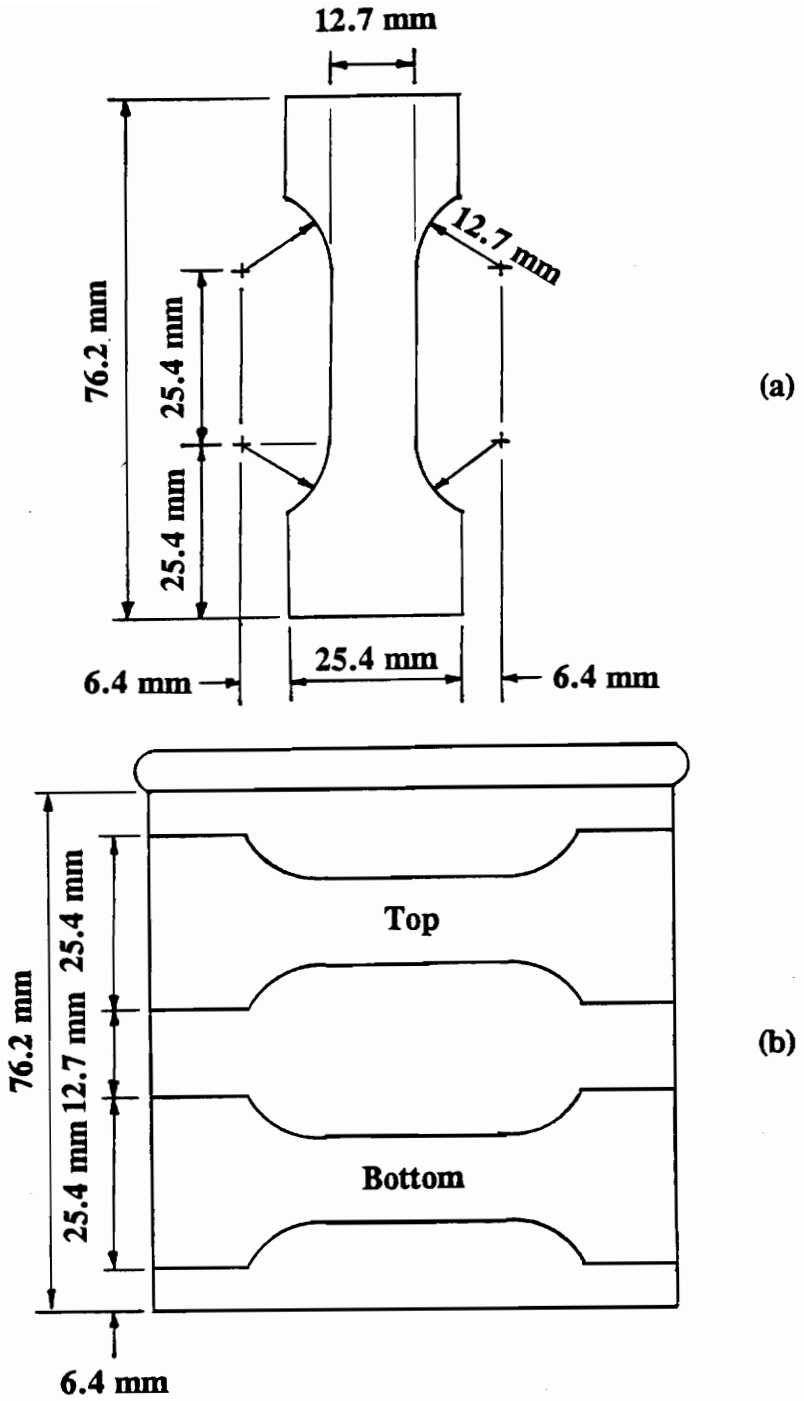

Figure 5. Tensile test specimen (a) geometry of the specimens (b) shows the locations of the specimen being cut from the injection molded plaque

the modulus of elasticity was not accomplished because of the difficulty of finding a linear tangent line from the origin. Lack of reproducibility was found when the yield strength and elongation-to-break were measured for each specimen.

3.4 Friction and Wear Testing

The friction and wear studies were conducted by sliding a steel (52100) ball with a diameter of 3.175 mm against a polymer disk using a pin-on-disk wear machine shown in Fig. 6. The steel ball was loaded by a pneumatic device against the rotating disk which is driven by a motor and a timing belt-pulley system.

A deflection of the cantilever beam to which the ball was attached was measured by a proximity transducer and calibrated to indicate the frictional force. The output of the transducer was continuously recorded on an Astro-Med plotter. The base of the cantilever beam was moved linearly to provide a desired radius of the wear track.

The apparatus was adjusted to run at two sliding speeds of 5 and 15 cm/s and two normal loads of 5 and 15 N. The operating conditions for each composition are listed in Table 4. Each test was conducted at room temperature. The sample disk was stopped at intervals of 600 cycles to look at the wear track by a Wild Heerbrugg macroscope and to measure the cross-section areas of wear track. The wear area was obtained by averaging areas at four locations 90° apart on the track using a Taylor Hobson Talysurf. Wear rates were evaluated by taking slopes of linear regression line on the plot of average wear areas versus number of cycles. The tests were terminated at 3600 cycles.

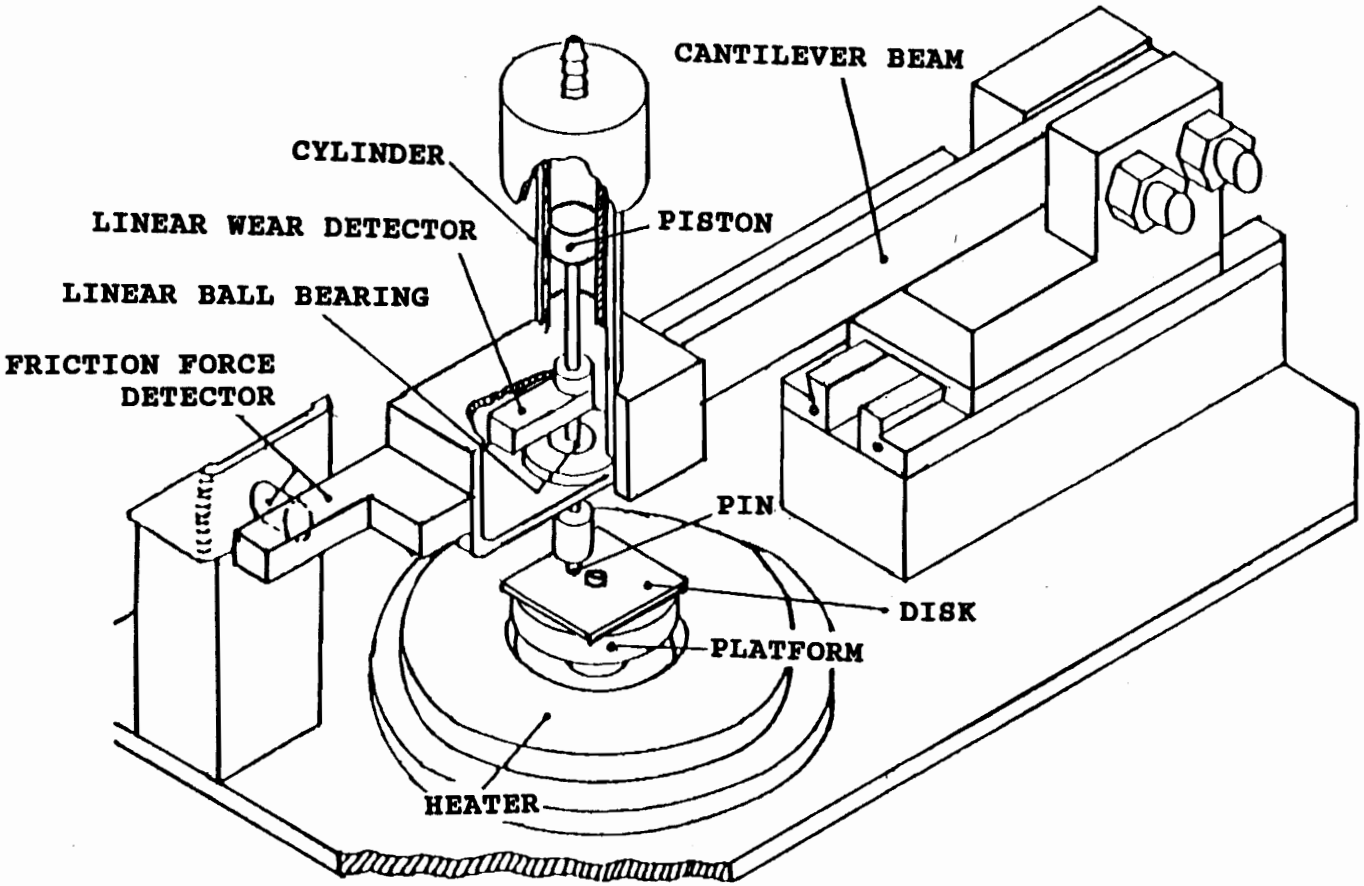

Figure 6. **The pin-on-disk wear machine**

TABLE 4. Operating conditions for friction and wear testing

	Normal Load	5 N		15 N	
	Sliding Speed	5 cm/s	15 cm/s	5 cm/s	15cm/s
	PEEK/PEI				
Unfilled	100/0	1†	1	-	-
	85/15	-	-	6	4
	70/30	4	-	2	4
	50/50	3	3	3	3
	0/100	3	3	3	5
Annealed	85/15	-	-	3	2
	70/30	-	-	3	3
	50/50	-	3	3	4
30 wt % CFR	100/0‡	-	-	3	3
	70/30‡	-	-	3	3
	0/100‡	-	-	3	3

† Number of tests under each set of conditions
‡ Relative weight % of the polymers; excluding weight fraction of carbon fibers

4. RESULTS

4.1 Morphology

The morphology characteristic of the tested samples was studied by heating small pieces of each sample from room temperature to 400 °C at a heating rate of 10 °C/min using Differential Scanning Calorimetry (DSC). Appendix C includes the DSC traces for all the tested samples. The observed glass transition temperatures (T_g) and the relative degree of crystallinity of PEEK for the tested PEEK/PEI blends are given in Table 5 as a function of weight composition. Note that, in Table 5, the 95% confidence limits are not included due to insufficient number of observations. Experiments were carried with basically three different samples; the PEEK/PEI blends as received from injection molding which will be called untreated, 30 weight % short carbon fiber reinforced blends that will be referred to 30% CFR, and the annealed blends that will be designated as annealed.

Untreated, 30% CFR, and annealed blends had single T_g's indicating the miscibility of PEEK and PEI. The T_g increased with increasing PEI incorporation in the blend. The observed values of T_g of the untreated obey the Flory-Fox equation which

TABLE 5. The relative crystallinity* of PEEK and the glass transition temperature(T_g) of tested samples

	PEEK/PEI	T_g (°C)	% Crystallininty
Untreated	100/0	144.6†	27.35
	85/15 (T)	155.4 ± 2.1‡	10.66 ± 2.90
	85/15 (B)	152.3	1.67
	70/30	159.4 ± 1.5	1.27 ± 1.73
	50/50	178.1	0.00
	0/100	213.0	-
Annealed	85/15	178.5	36.69
	70/30	186.0	37.91
	50/50	194.2	26.62
30 wt % CFR	100/0	157.4	16.43
	70/30	173.9	18.37
	0/100	214.1	-

* % of the PEEK crystallized relative to the PEEK content in the blend
† Mean
‡ Mean and 95% confidence limits
(T) Samples which were obtained from the plaque closest to the manifold
(B) Samples which were obtained from the plaque farthest from the manifold.

is noted earlier in Eq. 1 and are very close to the reported values that were found in references 15 and 17. For the 30% CFR, the T_g's were 13 °C higher than those of the untreated. The annealed blends further increased the T_g's 16 to 26 °C as compared to those of the untreated. Figure 7 displays these observations clearly. The glass transition temperature is the temperature at which the amorphous part of polymer changes from brittle glassy solid to a rubbery or viscous solid. T_g is affected by various physical and chemical factors that influence the mobility of the amorphous chains. For the 30% CFR and the annealed blends, the lamellae exist due to the crystallization. These lamellae may restrict the relaxation movements of the amorphous molecules and may be responsible for the increased T_g's.

The relative crystallinity of PEEK for the each sample is shown in Fig. 7. Even though the PEEK/PEI blends were quenched by injecting the melt at 410 °C into the mold at 90 - 100 °C and then cooled for 60 sec, a degree of crystallinity of 27% was observed for 100% PEEK of the untreated samples. As the degree of the crystallinity increased the plaques became more opaque. The plaques of the 85/15 blends of PEEK and PEI were opaque closest to the manifold and transparent farthest from the manifold. DSC results indicated 11% crystallinity for the former and 2 % for the latter. As PEI was incorporated into the blends, the crystallization process was retarded. The degree of crystallinity of the 50/50 blend and 100% PEI was zero thus they were completely amorphous materials. Among the 30% CFR blends, the 70/30 PEEK/PEI blend possessed the highest crystallinity, 18%. The annealed blend also exhibited the highest crystallinity at intermediate compositions, 70/30. Harris and Robeson [15] also found

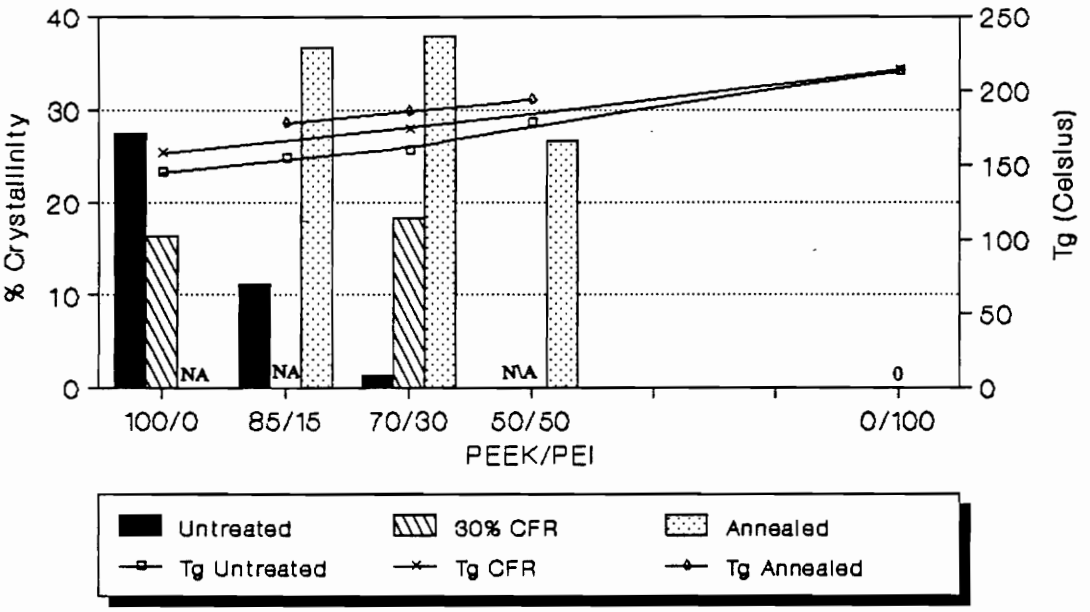

NA = not available

Figure 7. Comparisons of the relative crystallinity of PEEK and the glass transition temperatures for the tested sample

the maximum degree of crystallinity at 30-40 wt % PEI concentration for the PEEK/PEI blends that were isothermally crystallized at 300 °C. Their explanation for the maximum crystallinity at intermediate compositions was that the presence of noncrystallizing diluent increases the mobility of crystallizable components in the interlamellar regions.

Upon the examination of the DSC traces, double melting peaks were observed for the annealed 70/30 and 85/15 blends of PEEK/PEI. The small endotherm was found at annealed temperature. Lustiger, et al. [18] also observed two endotherms for the samples that annealed at temperatures above T_g.

4.2 Tensile Strength and Elongation-to-Fracture

In an attempt to find the correlationship with mechanical properties with friction and wear test results of PEEK/PEI blend composites, the tensile tests and fracture toughness tests were performed. Compact specimens (see Appendix A for geometry) were machined out of the molded plaque to measure the fracture toughness of the pure PEEK and PEI. However the specimens were too thin; i.e., the specimen of the PEI buckled and shortly after fractured and the specimen of the PEEK buckled in spite of a small crack at the notch. Therefore, the results of the fracture toughness tests were omitted and only the tensile test results were presented in this section.

The dog-bone shaped specimens were used for the tensile test of the PEEK, PEI, and 50/50 blend of PEEK and PEI. The experimentally obtained values of the yield

strengths and elongation-to-breaks are listed in Table 6. The representative stress-displacement responses exhibited by three different blends are shown in Fig. 8. The PEI specimens exhibited the highest yield strength and the lowest elongation-to-fracture. After the yield strength the PEI specimens formed a small neck and ruptured. The PEEK displayed a short strain-softening followed by an extended neck formation at constant stress level. The 50/50 blend had a similar mean value of the yield strength to that of the PEEK and the longest elongation-to-break among those three different compositions. The stress-displacement curve of the 50/50 blend exhibited some fluctuations after its yield point. The reduction of the cross-sectional area or the neck formation which is referred to as the strain softening resulted in a decrease of the stress level. The increase in stress represents the strain hardening which occurred as the necked region was further elongated. As the stress level increased due to the strain hardening, another neck developed at another weak region. This process of the strain softening followed by the strain hardening recurred until the entire length of the specimen was necked down. These repeated neck formation processes caused the fluctuations shown on the stress-displacement curve for 50/50 blend.

The hardness of a material is approximately three times its yield strength and the ductility is frequently quantified as the percent elongation-to-break. The term toughness is conveniently defined as the total area under the stress-strain curve. Therefore, PEI is harder, less ductile, and less tough than PEEK. From Figure 8, the 50/50 blend displays the highest toughness. However this would not be true if the PEEK specimens were quenched so that there was no crystalline regions in the PEEK specimens. Because,

TABLE 6. Tensile test results of PEEK, PEI, and 50/50 blend

	Y.S. (MPa)	Elongation-to-fracture(%)
100% PEEK†	82.1 ± 11.9[a]	60.3(26.74) ± 42.6
50/50 PEEK/PEI‡	80.0 ± 0.0	91.8(14.2) ± 127.5
100% PEI†	97.4 ± 3.8	21.5(7.61) ± 12.1

† 4 specimens were tested
‡ 2 specimens were tested
[a] Mean values and 95% confidence limits
( ) Standard deviation

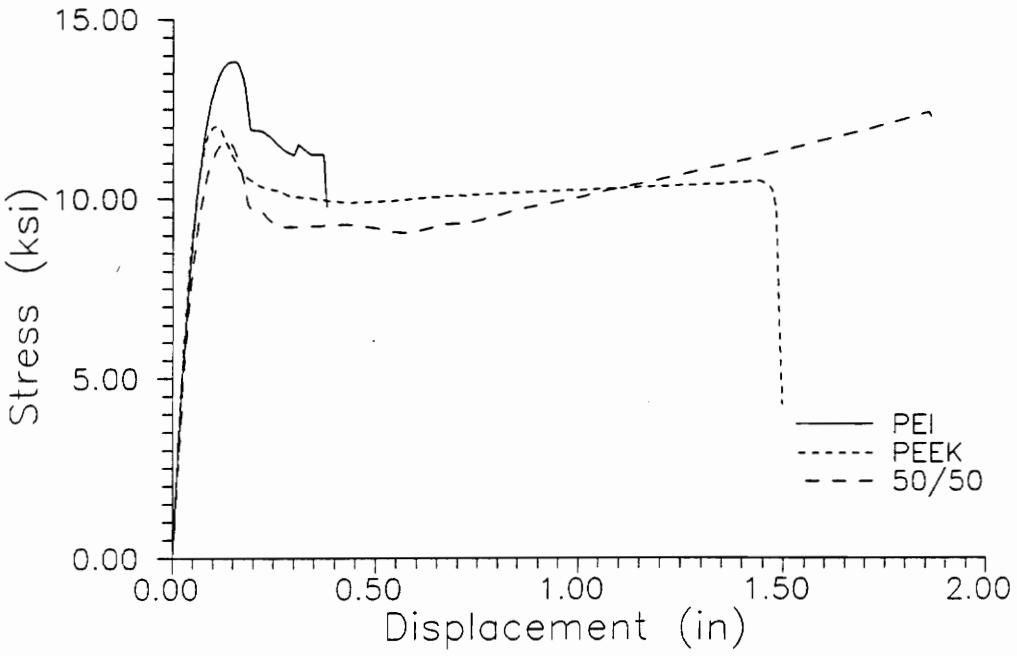

Figure 8. Representative stress-displacement curves of the PEI, PEEK, and 50/50 blend

as noted earlier, a decrease in crystallinity decreases yield strength but increases the elongation-to-break [11,18,19,20]. It is anticipated that PEEK with no crystallinity would have a longer elongation to break than the 50/50 blend did. Since PEEK and PEI are completely miscible in the amorphous state, the 50/50 blend should possess the mechanical properties that are intermediate between the properties of PEEK and PEI.

One thing that is noticeable between the PEEK and the 50/50 blend in Fig. 8 is the PEEK ruptured before any strain hardening occurred whereas the 50/50 blend experienced strain hardening. Differences between the PEEK and the 50/50 blend are the PEEK did have 27% relative crystallinity and no PEI content while the 50/50 blend was totally an amorphous material. Since the PEI broke shortly after the neck formation, the physical nature of the PEEK and the crystallinity play a dominant role in their difference. During the elongation the amorphous and coiled molecule chains of the PEEK were reoriented and aligned. However, the presence of crystals may act as crosslinks and prevent further elongation. The strain hardening of the 50/50 blend may result because of higher density of amorphous materials; consequently, molecule chains were more entangled. Therefore gradually increased force may be required to reorient those chains.

4.3 Friction

Friction responses for all tested samples were categorized into two general

classes: class A represents samples that generated wear debris and class B describes samples which did not produce wear debris. For class A samples, somewhat time dependent behavior of friction was subdivided into three stages based on experimental observations as shown in Fig. 9. A short period after sliding between steel ball and sample started, the coefficient of friction increased sharply with low frequency squeaking sounds in stage I. In the following stage II, the coefficient of friction rose more slowly and little wear debris was detected with the naked eye; and the frequency of the squeaking sound also increased. Eventually the coefficient of friction reached steady state and the wear track became very smooth.

When the sample did not produce wear debris detectable with the naked eye or even with the optical macroscope which has a maximum magnification of 80 times, the coefficient of friction remained below 0.15 and very slowly decreased. Untreated 100% PEEK did not produce any detectable wear debris at any normal test conditions and its steady state or kinetic coefficient of friction was recorded as 0.15 and 0.11 at 5N-5cm/s and 5N-15cm/s respectively. Also untreated 70/30 PEEK/PEI blend at 5N-5cm/s did not show wear debris while wear debris had been observed at the high normal load(15N) conditions. Figure 10 shows typical friction responses of the untreated 70/30 blend at three different testing conditions. Some of the untreated 70/30 and 85/15 blends and annealed 85/15 blends did not produce wear debris even at the higher normal load.

Some noticeable difference in friction response was observed with untreated 100% PEI at 15N-15cm/s and the 30% CFR of the pure PEI at high load (15N) wear conditions. For the untreated pure PEI, the steady state friction was exceptionally high,

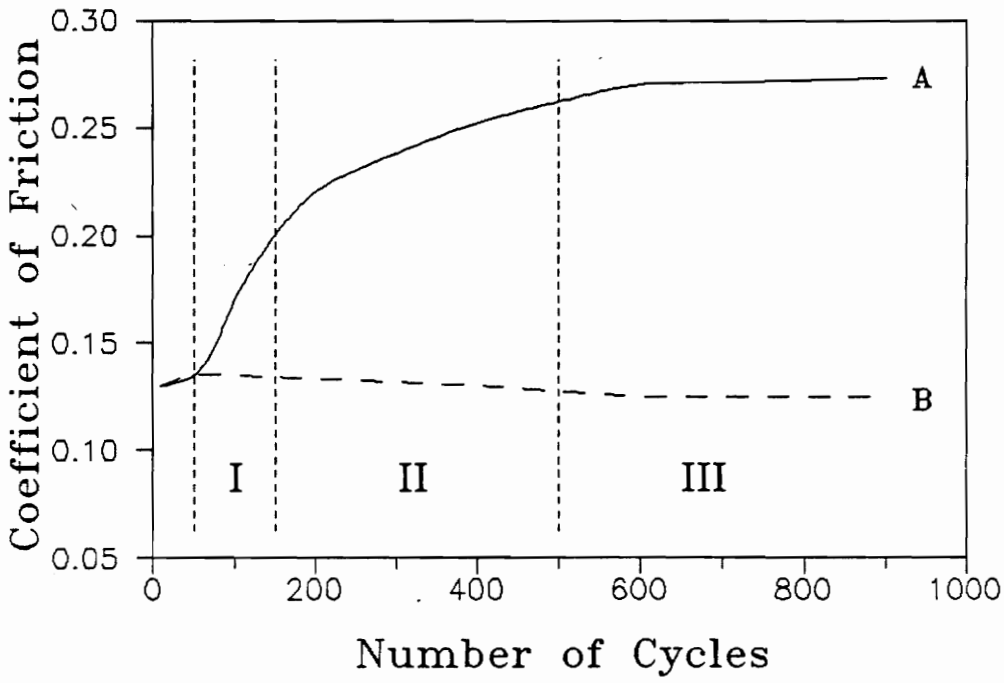

Figure 9. **Schematic representation of two categorized friction responses (solid line A represents a sample which generated wear debris and dashed line B represents the sample with no wear debris generated)**

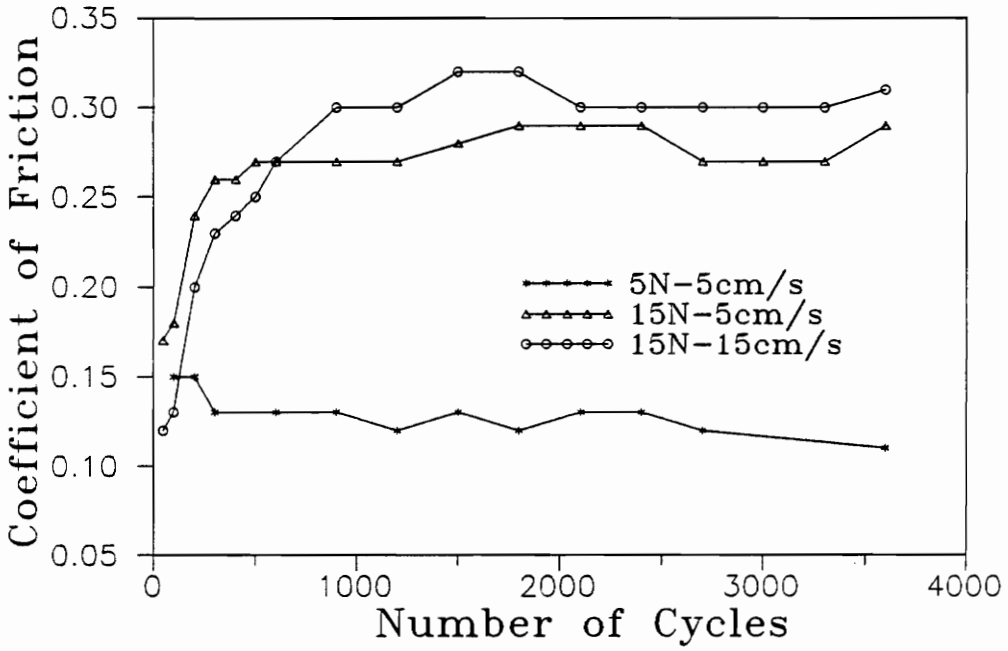

Figure 10. Coefficient of friction vs. number of cycles for the untreated 70/30 PEEK/PEI blend

i.e., 0.34. The 30% CFR PEI showed the second increase of the coefficient of friction after a short period of the steady state. Figure 11 exhibits the friction response of the 30% CFR PEI. The steady state coefficient of friction only lasted about 400 cycles and started to increase after 600 cycles. At the end of the test, 3600 cycles, the coefficient of friction reached 0.39. Other 30% CFR specimens showed a slight increase of friction after they entered the steady state stage as described in Fig. 9.

The steady state or kinetic coefficients of friction (μ_k) for all tests were averaged and are listed in Tables 7, 8, and 9. There was no significant differences among the different compositions of PEEK and PEI except the (a) untreated pure PEEK and (b) 70/30 blends at low load tests, which did not produce wear debris and (c) the untreated pure PEI at 15N-15cm/s, which had the highest wear rate among all samples. An increase in normal load and/or sliding speed also did not change μ_k. Figures 12 and 13 compare the mean values of the kinetic coefficient of friction between the untreated, annealed, and CFR specimens. The coefficient of friction as a function of the number of cycles for each test is given in Appendix D.

If the coefficient of friction at 10 cycles are compared for all tests, the 30% CFR pure PEI had the highest μ_{10} which was 0.22 ± 0.04 (95% confidence limits) while others were below 0.2. The 30% CFR PEI had the roughest surface before the test as shown in Table 10.

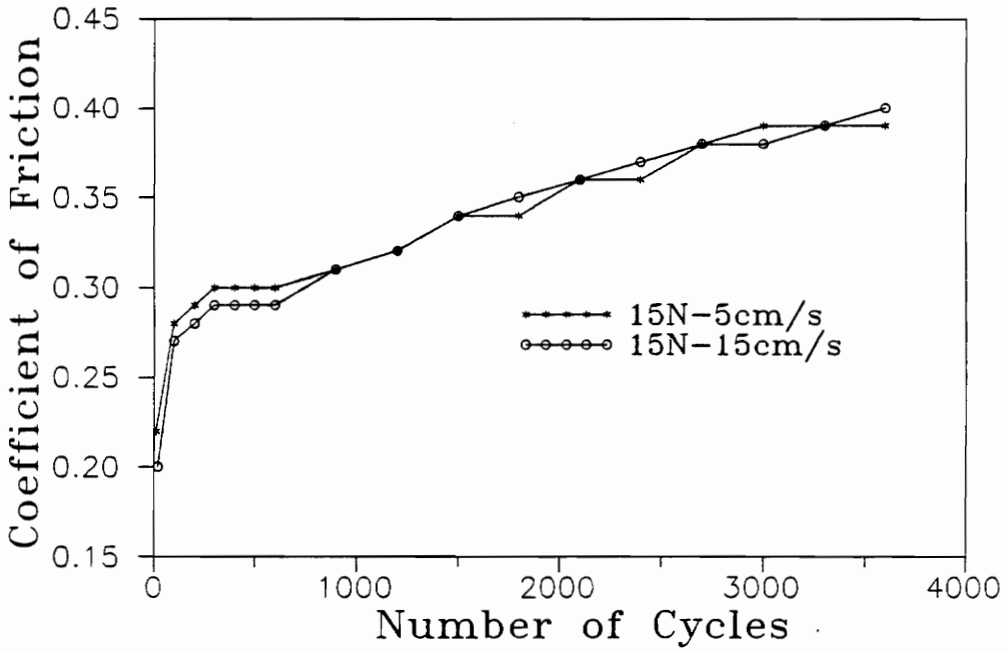

Figure 11. Coefficient of friction vs. number of cycles for the 30% CFR PEI

TABLE 7. Kinetic coefficient of frictions for the untreated specimens

PEEK/PEI	5N-5cm/s	5N-15cm/s	15N-5cm/s	15N-15cm/s
100/0	0.15 ± -	0.11 ± -	-	-
85/15(T)	-	-	0.27 ± 0.06†	0.28 ± 0.05
85/15(B)	-	-	0.28 ± 0.06	0.27 ± 0.06
70/30	0.13 ± 0.01	-	0.27 ± 0.14	0.28 ± 0.05
50/50	0.27 ± 0.05	0.28 ± 0.02	0.27 ± 0.01	0.27 ± 0.01
0/100	0.29 ± 0.04	0.27 ± 0.02	0.29 ± 0.04	0.34 ± 0.02

† Mean values and 95% confidence limits
(T) Samples which were obtained from the plaque closest to the manifold
(B) Samples which were obtained from the plaque farthest from the manifold.

TABLE 8. Kinetic coefficient of friction for the annealed specimens

PEEK/PEI	5N-15cm/s	15N-5cm/s	15N-15cm/s
85/15	-	0.23 ± 0.02†	0.27 ± 0.27‡
70/30	-	0.25 ± 0.01	0.25 ± 0.02
50/50	0.23 ± 0.01	0.23 ± 0.02	0.32 ± 0.06

† Mean values and 95% confidence limits (3 samples were measured)
‡ 2 samples were measured

TABLE 9. Kinetic coefficient of friction for the 30% CFR specimens

PEEK/PEI	15N-5cm/s	15N-15cm/s
100/0	0.24 ± 0.01†	0.23 ± 0.02
70/30	0.25 ± 0.01	0.25 ± 0.00
0/100	0.30 ± 0.01	0.29 ± 0.02
	(0.38 ± 0.02)	(0.39 ± 0.01)

† Mean values and 95% confidence limits
( ) The coefficient of friction at 3600 cycles

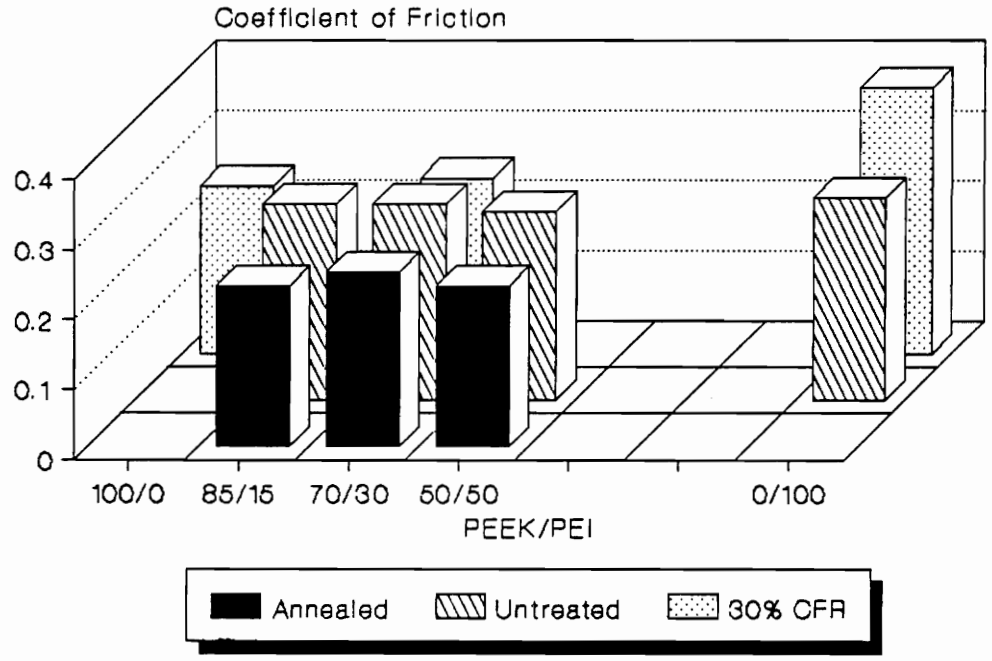

Figure 12. Comparisons of the kinetic coefficient of friction of the untreated, annealed and 30% CFR specimens at 15N-5cm/s

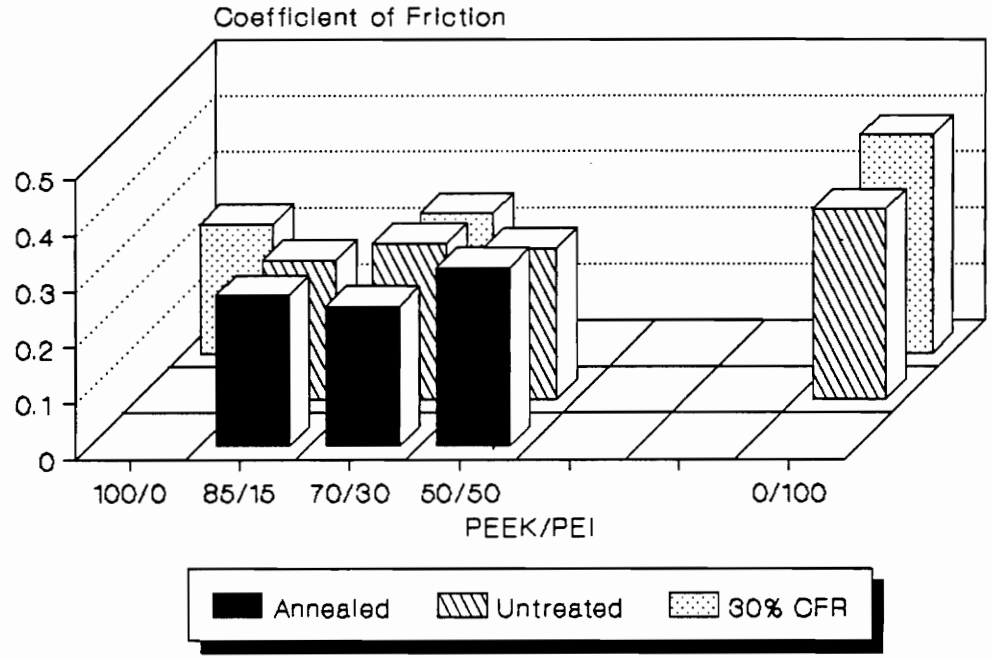

Figure 13. Comparisons of the kinetic coefficient of friction of the untreated, annealed and 30% CFR specimens at 15N-15cm/s

TABLE 10. The CLA surface roughness (Ra)‡ of the tested samples

PEEK/PEI	Untreated (μm)	Annealed (μm)	30% CFR (μm)
100/0	0.85 $\pm$ 1.91†	-	1.75 $\pm$ 0.34
85/15	0.70 $\pm$ 0.12	0.87 $\pm$ 0.40	-
70/30	0.69 $\pm$ 0.07	0.94 $\pm$ 0.21	1.01 $\pm$ 0.08
50/50	0.76 $\pm$ 0.07	0.61 $\pm$ 0.12	-
0/100	0.75 $\pm$ 0.14	-	2.77 $\pm$ 1.37

‡ Measured before the wear test
† Mean values and 95% confidence limits

4.4 Wear

The ASTM [43] definition of wear is "damage to a solid surface, generally involving progressive loss of material, due to relative motion between that surface and a contacting substance or substances." There might be a case in which no loss of material occurs and only displacement of material is present. Another case may be the net change of mass or volume from at least one of the interacting components and the observation of loose wear debris. In this paper, a net volume loss of polymer disk is measured as the wear.

The wear mechanism of PEEK consisted of the ball plowing a groove into the surface of the disk. However, there was no loss of material from the surface. At the lower load (5N) condition, PEEK did not show any wear debris under the optical macroscope. Even though there was a visible track where sliding occurred, the surface profile meter could not detect any loss of material. The load and speed were increased to determine the conditions to produce PEEK wear. At 26.4N and 25cm/s, few wear debris were observed after 3000 cycles. And at 26.4N and 50cm/s, one test showed few wear debris while the other did not. However the PEEK wear groove had large adjacent ridges which were formed by plastic deformation. In some cases, the cross-sectional area of the ridges was larger than that of groove.

As the percentage of PEI in the untreated and annealed blends was increased, the wear mechanism changed from plowing to the generation of small flake-like particles after certain number of cycles. However there was a different wear mechanism in

carbon fiber reinforced samples. As the steel ball started to slide against the disk, the polymer matrix formed a film-like layer over the sliding surface before 30-50 cycles as shown in Fig. 14. Then this layer was slowly worn out after few hundreds of cycles. Broken carbon fibers also observed in the wear debris.

Table 11, 12 and 13 give the average wear rates and 95% confidence limits for the untreated, annealed, and 30% CFR. In Appendix E, the average cross-sectional areas of the wear track for each tested samples are listed. Upon examining the wear rates in Table 11, 12 and 13, it is noted that either increase in normal load or sliding speed increased the wear rates. The two-way analysis of variance (ANOVA) indicated that the increase in load by a factor of 3 resulted in more than twice as much wear than occurred when the sliding speed increased by a factor of 3 for the untreated pure PEI and 50/50, and the annealed 50/50 blend. The highest increase in the wear rate as a function of load was observed in the untreated 50/50 blend. In order to study the effect of the variance of load and/or sliding speed on the mean wear rates, the untreated pure PEI and 50/50 blend were subjected to the two-way analysis of variance (ANOVA). As a result, the effect of load change was the highest and the interaction between load and speed had as much as effect on wear as did the sliding speed, and they were all significant at 0.05 level of significance. The results of the statistical analysis are in Appendix F. For the untreated 70/30, 85/15 blend and all of the annealed and 30% CFR compositions, there was no significant effect of sliding speed on wear rate except the annealed 50/50 blend at high load condition.

Figure 15 shows wear rates of the untreated, annealed, and 30% CFR at the high

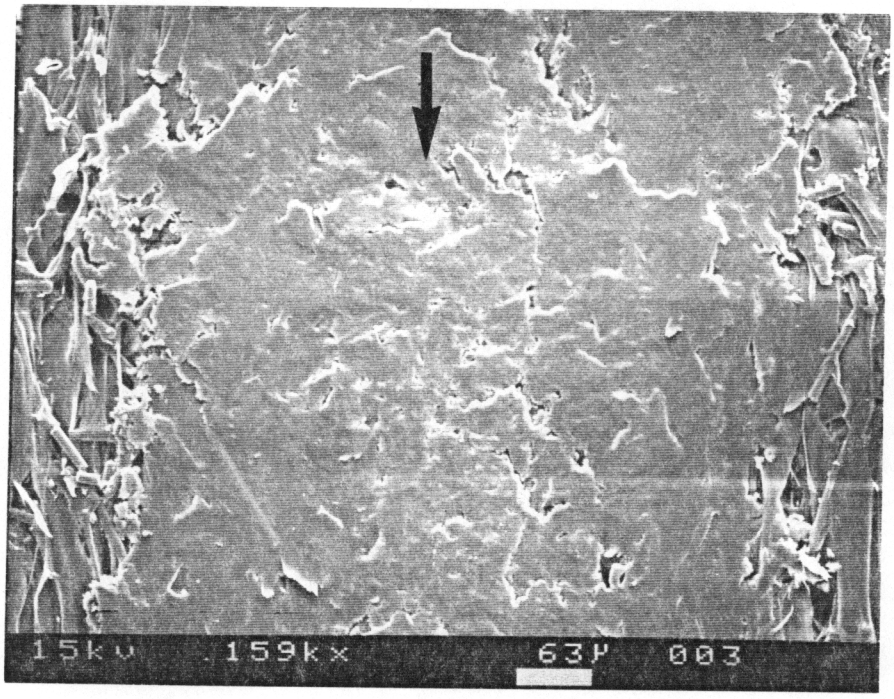

Figure 14. **SEM micrograph of the sliding surface of 30% CFR PEEK (15N-15cm/s at 3600 cycles; arrow indicates sliding direction)**

TABLE 11. Wear rates (μm^2/cycle) for the untreated specimens

PEEK/PEI	5N-5cm/s	5N-15cm/s	15N-5cm/s	15N-15cm/s
100/0	0.0	0.0	-	-
85/15(T)	-	-	0.405 ±0.620†	0.379 ±1.626
85/15(B)	-	-	0.226 ±0.283	0.181 ±0.216
			0.298±0.163‡	0.280 ±0.248‡
70/30	0.0	-	1.227 ±1.725	1.429 ±0.936
50/50	0.777 ±0.050	1.295 ±0.939	3.128 ±0.465	65.986 ±9.762
0/100	2.289 ±0.142	2.384 ±0.035	8.898 ±1.190	66.122 ±13.688

† Mean values and 95% confidence limits
‡ Mean values and 95% confidence limits for all of 85/15(T) and 85/15(B)
(T) Samples which were obtained from the plaque closest to the manifold
(B) Samples which were obtained from the plaque farthest from the manifold.

TABLE 12. Wear rates (μm^2/cycle) for the annealed specimens

PEEK/PEI	5N-15cm/s	15N-5cm/s	15N-15cm/s
85/15	-	0.169 ± 0.065†	0.286 ± 1.105
70/30	-	0.443 ± 0.196	0.328 ± 0.144
50/50	0.492 ± 0.142	1.132 ± 0.482	10.192 ± 5.182

† Mean values and 95% confidence limits

TABLE 13. Wear rates (μm^2/cycle) for the 30% CFR specimens

PEEK/PEI	15N-5cm/s	15N-15cm/s
100/0	0.243 ± 0.137†	0.504 ± 0.368
70/30	0.287 ± 0.149	0.298 ± 0.154
0/100	1.414 ± 0.224	1.581 ± 0.847

† Mean values and 95% confidence limits

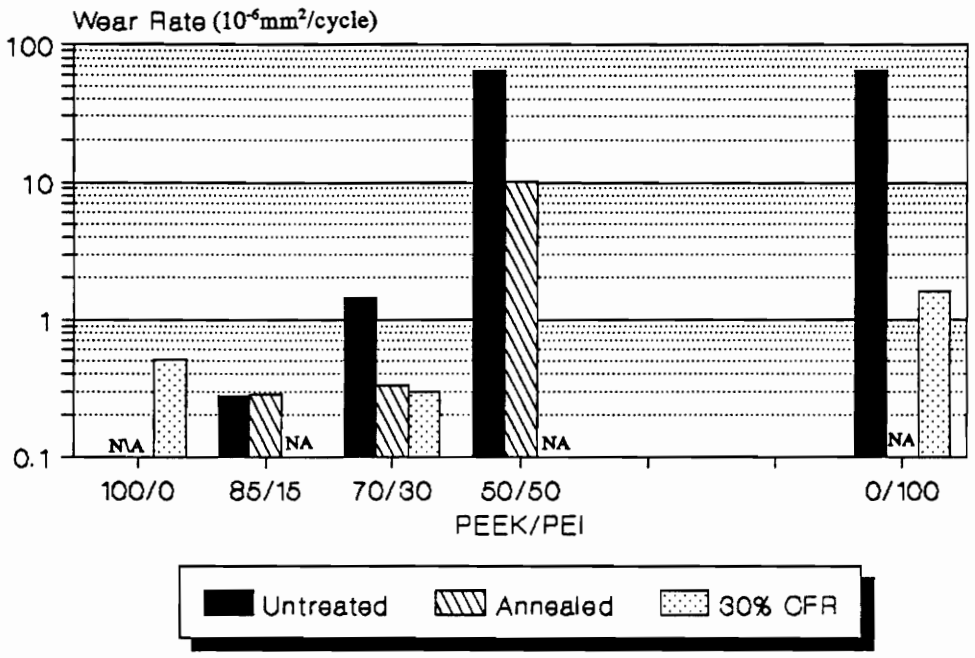

NA = not available

Figure 15. Wear rate comparisons at 15N-15cm/s

load and high sliding speed (15N-15cm/s). Two regimes of wear were observed. The first regime includes the PEEK/PEI compositions of 100/0, 85/15, and 70/30 which all exhibited very low wear rate and had a higher weight percentage of PEEK than that of PEI. For 50/50 blend and pure PEI which are classified as the second regime compositions, the wear rate was 46 times that of the first regime compositions. The difference of the wear rates between 50/50 and pure PEI was insignificant from the Duncan's multiple range test (see Appendix F.) Figure 16 shows wear rate at the high load and low sliding speed (15N-5cm/s) and it is recognized from Fig. 16 that the relationship between PEI composition from 30 to 100 percent and wear rate is linear. Even though the linearity still exists in the annealed and the 30% CFR compositions, the Duncan's multiple range test (Appendix F) indicated no significant difference between 100/0, and 70/30 compositions.

The reductions of wear rates by annealing and carbon fiber reinforcement were observed in all PEEK/PEI compositions except the pure PEEK shown in Table 14. The 30% CFR PEEK had an increase in wear rate and coefficient of friction. The reduction of wear rate was more pronounced as PEI composition increased. Generally for both high speed and low speed, the effects of the carbon fiber reinforcement on the wear rate were greater than those caused by the increase in crystallinity by annealing.

4.5 Scanning Electron Micrographs

The worn surface of the tested specimens were examined in a Scanning Electron

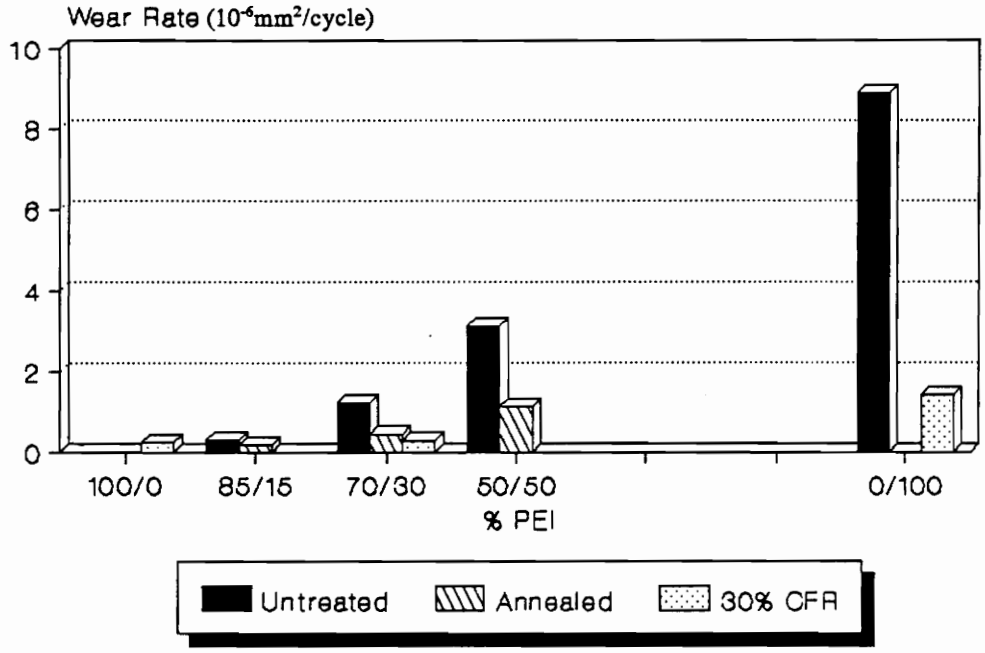

Figure 16. Wear rate comparisons at 15N-5cm/s

TABLE 14. Wear rate reduction factor over the untreated blends by annealing and CF reinforcement

		Untreated (PEEK/PEI)			
		85/15†	70/30	50/50	0/100
Annealed	15N-5cm/s	1.8	2.8‡	2.8	-
	15N-15cm/s	1.0	4.4	6.5	-
30% CFR	15N-5cm/s	-	4.3	-	6.3
	15N-15cm/s	-	4.8	-	41.8

† Averaged all of 85/15(T) and 85/15(B) and calculated
‡ Mean values and 95% confidence limits

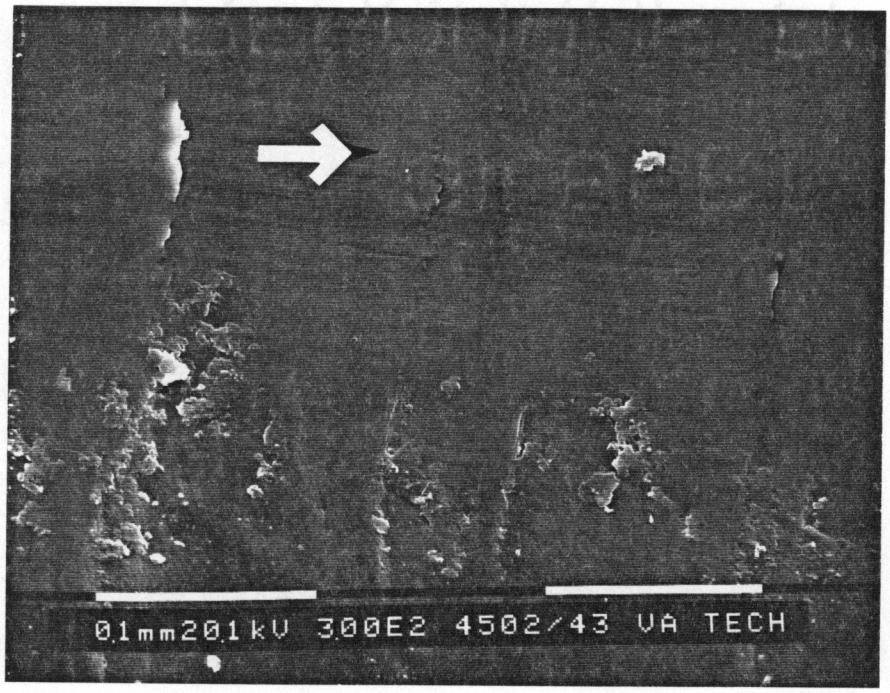

(a)

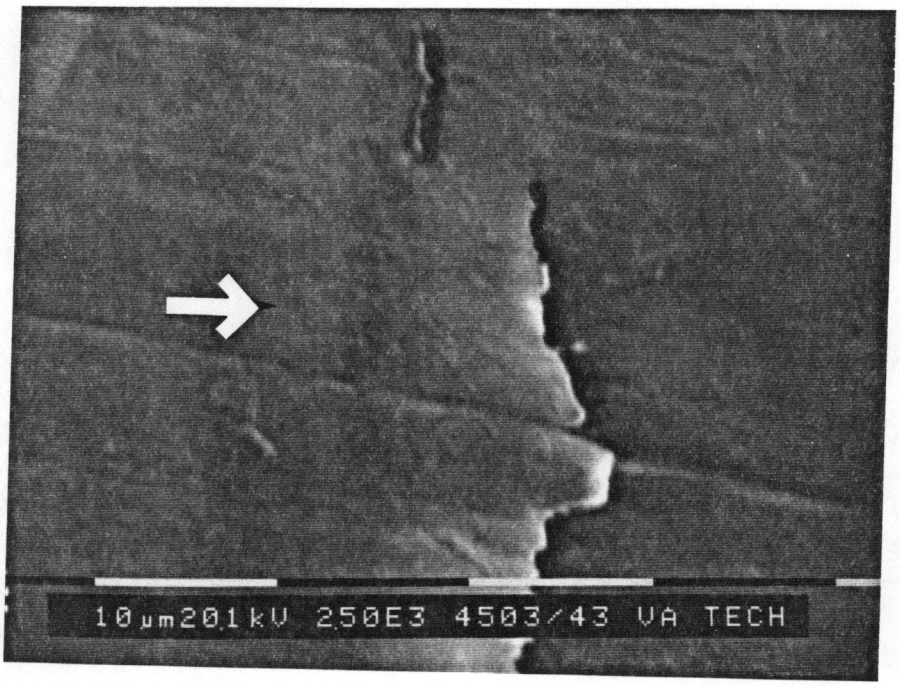

(b)

Figure 17. **SEM micrographs of wear track of the untreated PEEK**
a) wear track at 3800 cycles (5N-15cm/s)
b) magnified view of (a) (arrow indicates sliding direction)

Microscope (SEM). All specimens were coated with gold to a thickness of 200 Å. In addition to the SEM micrographs, a few optical micrographs were taken.

Figure 17(a) shows several cracks that were perpendicular to the sliding direction on the untreated 100% PEEK at 5N-15cm/s. These cracks were not due to tensional stress field generated by sliding of steel ball but were produced by normal and tangential forces exerted from the ball pushing the polymer forward to the sliding direction. The magnified picture (Fig. 17b) clearly illustrates that the left side region respect to the crack line was lifted up and overlaid to the right. Figure 18 shows similar appearance that was found in the untreated 70/30 and annealed 85/15. This pushed-forward like deformations were very periodic and observed in all specimens except the CFR specimens.

The PEEK tested under severe conditions (20N-35cm/s), which generated few wear debris, showed many bulges in the track as shown in Fig. 19. The bulges are either wear debris embedded into the wear track by the sliding action or incipient wear particles about to become loose from the surface. Figure 20(a) shows similar bulges that were found in the wear track of the untreated 85/15 PEEK/PEI blend. Under the optical macroscope, these bulges rather look like tearing of surface as shown in Fig. 20(b).

The wear tracks of the CFR were different from those observed in the cases of the untreated and annealed specimens. Matrix was smeared out and smoothed the wear track. This film-like layer had already been present when cross-sectional wear area was measured at 600 cycles or early stage of the sliding. Figure 21 displays incipient wear particles of the 30% CFR similar to those predicted by the delamination theory, which

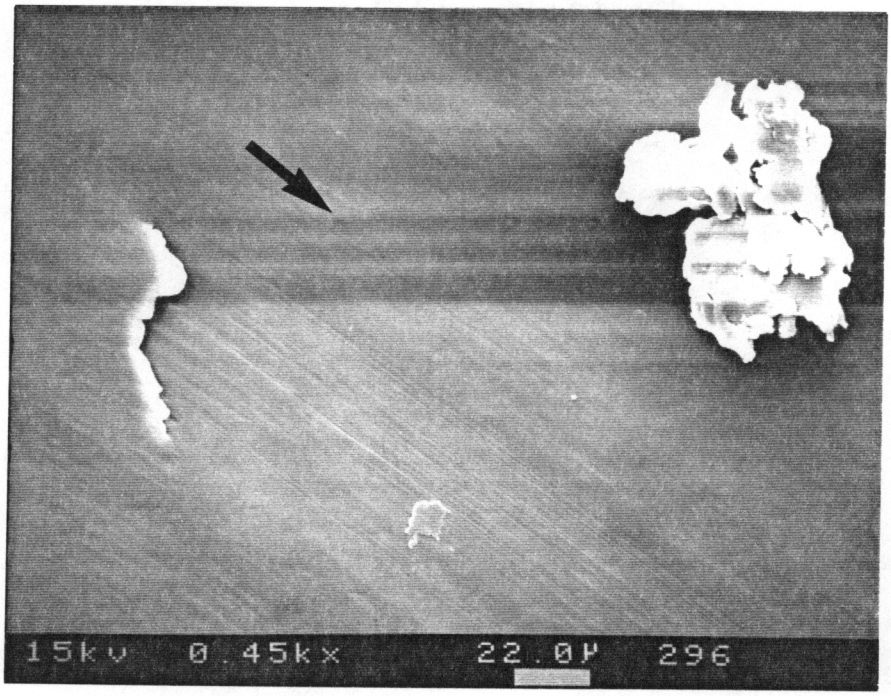

(a)

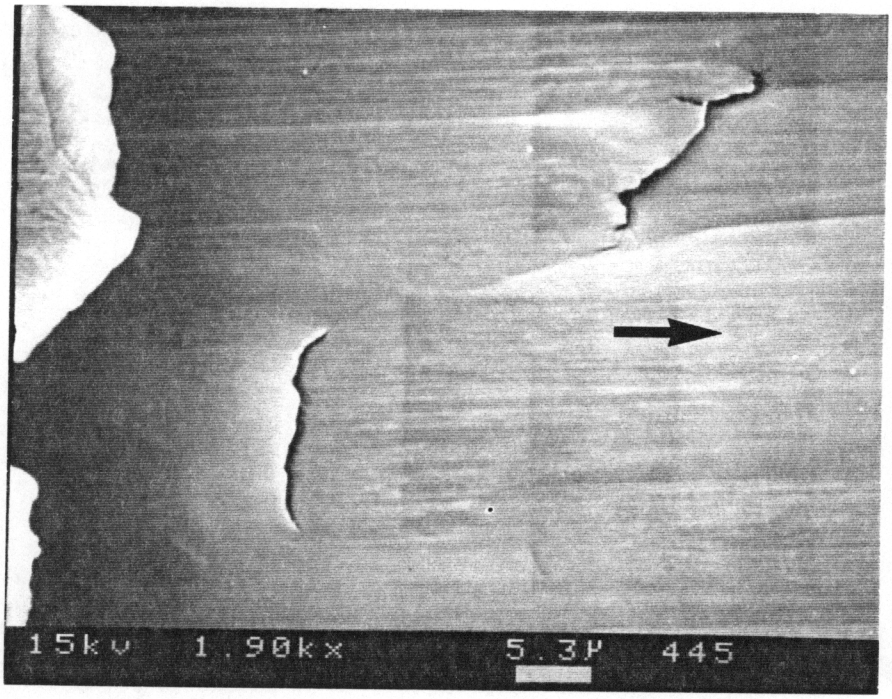

(b)

Figure 18. **SEM micrographs of the pushed forward cracks, arrow indicates a sliding direction a) Untreated 70/30 at 3600 cycles (5N-15cm/s) b) Annealed 85/15 at 3600 cycles (15N-15cm/s)**

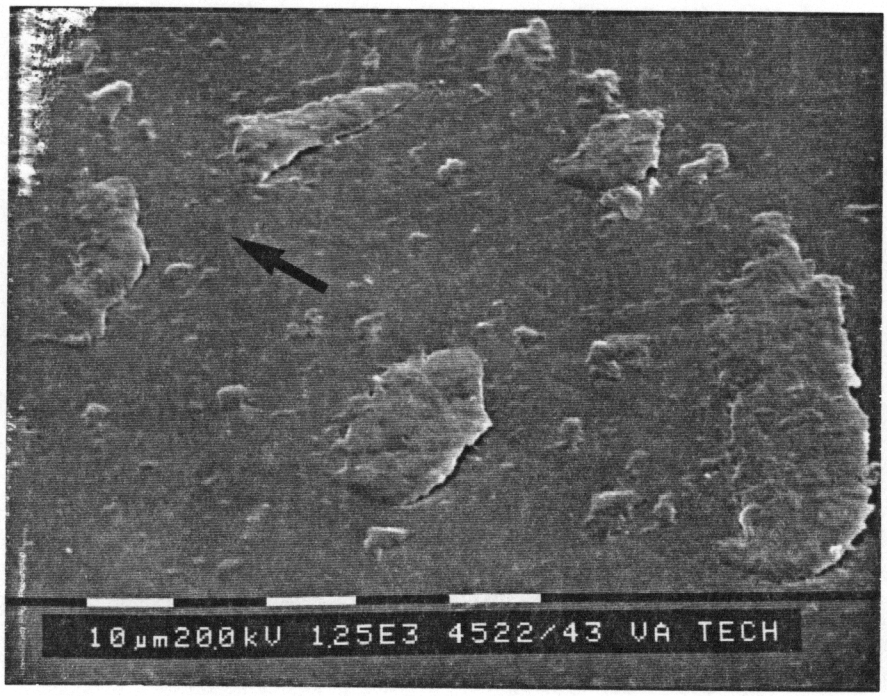

Figure 19. **SEM micrograph of wear track of the untreated PEEK, arrow indicates a sliding direction (20N-35cm/s)**

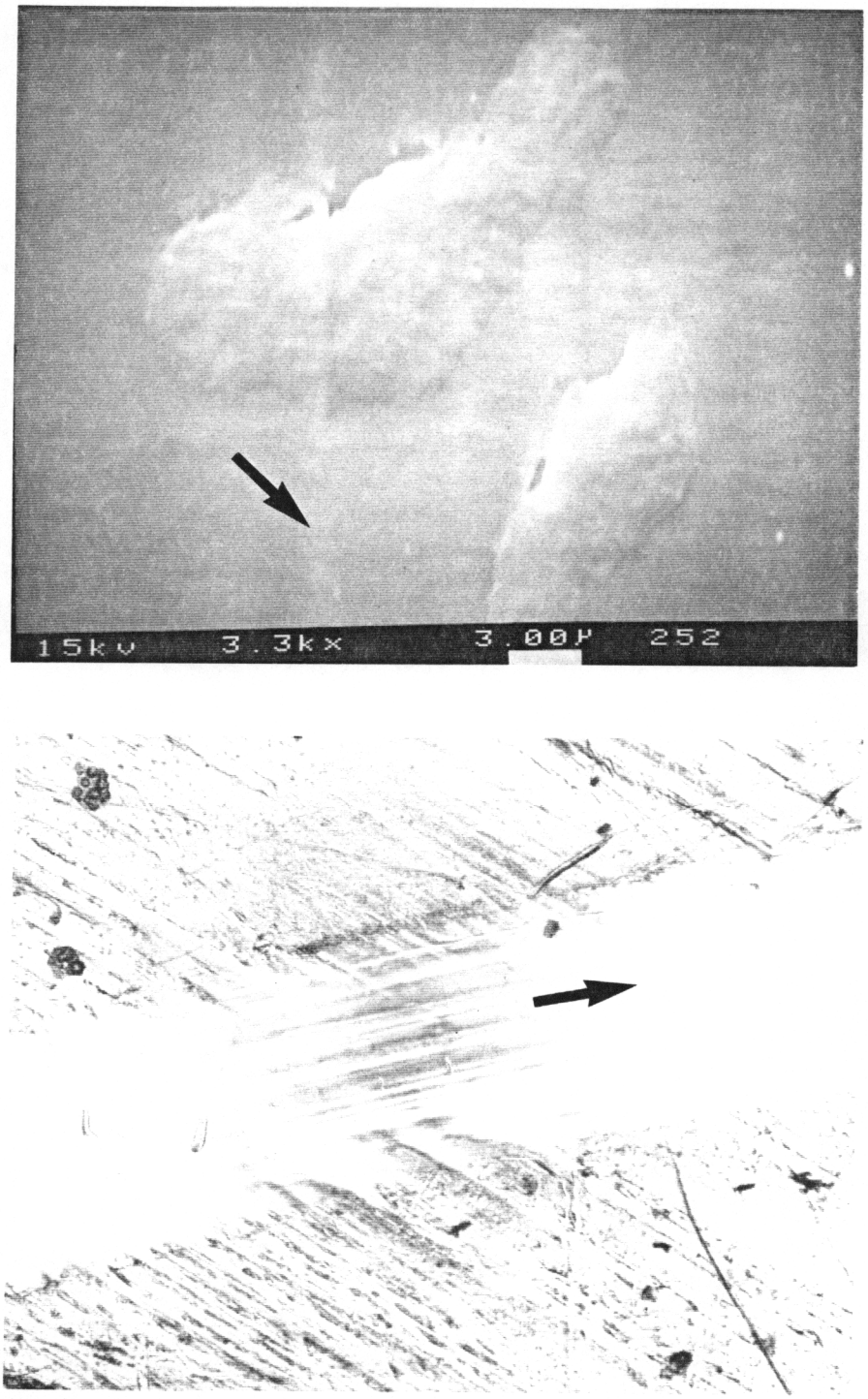

(a)

(b)

Figure 20. **The bulges on the wear track of the untreated 85/15 blend**
a) SEM micrographs of wear track at 1200 cycles (15N-5cm/s)
b) Optical micrograph of wear track at 1200 cycles (15N-5cm/s, 80x)

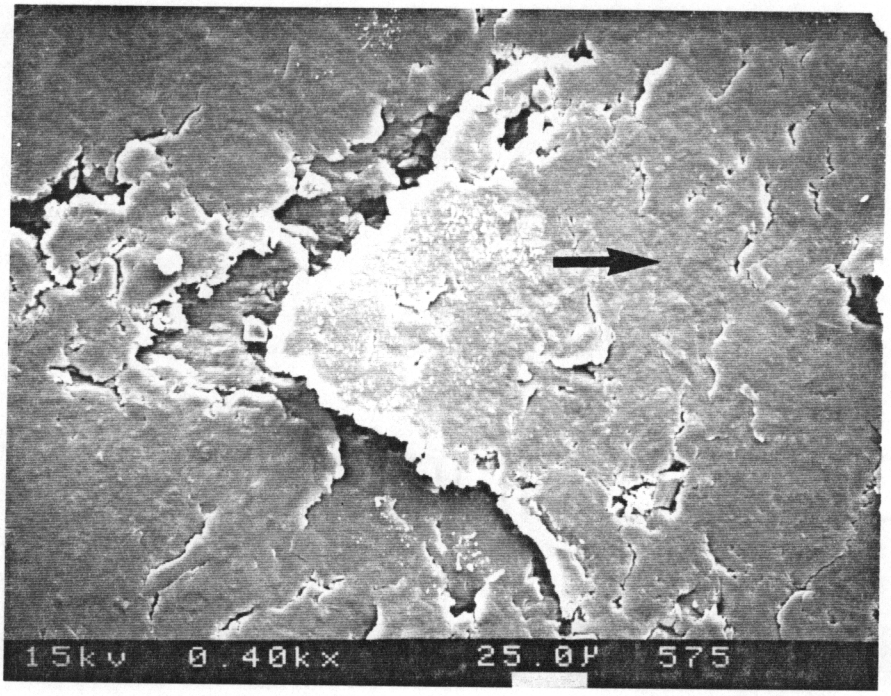

(a)

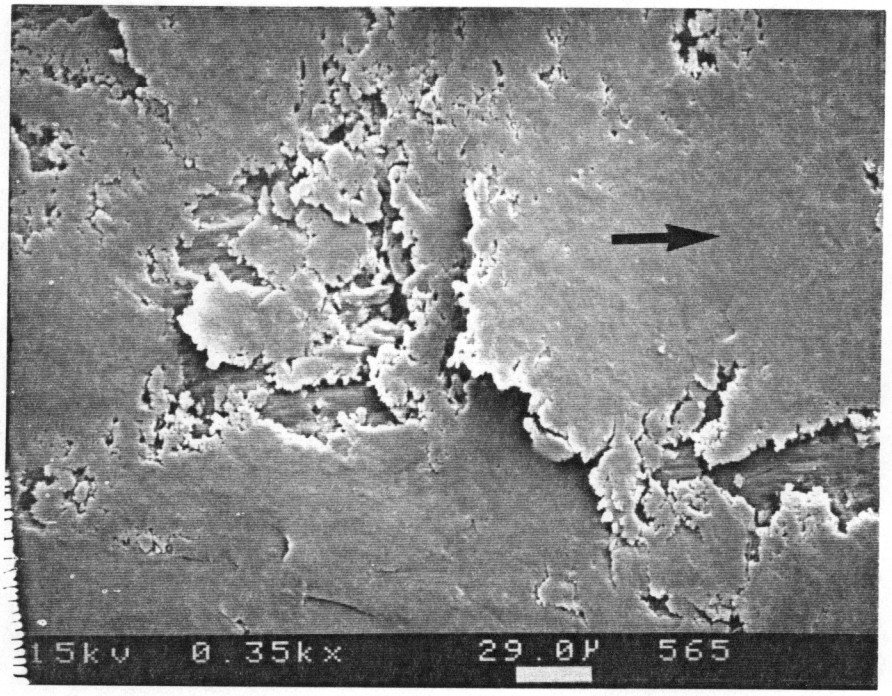

(b)

Figure 21. **SEM micrographs of wear track of the 30% CFR at 3600 cycles a) 70/30 blend (15N-5cm/s) b) 100% PEI (15N-15cm/s) (arrow indicates direction of sliding)**

is pulling away from the tail part. It had been observed that the short carbon fibers were highly aligned along the mold filled direction. The damages on the wear track were somewhat dependent on the fiber direction. Figure 22 (a) and (b) exhibit that a long axis(↕) of the wear scar(Y) had tendency to follow the fiber direction. A plausible explanation for this tendency is that the matrix film-like layer overlaid the fibers thinner and it may tend to get thicker between the fibers. Also the hardness of the fiber induced a high stressed area over the fiber whereas area over the matrix cushioned the stress. Therefore film-like layer over the fiber was worn quicker than that over the matrix. Figure 23(a) depicts the damaged spot which revealed the fibers on the surface and shows a broken fibers being embedded into the film-like layer. The pulled-out fibers tend to align with the sliding direction. This spot is either an area where the film-like layer had not smeared into yet or where a large fragment had peeled off. Figure 23(b) is a magnified view of the broken fibers that are shown in Fig. 23(a). The fibers were pulverized and were about to debond from the matrix.

One big surprise from the SEM micrographs is the discovery of very few wear debris of PEEK tested under normal conditions. which was not seen in the optical macroscope. Figures 24 (a) and (b) reveal the very thin plate-like wear debris found inside wear track. The shape of wear debris found at the outside of the wear track is flake-like and agglomerated. Figures 25 to 28 show wear debris of all compositions. There are no dramatic differences in their appearances.

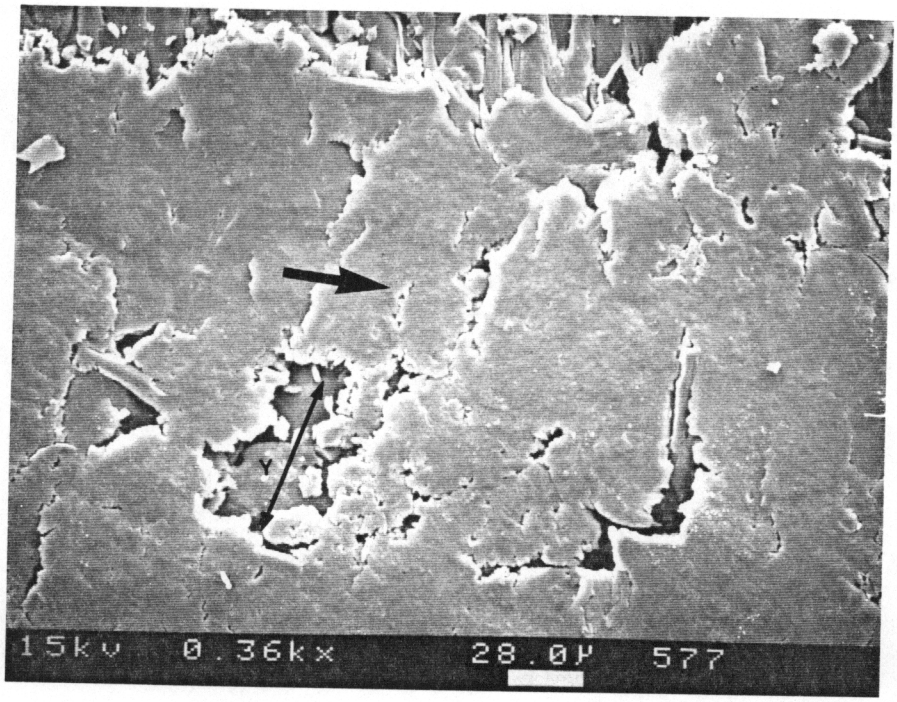

(a)

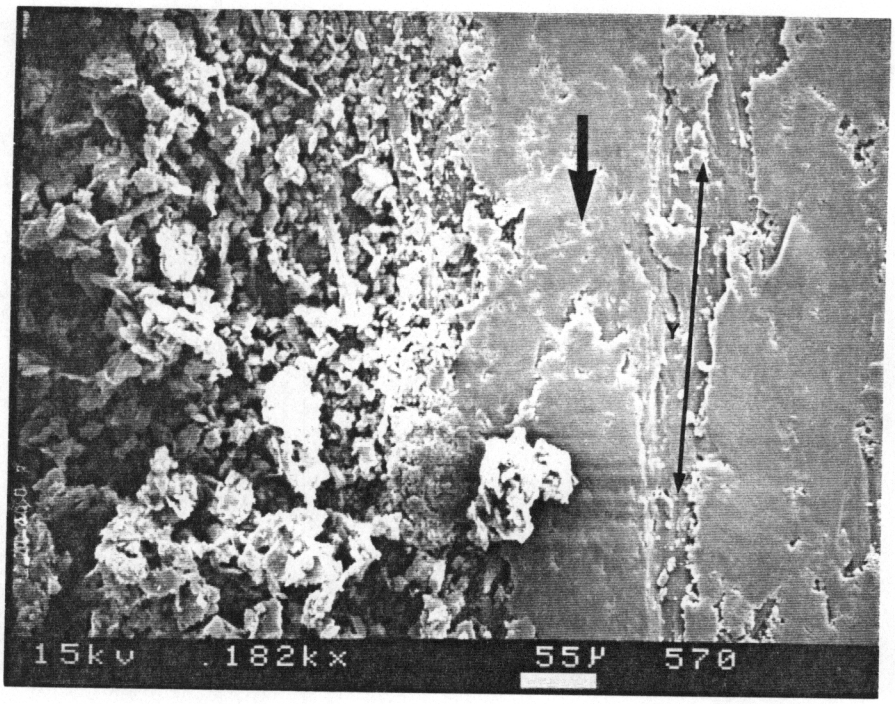

(b)

Figure 22. **SEM micrographs of wear track of the 30% CFR at 3600 cycles a) 70/30 blend (15N-5cm/s), sliding is perpendicular to fiber direction b) 100% PEI (15N-15cm/s), sliding is parallel to the fiber direction**

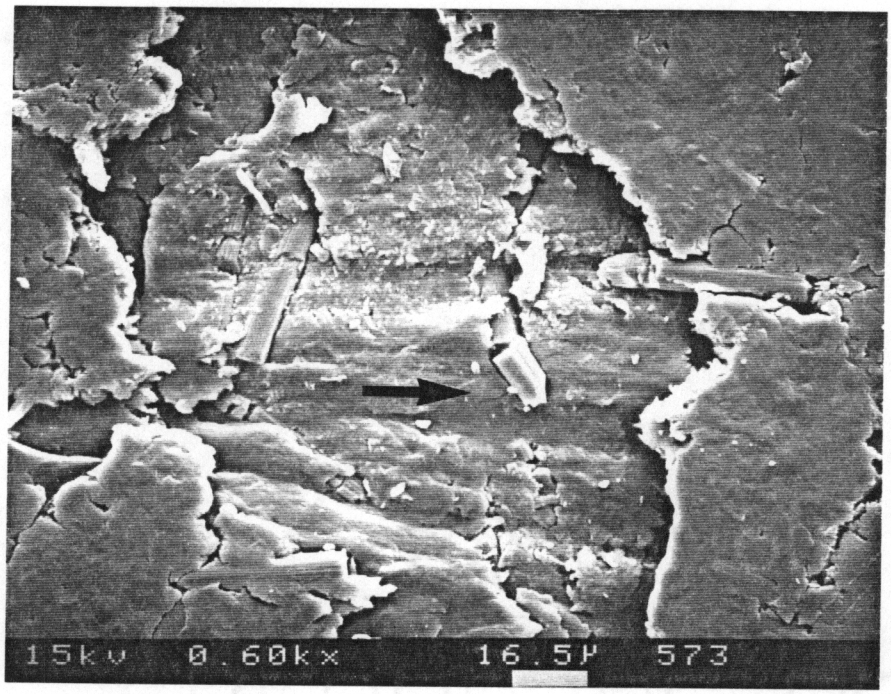

(a)

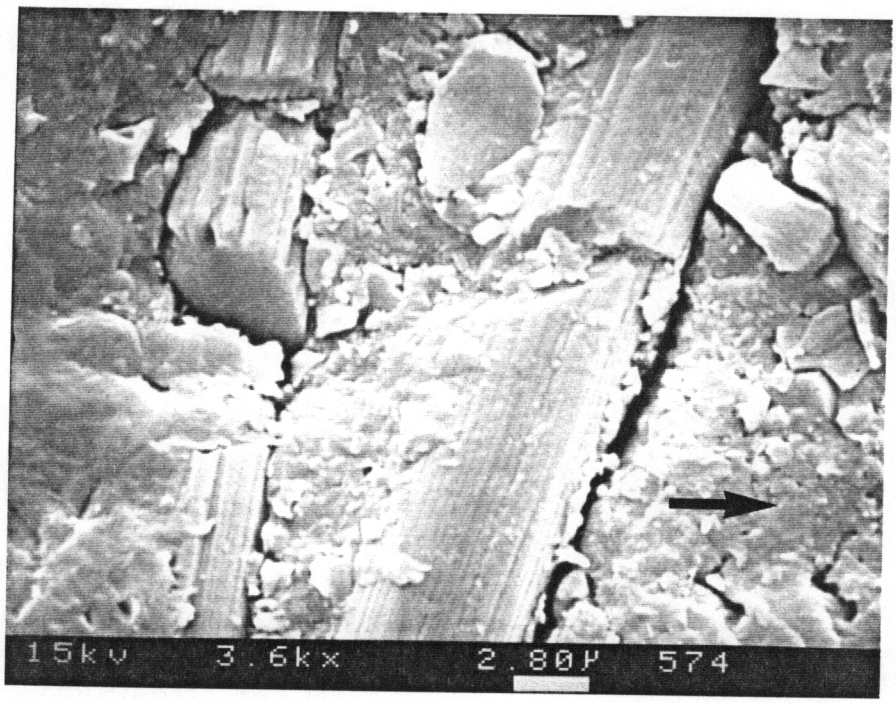

(b)

Figure 23. **SEM micrographs of wear track of the damaged spot of 30% CFR a) 70/30 blend at 3600 cycles (15N-15cm/s) b) magnified view of (a), arrow indicates direction of sliding**

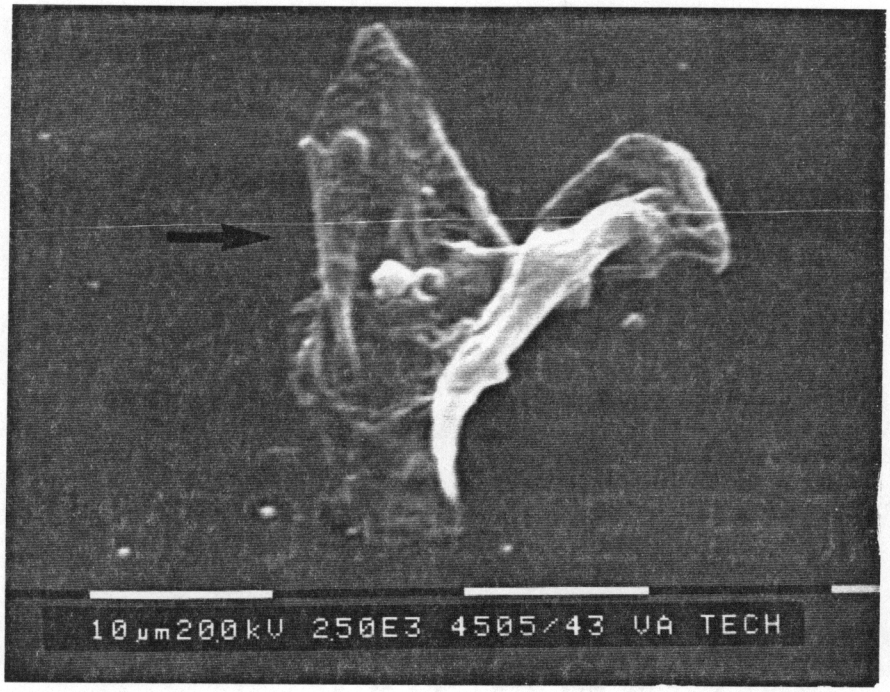

(a)

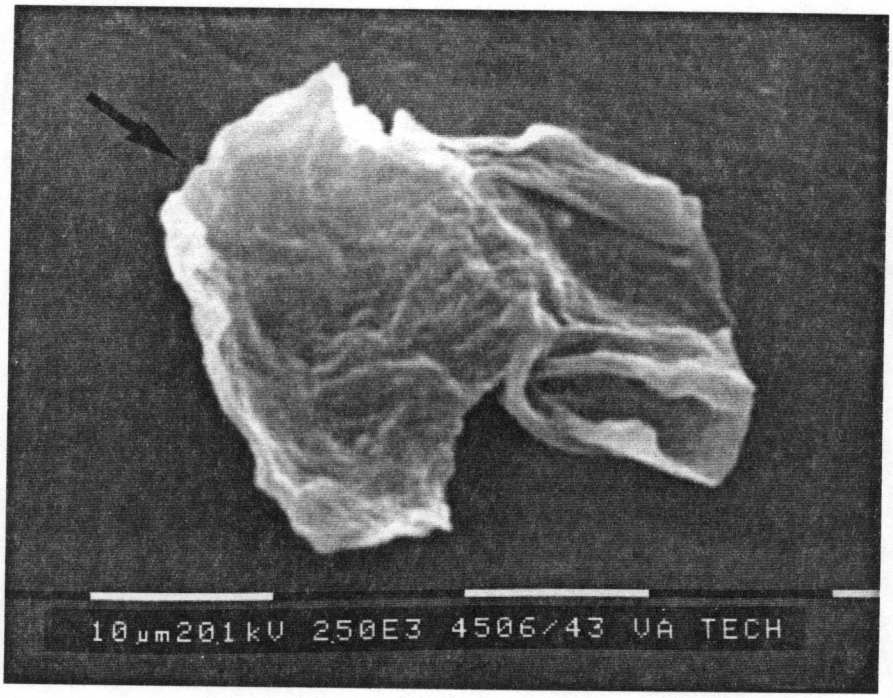

(b)

Figure 24. **SEM micrograph of wear track of the untreated PEEK (a) and (b) at 3800 cycles (5N-15cm/s)**

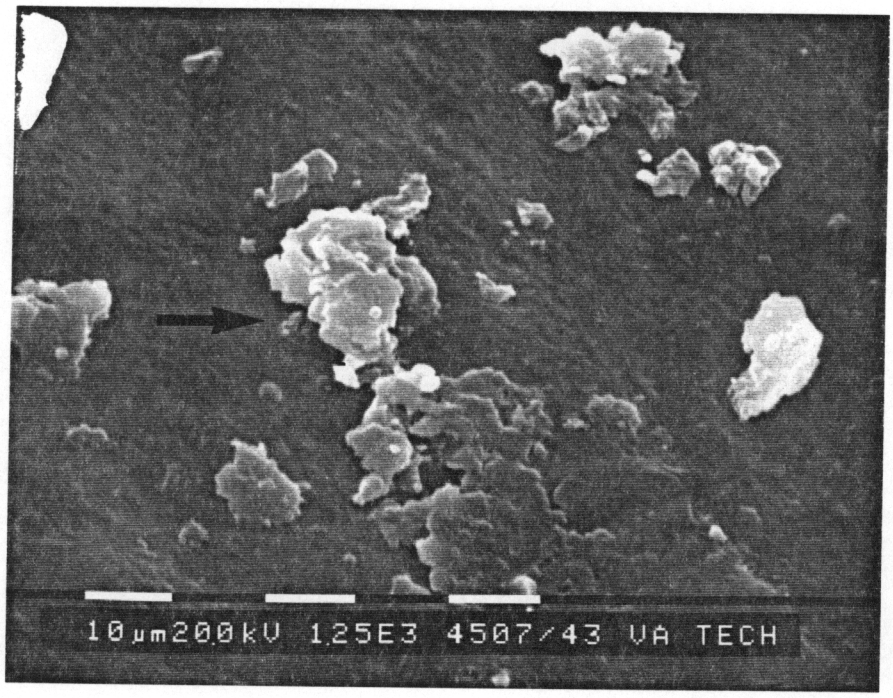

(a)

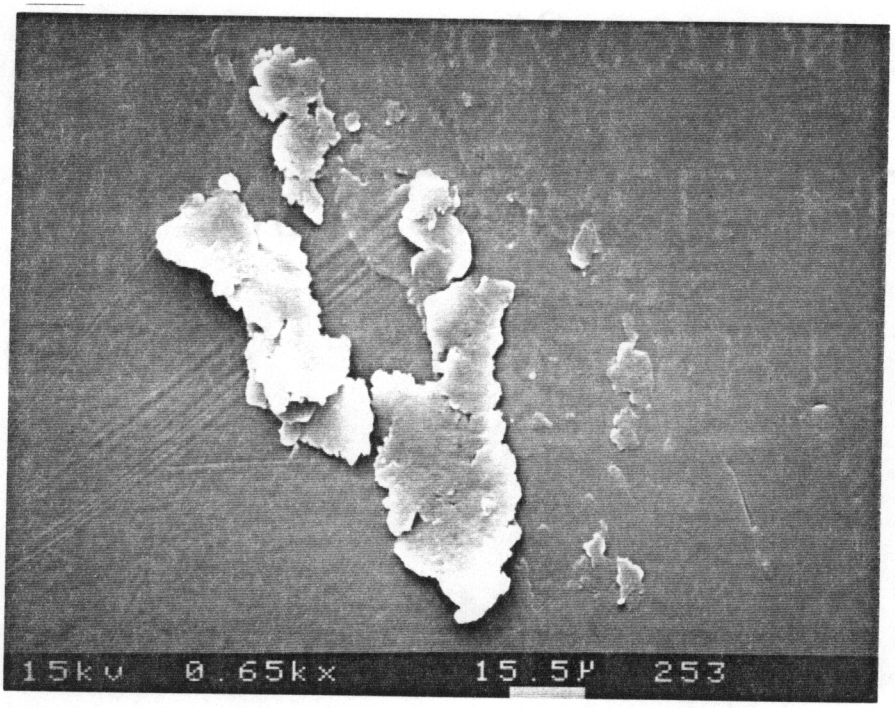

(b)

Figure 25. **SEM micrographs of wear debris**
a) Untreated PEEK (5N-15cm/s)
b) Untreated 85/15 blend (15N-5cm/s)

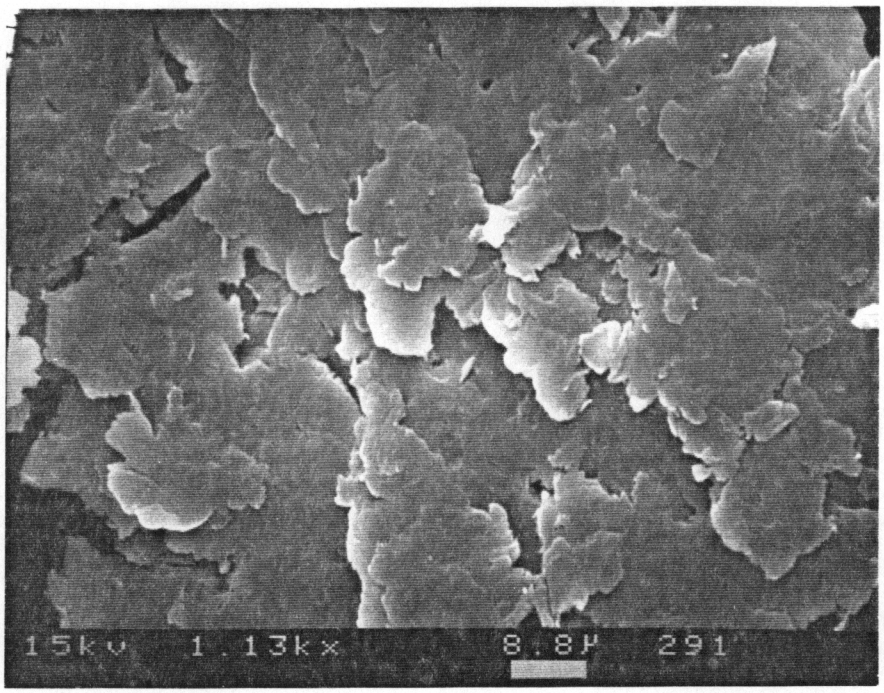

(a)

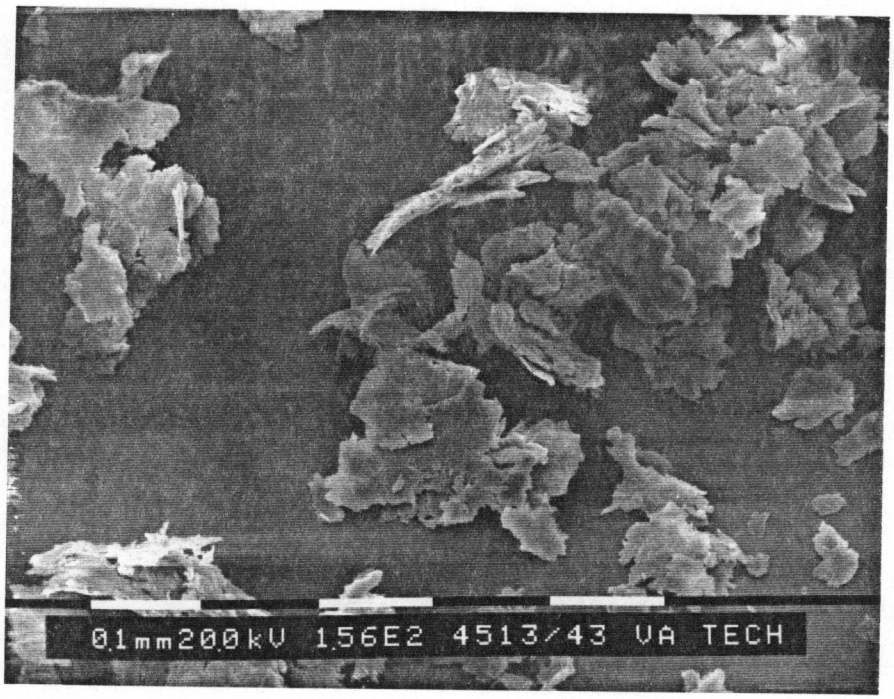

(b)

Figure 26. **SEM micrographs of wear debris**
a) Untreated 70/30 blend (15N-5cm/s)
b) Untreated 85/15 blend (5N-15cm/s)

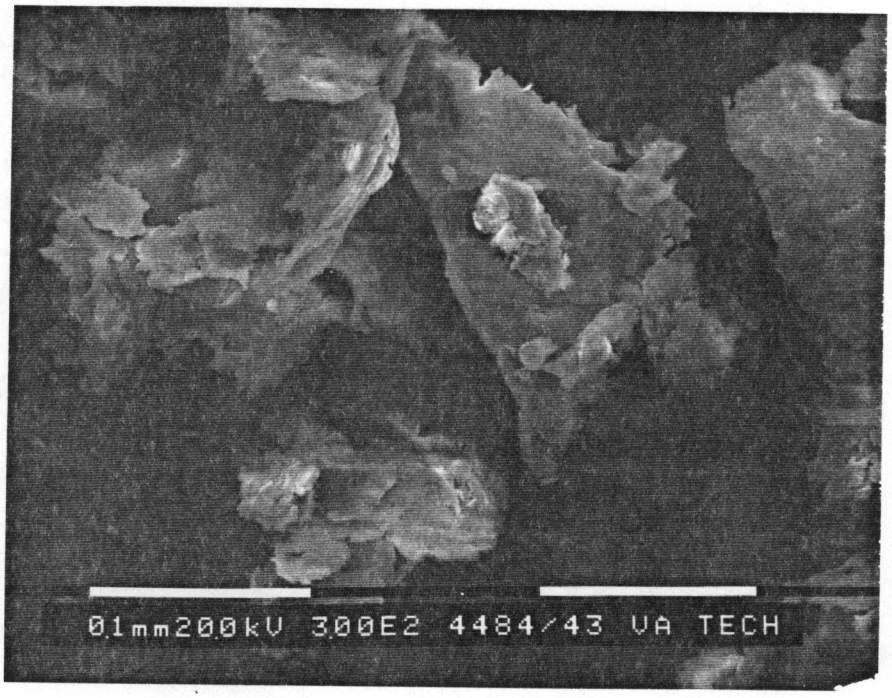

(a)

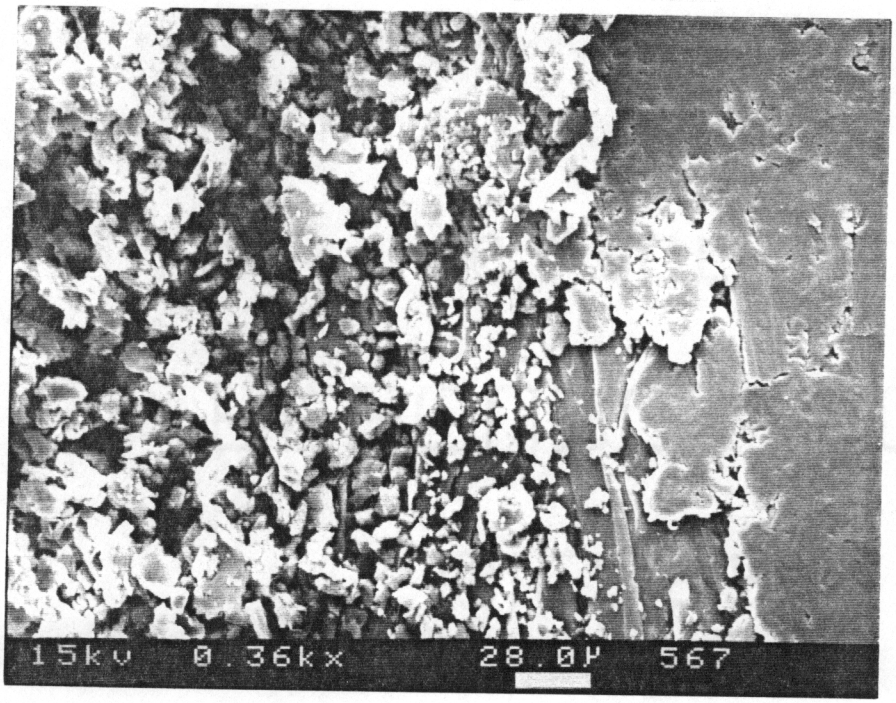

(b)

Figure 27. **SEM micrographs of wear debris**
a) Untreated PEI (15N-5cm/s)
b) 30% CFR PEI (15N-15cm/s)

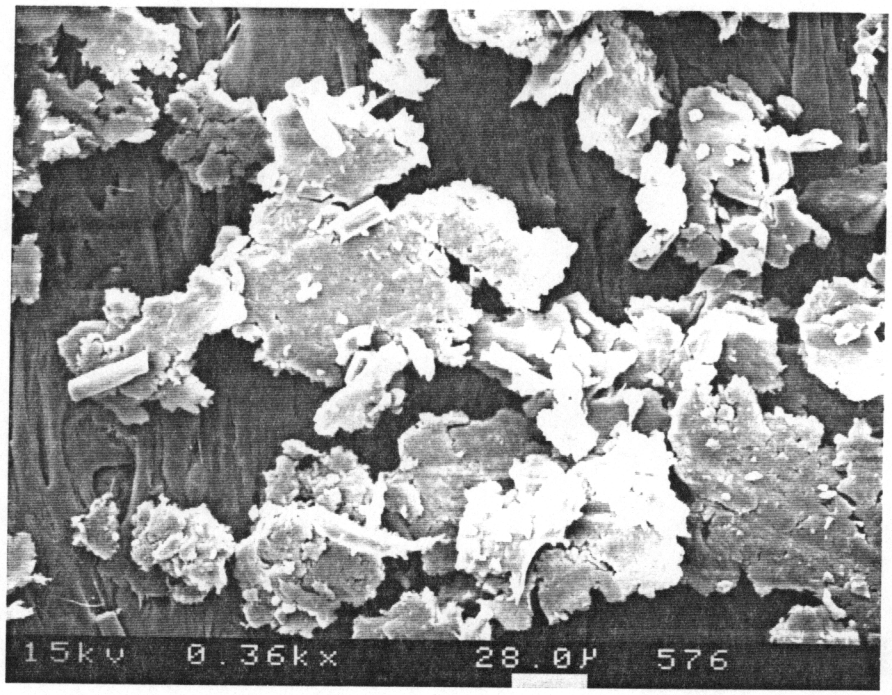

(a)

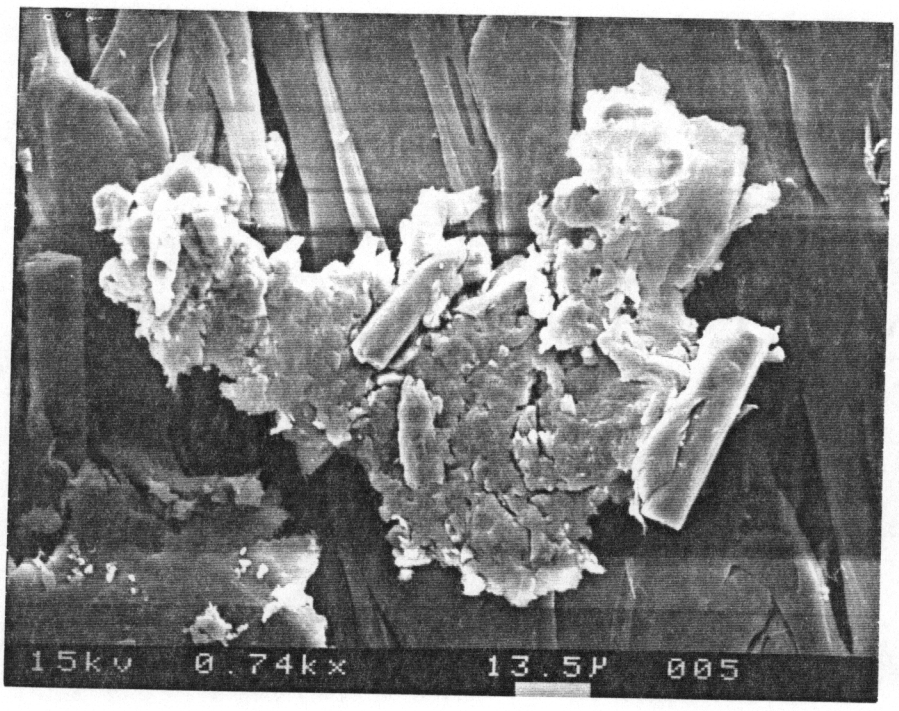

(b)

Figure 28. **SEM micrographs of wear debris**
a) 30% CFR 70/30 blend (15N-5cm/s)
b) 30% CFR PEEK (15N-5cm/s)

5. DISCUSSION

In this chapter, the tribological behaviors of PEEK/PEI polymers and composites were examined with the morphological and mechanical test results obtained in the previous chapter.

5.1 Wear

Based on the observations of the optical macroscope and SEM micrographs, the wear track of the untreated and the annealed polymer specimens had many periodic plastic deformations and that of the CFR composite specimens formed film-like layer over the track. Therfore, different wear processes have been hypothesized for the untreated and the annealed polymer specimens and for the CFR composite specimens. The assumed wear process of the untreated and the annealed samples is as follows. When the steel ball starts to slide over the polymer disk, the load that is exerted from the ball is carried by the asperities of the disk. The pressure on the asperities increases rapidly to the plastic flow and therefore junctions are formed at asperity tips. Even though there is relative motion between the surface during sliding, the junctions adhere

and shear occurs within the asperities. As this process of the removal of asperities by adhesion continues, a smooth sliding track is formed. The adhesive transfer occurs without measurable wear of the polymer disk. The evidence of the adhesive transfer is shown in Fig. 29. After a wear groove is initiated the wear debris adhered to the steel ball slowly removes. This is shown in Fig. 30 (a) and (b). Therefore some loosely attached fragments are seen on the ball in these figures.

When a track becomes smooth, subsequent sliding of the ball induces a shear of material or piling up ahead of the ball and the wave pattern is produced as shown in Fig. 31. Several repeating cycles cause more deformation and thus generate subsurface cracks (see Fig. 32a) by fatigue wear mechanism and they propagate to the surface. Loose wear debris are formed as shown in Fig. 32b and they are squashed by the ball and carried to the next pushed-forward deformed area (Fig. 32c). At the next cycle, the wear debris is pressed into the surface and piled up in front of the ball as shown in Fig. 31. After material breaks off, the above process will repeat. Figures 33, 34, and 35 show the wear track of the untreated 85/15 blend tested under 15N load and 15cm/s sliding speed. The smooth track was observed up to 1200 cycles and the wavy deformation was seen from 1200 cycles to the end of the test.

The hypothetical wear process of the CFR materials is as follows. The surface matrix which is over the fibers easily smears out under the applied normal and tangential forces because of the stiffness of the carbon fibers. During the first few hundreds of cycles, the initial composite surface topography will be modified significantly by the sliding process. The sliding track will be covered up with the matrix film-like layer.

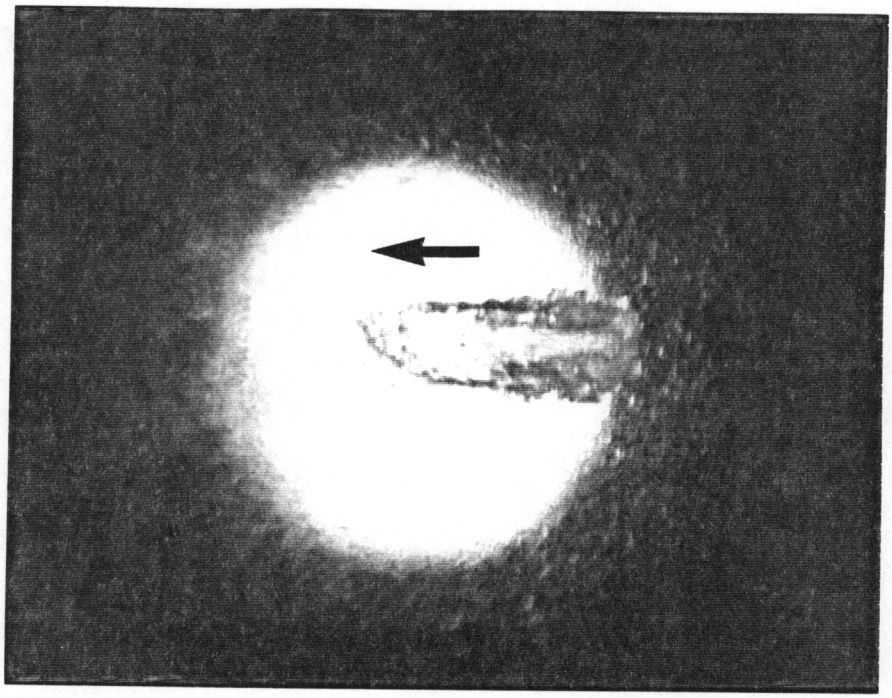

Figure 29. **Optical micrograph of the adhered wear debris on the steel ball (arrow indicates direction of disk rotation)**

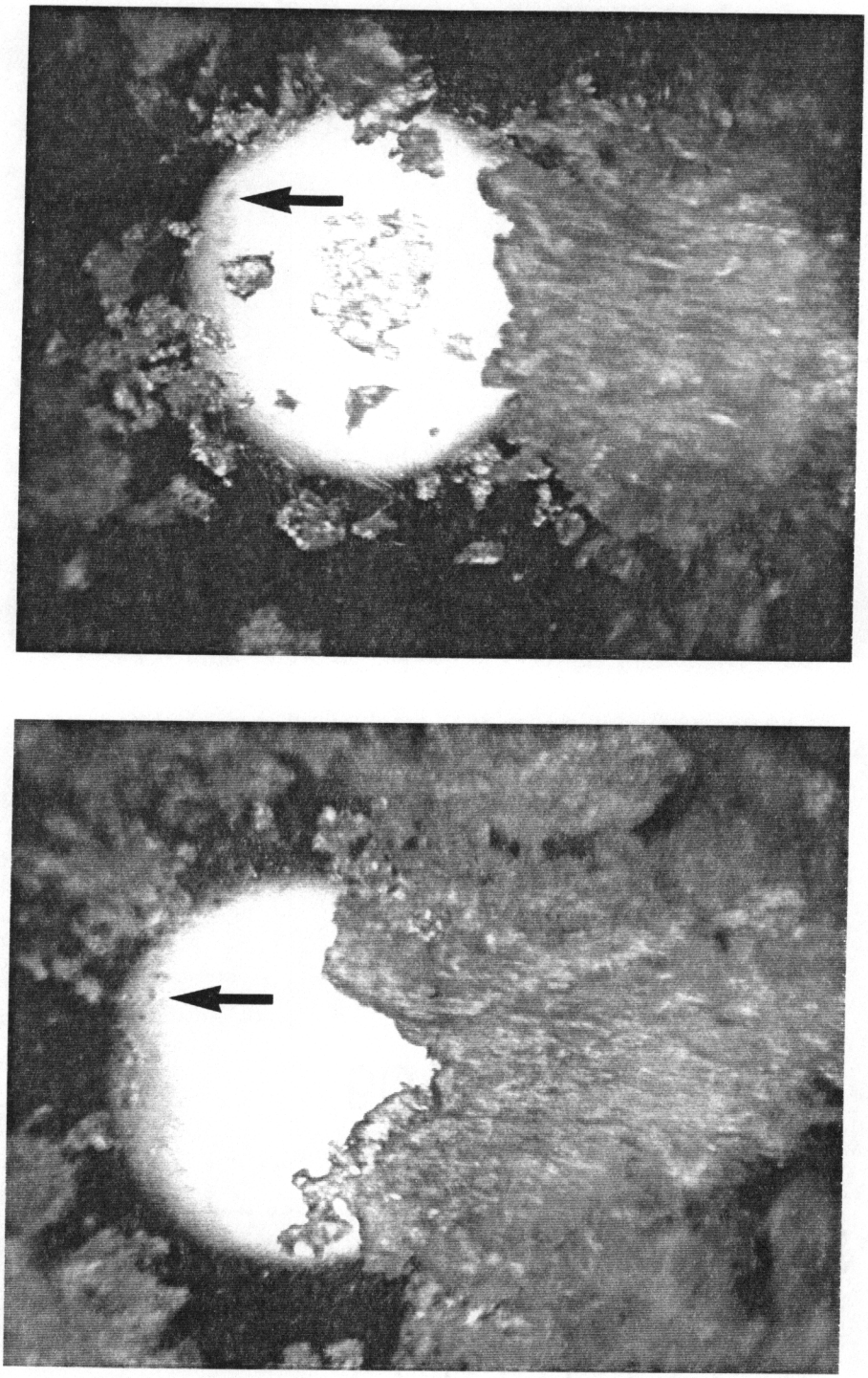

(a)

(b)

Figure 30. **Optical micrographs of the steel ball on the untreated 70/30 blend at 15N-5cm/s (arrow indicates direction of disk rotation) a) after 200 cycles b) after 600 cycles**

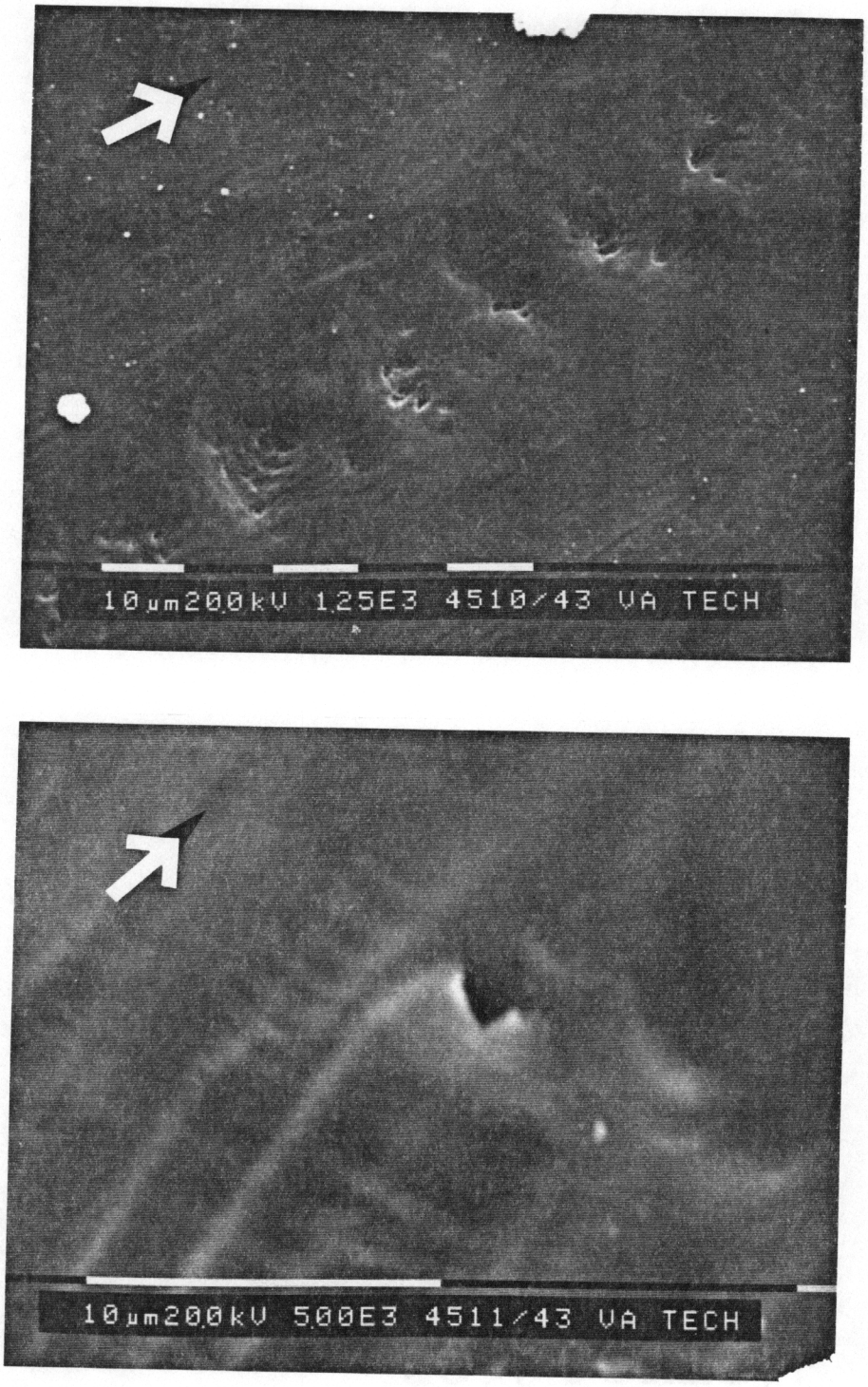

Figure 31. SEM micrograph of the wave pattern on the surface (arrow indicates direction of sliding) a) Untreated 50/50 blend (5N-15cm/s) b) magnified view of (a)

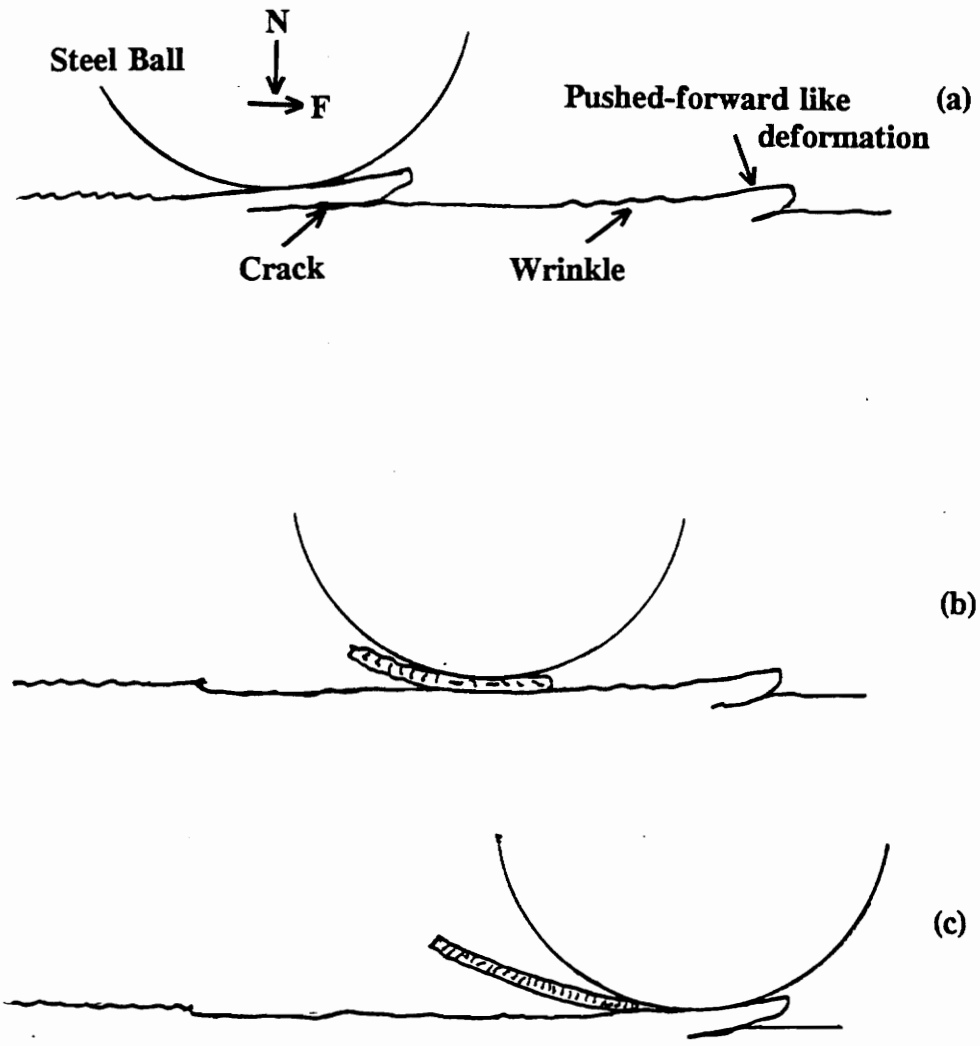

Figure 32. Schematic representation of the wear debris generation of the untreated and annealed samples (a) debris is about to brcome loose (b) loose debris is carried by ball (c) debris is seperated from the ball

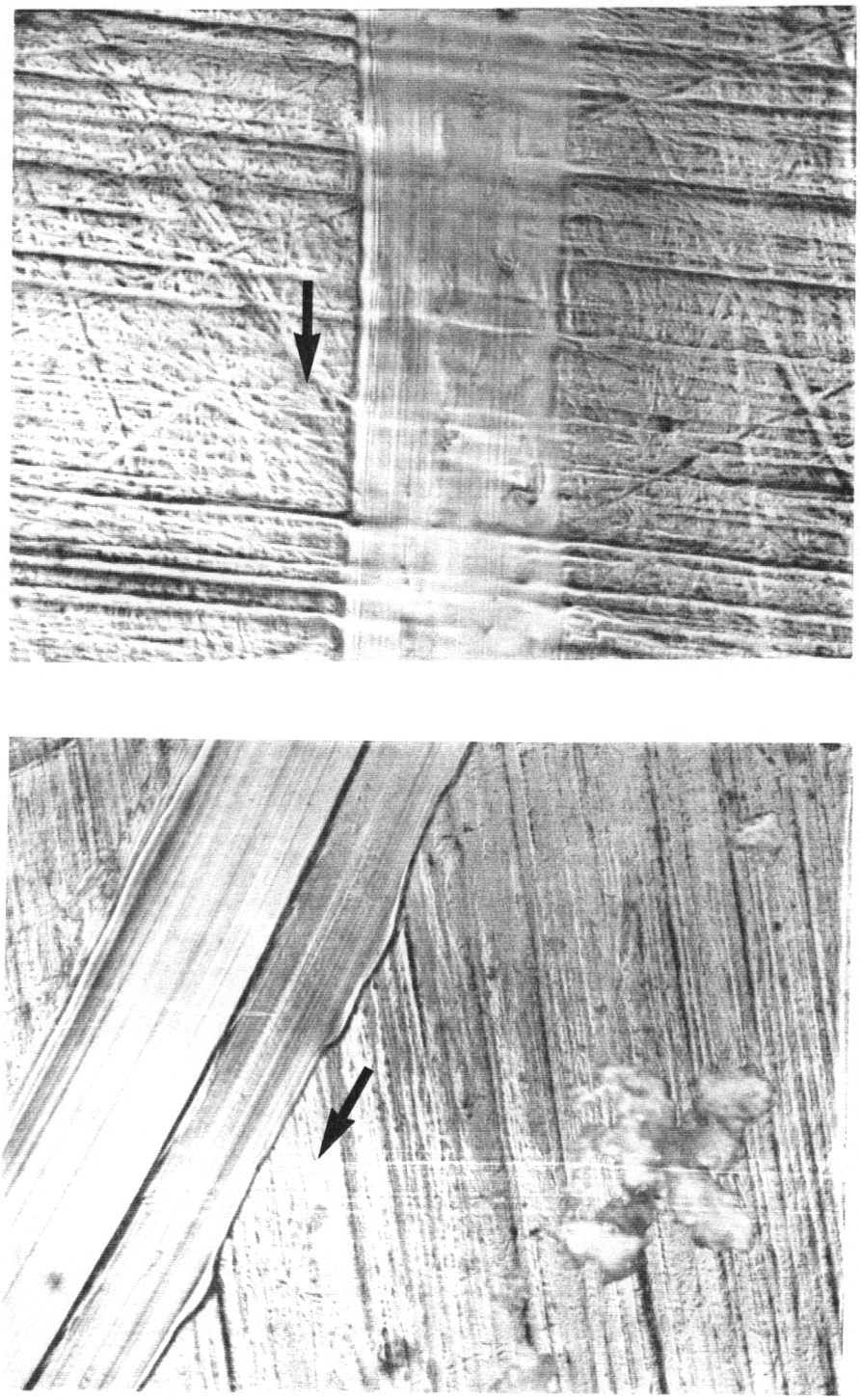

(a)

(b)

Figure 33. **Optical micrographs of the wear track of the untreated 85/15 blend at 15N-5cm/s a) after 600 cycles b) after 1200 cycles**

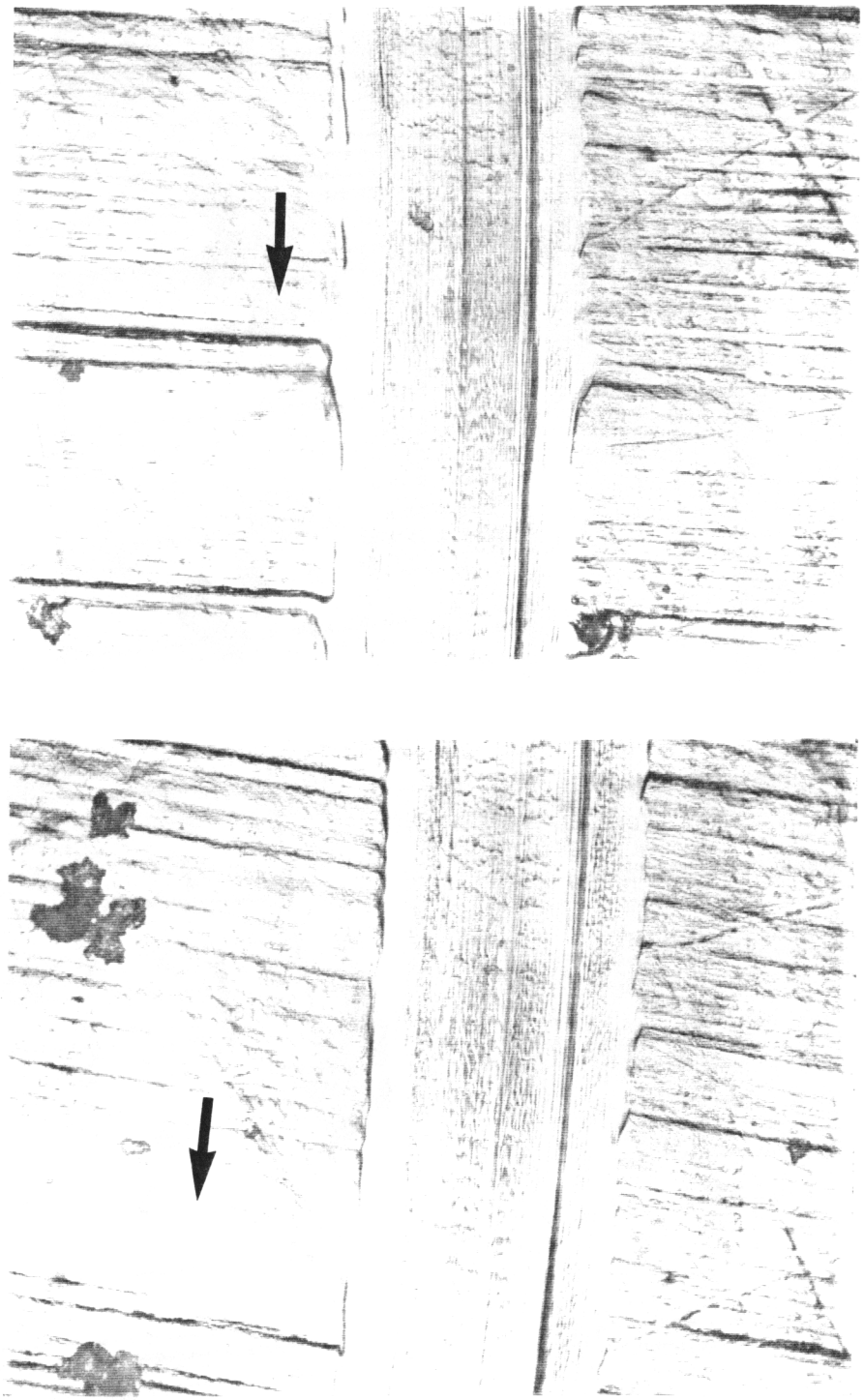

(a)

(b)

Figure 34. **Optical micrographs of the wear track of the untreated 85/15 blend at 15N-5cm/s a) after 1800 cycles b) after 2400 cycles**

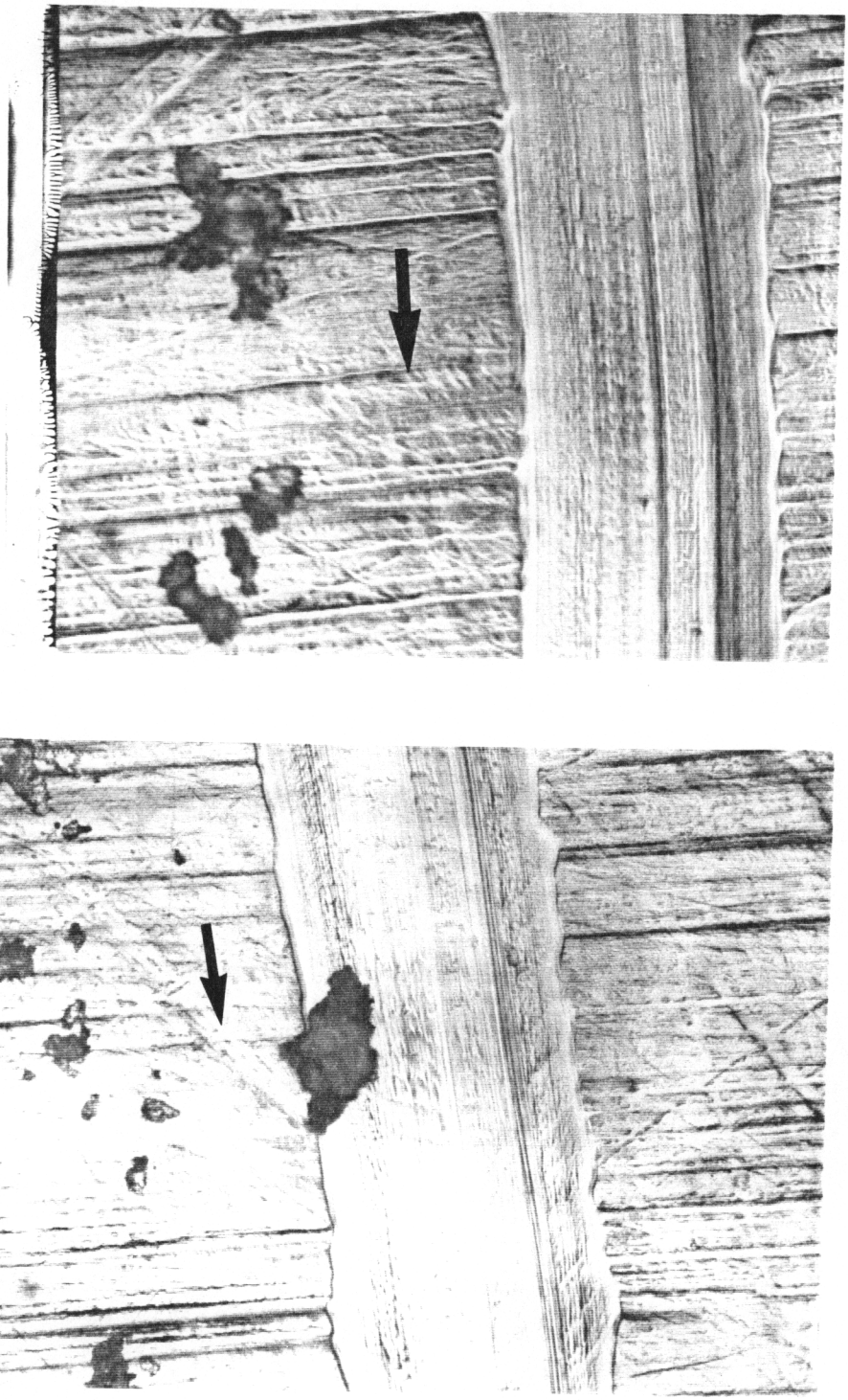

(a)

(b)

Figure 35. Optical micrographs of the wear track of the untreated 85/15 blend at 15N-5cm/s a) after 3000 cycles b) after 3600 cycles

After a few more hundred cycles, cracks developed in the film-like layer mostly at the centerline due to alternating compressive and tensile stresses. Development of the subsurface cracks eventually produces loose wear debris which are transported by the ball to new locations. Because of many cracks and wear scars on the wear track, much of the wear debris is easily stuck or embedded to the film-like layer. Spots in the track where fragments of film-like layer were pulled off are quickly covered up by adjacent film-like layer. Thus the steel ball has little opportunity to contact the material beneath the layer.

The wear of the CFR materials, unlike the wear of the untreated samples, did not seem to have an adhesive transfer film on the steel ball during the initiation of the sliding track. Numbers of speculations can be made: First, since fibers support a large portion of the load, less asperities of the matrix carry the load. Second, the carbon fiber reinforcement is susceptible to deform at initial contact mainly because of its less dense at the surface. Figure 36 shows many gaps on the surface of the 30% CFR PEEK before wear test. Therefore, the relative groove formation rate is highest at initial sliding and gradually decreases for subsequent cycles. Indeed one of the 30% CFR PEI specimens tested at 15N-5cm/s exhibited 20 $(\mu m)^2$/cycle from the beginning to 20 cycles, 2$(\mu m)^2$/cycle from 20 to 150 cycles, and 1 $(\mu m)^2$/cycle relative groove area formation rate from 150 to 600 cycles. Finally, if an adhered transfer film existed, it would be scraped out by the fibers on the surface of the sliding track.

Schelling and Kaush [2] and Mody, et al. [9] have noted that carbon fibers lower wear rates of composites because the fibers have high elastic modulii and therefore carry

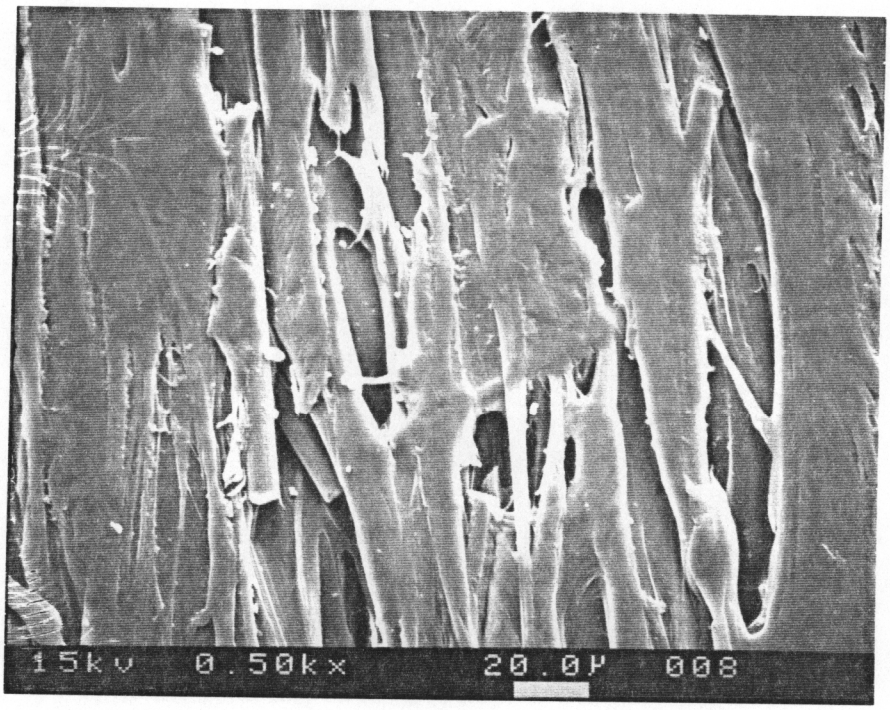

Figure 36. SEM micrograph of the original surface of the 30% CFR PEEK

a large portion of the applied load. The same reasoning can be applied to theses experiments; the wear is reduced because the fibers support the applied loads.

By comparing wear of PEEK of the untreated and the carbon fiber reinforced samples, it was supposed that the formation of groove and generation of wear debris of the 30% CFR were mainly due to the different physical nature of the carbon fiber reinforcements. As shown in Table 10, the surface roughness of the 30% CFR specimens is twice as great as that of the untreated ones. Therefore, before sliding track formation started, less number of asperities of the 30% CFR supported the load and thus they were subjected to the high stress. After the film-like layer covered the sliding track, the layer over the fibers was under high stress when it contacted the ball due to the stiffness of the fibers; therefore the layer was easily deformed and broke off. Consequently, a groove and many wear debris were observed in the 30% CFR PEEK.

Upon the examination of the wear rates of the PEEK/PEI blends, it is recognized that an increase in percentage of PEEK in the blend, lowers the wear rate. The wear data indicates that the material properties of PEEK dominate in pure PEEK, 85/15 and 70/30 compositions while those of PEI dominate in 50/50 and pure PEI compositions. As noted earlier in Chapter 4.2, PEEK is more ductile, tougher, and softer than PEI, and has a longer elongation-to-break. The stress exerted by the steel ball caused PEEK to plastically deform in the manner indicated earlier which produced very few wear debris. On PEI which is more brittle than PEEK, the stresses cause many transverse cracks and tears shown in Fig. 37 which join up to produce wear particles. For the PEEK dominated compositions, material failure by shear probably occurred at the subsurface

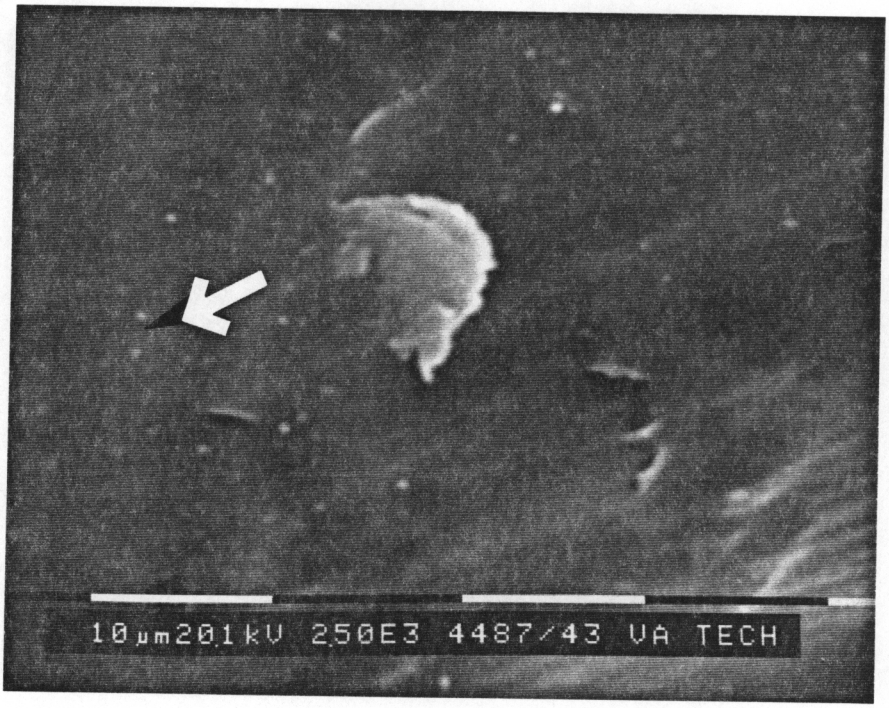

Figure 37. **SEM micrographs of the wear track of the untreated PEI at 3000 cycles(15N-5cm/s)**

of the circular region of contact subject to a hemispherical Hertzian normal and tangential forces as described by Hamilton and Goodman [44]. However, for the PEI dominated compositions, the maximum tensile stress that occurred upon the surface as sliding proceeded seemed to govern the failure of material. Thus the wear debris from the PEI dominated composition were generated by the fatigue wear, and the surface damage in the PEEK dominated composition was controlled by shear and plastic flow. The material failures were apparently related to the mechanical properties. However, the high elongation-to-break found in the untreated 50/50 blend appears to negate the above explanation. This apparent discrepancy may be explained by comparing strain rates in sliding with those in the tensile test. It is possible that high strain rate applied at the sliding wear test would not provide an enough time for molecule chains to reorient into the sliding direction which would cause failure to occur at short elongation whereas in the tensile test the lower strain rate (head speed was 0.5 mm/min or 0.02 in/min) would allow chains to reorient, thus resulting in high elongation-to-fracture.

It is generally known that a semicrystalline polymer is stronger than an amorphous polymer of the same kind. According to Hornbogen and Schafer [5], a high crystallinity produces better intermolecular cohesion and thus increases wear resistance. Voss and Friedrich [22] observed improvement of the wear resistance of the annealed materials. They claimed that a high degree of crystallinity in the polymer resulted in an increase in the material's hardness without reducing the toughness. Jones and Eiss [29] have claimed that a high degree of crystallinity inhibits crack propagation. Since in crystalline polymers, polymer chains can not reorient to allow slippage, crack propagation involves

the breaking of primary bonds which is difficult. In these experiments, an increase in the relative crystallinity by annealing decreased the wear rates of the PEEK/PEI blends as shown in Fig. 38. The apparent difference in wear rate for the 10.7% relative crystallinity (85/15T) and the 1.3% crystallinity (85/15B) was shown to be not significant at the 95% confidence level (see Table 11.)

Tanaka and Ueda [21] have observed a minimum wear rate at the spherulite size corresponding to the friction minimum in the sliding wear test of a polypropylene pin on the polished NAK 55 steel disk (Ra$\approx$0.02 μm). However the wear rate of an annealed polypropylene was not changed with spherulite size. They have suggested that the specimens without annealing include more defects than the annealed specimens and therefore the molecules are more easily drawn out of the spherulites at the frictional surface. As described in Chapter 4.1, the polymer blends were injected into 90-105 °C mold and cooled for one minute. During this time, temperature of the injection polymer had stayed above 145 °C which is the T_g of PEEK and thus the crystallization process had started. Because the crystallization temperature was very close to the T_g and lasted only for short period of time, the size of the spherulites, if any existed, would be smaller and the structure of spherulites would be imperfect. This has observed in other literature [11,24]. Therefore as Tanaka and Ueda [21] described, more defects in crystalline molecules of the 85/15(T) may cause higher wear rates than otherwise.

Jones and Eiss [29] observed that the increased in wear rate increased as the T_g increased for polyimide films on a pin-on-polymer disk apparatus. Since polymers with stiff molecular chains have high T_g's, they explained this result by claiming that stiff

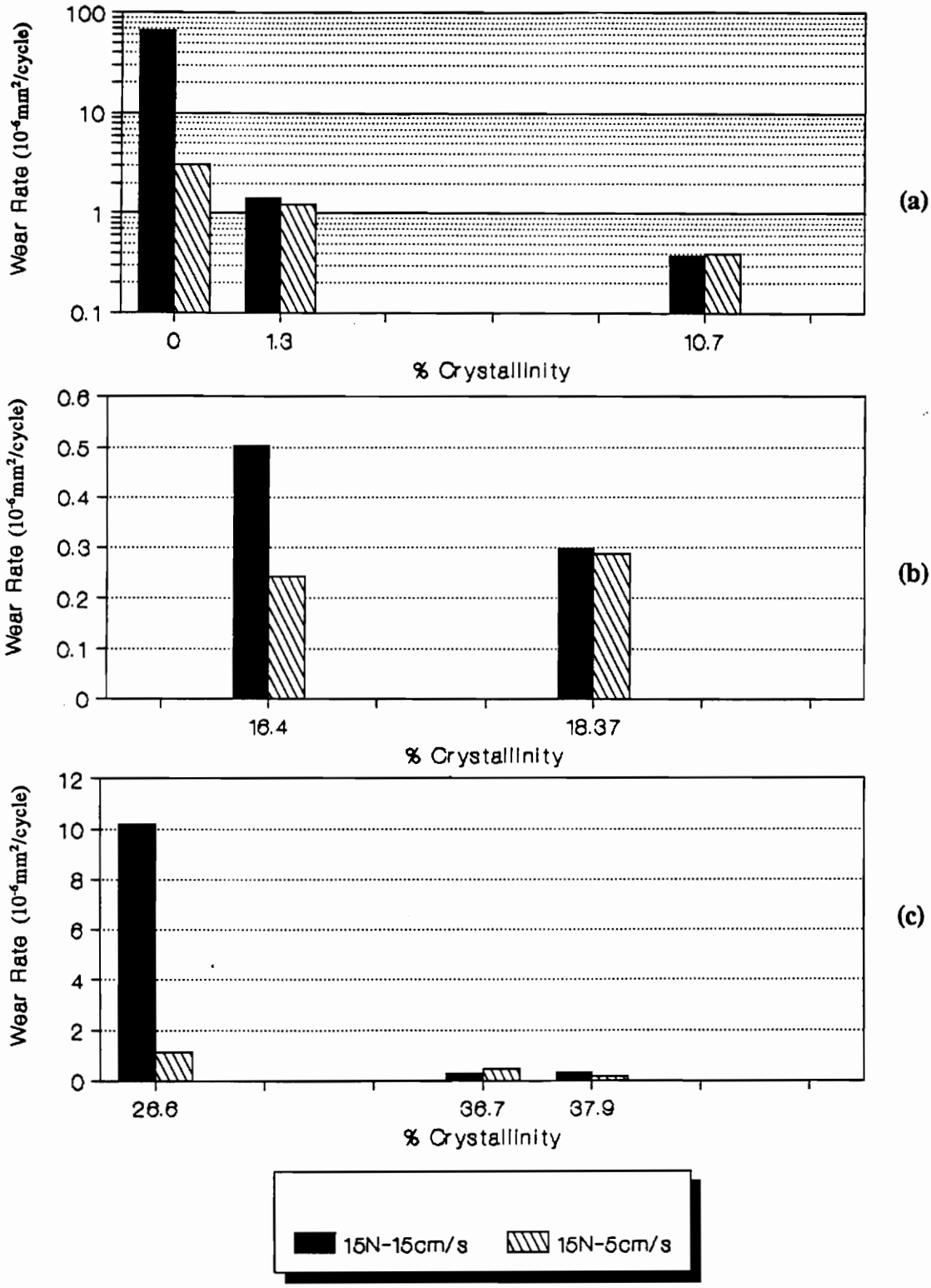

Figure 38. The crystallinity effects on wear rates a) Untreated, b)30% CFR, c) Annealed.

chains can not rotate to accommodate the stresses and thus fracture more readily. In this study, a correlation between the T_g and wear rate was observed in the untreated samples only. However, an opposite correlation -- a higher T_g and lower wear rate was noted when the wear rates of the untreated and the annealed samples were compared. Probably, the wear rates of this type of polymer blend are more related to the crystallinity and its perfection than the chain rigidity.

5.2 Friction

In the previous section, two hypotheses of wear mechanisms for the untreated and annealed polymer specimens and the CFR composite specimens were discussed. It is possible that two different wear mechanisms will affect differently on the friction behaviors of the specimens. Therefore in this section, possible connection between wear mechanism and coefficient of friction is examined.

In general, the frictional force results from surface layer deformation and adhesion. This is represented as

$$F_F = F_{adh} + F_{def} \qquad (9)$$

where F_F = the total frictional force

F_{adh} = the adhesion friction

F_{def} = the deformation friction.

Therefore, in this experiment, the frictional force will increase if either of the shear strength of the junction, the real area of contact, or the viscoelastic-plastic losses in polymers increases.

As Figure 9 shows, two types of the coefficient of friction responses were observed. Whenever wear debris were produced, a class A type of the friction response was seen and otherwise a class B type response was noticed. For class A samples, the driving mechanism for increasing the coefficient of friction at stage I of the 30% CFR specimens was little different from that of the untreated and annealed materials.

For the 30% CFR materials at the stage I, the applied normal and tangential forces plastically deformed the asperities of the disk so that surface matrix over the fibers started to smear out and a groove was easily formed due to the low density at the surface. The sharp increase in friction was contributed by the deformation loss of the asperities and by lesser an increase in contact area which was due to changes in the configuration from ball-on-flat to ball-on-groove. During stage II, a film-like layer fully developed so that fibers could not be seen on the surface of the sliding track. During this stage the cross-sectional groove area did not increase much; thus plastic displacement probably accounted for the increased coefficient of friction. Stage II was generally longer than stage I. A few wear debris were discovered at this stage but they were believed to be from the deformation of the initial asperities; debris stuck to the ball and

then was removed. At stage III, accumulated plastic deformation during the stage II finally caused cracks at the centerline of the wear track and the film-like layer produce loose wear debris. Even though the number of stress cycles to generate loose particles at stage III varied from specimen to specimen, prolonged cycles were required. Therefore fatigue wear is proposed as the predominant wear mechanism.

For the untreated and annealed materials, as the ball started to slide, junction growth occurred at asperity tips of the disk. Asperities were removed by adhesive wear and thus contact area was slightly increased. As the track became smooth, the stage I friction response was observed. The increase in the real area of contact caused by the smooth sliding track increased the coefficient of friction. During this stage, the frictional work was dissipated by generating low frequency noise, heat, and a series of cyclic deformations in the contact region. At the stage II, a transition from the sliding track from which no loss of material was observed to the wear track where many loose wear debris were generated occurred. Unlike the 30% CFR case, stage II was short compared to that of the stage I. Wear debris adhered loosely to the ball, fractured, and became loose. At the stage III, the wavy surface roughness probably resulted from plastic flow; the accumulated plastic strain caused crack generation and propagation to form wear particles. The steady state of the coefficient of friction was obtained, probably because the rate of the creation of the cracks and wavy deformations was same as the rate of the wear debris generation.

For class B samples, no sharp increase in the coefficient of friction was seen even though small grooves were formed. Usually, the groove of the class B sample was

below the sensitivity of the surface profile meter. Under the optical macroscope, the original surface machine marks were still visible even at 3600 cycles but the track looked smooth. This example is shown in Fig. 39. The decrease in the coefficient of friction as the sliding cycles increased was probably due to a work hardening effects which reduced deformation. Hornbogen and Schafer [5] have claimed that during the sliding, the molecules are aligned in the direction of sliding and a considerable amount of work hardening occurred in the sliding direction. This change of the surface structure can lead to a decreasing coefficient of friction due to increase of hardness and a decreasing contact area. If the work-hardening is assumed during the sliding, it is questionable why the class A samples did not see the work-hardening effect. Since wear debris were generated in the class A samples, new surface was exposed each time wear debris was generated. Then, the material at newly exposed area must break off before enough numbers of cycles to work harden occur.

It is speculated that at high sliding speeds, surface temperatures may rise high enough to soften the contact surface. Thus less frictional force at high sliding speed will be required to get the same amount of accumulated plastic strain which can be produced at low sliding speed. In other words, with the same frictional force, higher amount of deformations will result at the high sliding speed. Since the coefficient of friction of all samples were same at 95% confidence level, it is unlikely that thermal softening occurred. In the preliminary study conducted in the tribology lab at VPI & SU by Brinkley and Eiss, they measured the temperature with a thermocouple placed in the pin holder about 10 mm from the contact. After 3600 cycles with same apparatus and

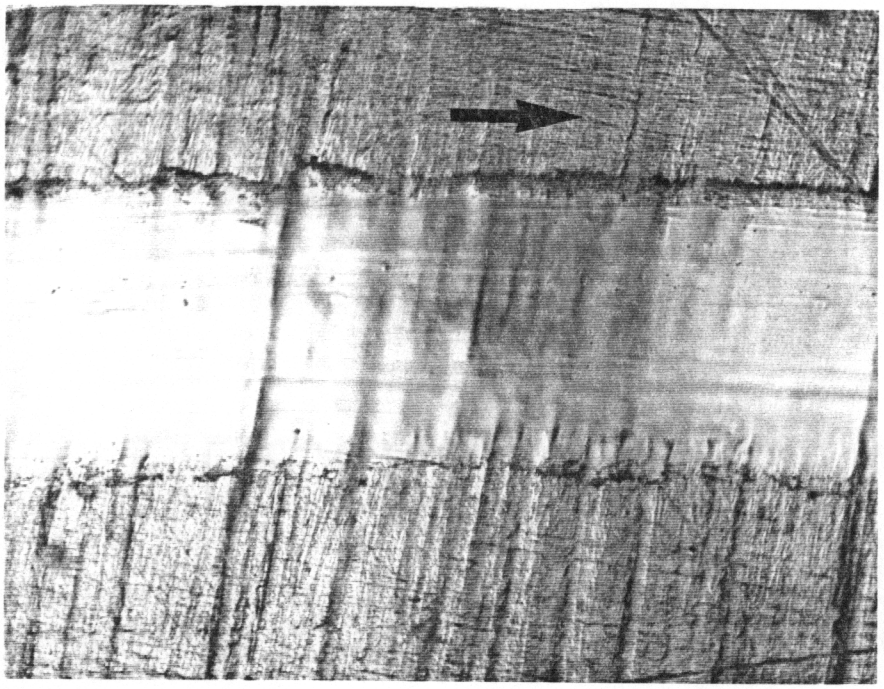

Figure 39 Optical micrograph of the wear track of the 85/15 blend at 3600 cycles

materials used in this experiment they observed a temperature rise of 5 to 8 °C at 5 cm/s and 8 to 15 °C at 15 cm/s sliding speed.

The increase in the coefficient of friction of the 30% CFR after the stage III is closely related to the increase in contact area. During the sliding, steel ball occasionally contacted the high strength fibers and slowly wore away. When steel ball slid against the 30% CFR PEI, the worn area of the ball was 0.253 mm^2, and when it slid against the 30% CFR PEEK, the area was 0.158 mm^2 while the size of wear debris was two orders of magnitude lower than those areas. Therefore the friction force would rise due to the deformation of the steel ball and carbon fiber reinforced specimen. The increase in contact area which resulted from the flattened tip of the steel ball also contributed to the rise in coefficient of friction. The untreated pure PEI had the exceptionally high coefficient of friction among all compositions along with the highest wear rate at 15N-15cm/s testing condition. An increase in contact area and many trapped wear debris particles between the ball and disk would significantly increase the coefficient of friction.

6. CONCLUSIONS

In this experiment, the incubation time before generating wear debris and the increase in the coefficient of friction when wear started suggested the predominant wear mechanism was fatigue.

As the percentage of PEI in the blend was increased the wear mechanism changed from plowing to the generation of small particles. Indeed, the blends of PEEK/PEI with compositions of 50/50 and 0/100 were amorphous and their wear rates were 46 times higher than the semicrystalline PEEK dominated blends. For the PEEK dominated compositions, material failure probably occurred by shear at the subsurface of the contact region. For the PEI dominated blends, the maximum tensile stress on the surface seemed to govern the failure of material. The wear mode of the untreated and annealed PEEK/PEI blends was initially adhesive and as the wear track was formed, the wave deformation occurred and loose particles were generated after multiple stress cycles.

The coefficient of friction for the untreated and annealed blends remained below 0.15 when wear particles were not produced. When wear particles were produced, the coefficient of friction ranged from 0.2 to 0.3 and was not significantly different among each composition.

For the pure PEI and 50/50 PEEK/PEI blends, the increase in load by a factor of 3 resulted in twice as much wear than occurred when the sliding speed increased by

a factor of 3 for the PEI dominated blends. Increasing speed did not seem to affect the wear rates of the PEEK dominated blends and the coefficients of friction of all tests.

Increasing the relative PEEK crystallinity by annealing reduced the wear rate of the PEEK/PEI blends but there was no significant differences in the coefficient of friction. However, the wear behavior of the untreated 85/15 blend may indicate that the crystalline perfection is more important factor for wear resistance of polymer materials than the degree of crystallinity of the blends.

30 weight % of the short carbon fibers improved the wear resistance of the unreinforced PEEK/PEI blends but not for pure PEEK. However the 30% CFR induced the counterface (steel ball) wear. During the test, a film-like layer covered the sliding tracks and after number of cycles it was worn out. The coefficient of friction for CFR PEI was higher than unreinforced PEI. The coefficients of friction for CFR PEEK and 70/30 blends were not significantly different and they are similar to those of the unreinforced samples.

The T_g of the PEEK/PEI blend can be increased from 145 °C for pure PEEK to 159 °C for 70/30 blend without significant increase in the wear rate of the materials. Annealing and reinforcement by the short carbon fibers further increased the T_g to 186 and 174 °C respectively for the 70/30 blend.

CONCLUSIONS

7. RECOMMENDATIONS

1. In this experiment, when PEEK/PEI blends were fabricated the crystallinity of the each composition was not the same. Consequently, the mechanical and wear properties were dependent on the composition and the crystallinity. Therefore it is desirable to have mechanical and wear tests of the quenched blends to reduce the crystallinity effect.
2. Tensile tests of the all blends are needed to compute the elastic contact area. However a better way to obtain mechanical properties has to be found because using the dog-bone specimen on the Instron testing machine produced many inconsistent results. When the tensile test specimens are cut from the plaque, the mold filled direction (MFD) should be concerned because the molecules are tend to align with MFD.
3. Although Tanaka and Ueda [21] already studied the spherulite size effect on wear and friction and found that the perfection of the crystalline lamellae and a state of the inter-lamellae molecules are more influential factors than size of spherulites in the wear of polymers, Cebe, et al. [11] found that an increase in spherulite size of PEEK would cause embrittlement and low strain to break. Therefore it will be interesting to see the effect of different size of spherulite on the tribological behavior. It is known that the semicrystalline polymer crystallized at near to the its melting temperature has larger size of the spherulite than polymer crystallized at near to the

glass transition temperature due to the increasing number of nucleation sites at lower temperature.

4. Investigation of the structure of the crystalline blends is highly needed to explain the controversial crystallinity effect on the untreated 85/15 blend. It is undesirable to look at the spherulites under the optical microscope because a small piece cut by a microtome always tends to curl up. Therefore solution etching method is recommended.

5. Since the PEEK/PEI blends are high temperature stable thermoplastics, they will be used at many high temperature applications. Therefore friction and wear tests should be conducted at elevated temperatures.

6. The applications of the PEEK and PEI include high pressure steam valves and automotive heat exchange components. Therefore the humidity effect on wear should be studied in order to determine the safe operation conditions.

7. The rate of stress application in sliding wear test and a tensile test are significantly different especially for the visco-elastic materials. Therefore more in-depth knowledge of the polymeric materials is required to better understand if tribological behavior is to be correlated with the mechanical properties. The latter must be obtained from test that can simulate the strain rate of the wear test.

8. In this experiment, PEEK showed good wear resistance whereas PEI displaced poor wear resistance. However Bijwe, et al. [3,7,8,35,36,37] observed PEI is good abrasive wear resistant material. Therefore it will be interesting to run a different wear test, such as an abrasive wear test.

References

1. ICI Brochure (Victrex® PEEK), *A Guide to Grades for Injection Molding,* ICI Advanced Materials, 1990.

2. A. Schelling and H. H. Kausch, "The Influence of Long Term Reciprocating Dry Friction on the Wear Behavior of Short Fiber Reinforced Composite Materials," *Proceedings of conference: congress "The Tribology of Composite Materials,"* Oakridge, Tenn. May 1990.

3. J. Bijwe, U. S. Tewari, and P. Vasudevan, "Friction and Wear Studies of Bulk Polyetherimide," *J. of Materials Science*, vol. 25, 1990, pp. 548-556.

4. U. S. Tewari, S. K. Sharma, and P. Vasudevan, "Polymer Tribology," *J. of Macromolocular Science - Review in Macromolecular Chemistry and Physics.* 1989, pp. 1-38.

5. E. Hornbogen and K. Schafer, "Friction and Wear of Thermoplastic Polymers," in *Fundamentals of Friction and Wear of Materials,* edited by D. A. Rigney, ASM, Ohio, 1981, chapter 11.

6. T. C. Ovaert, and H. S. Cheng, "The Unlubricated Sliding Wear Behavior of PEEK against Smooth Mild-Steel Counterfaces," J. of Tribology, v.113, No.1, Jan. 1991, pp.150-157.

7. J. Bijwe, U. S. Tewari and P. Vasudevan, "Friction and Wear Studies of Polyetherimide Composites," *Wear of Materials 89* , vol. 2, ASME, 1989, pp. 507-515.

8. J. Bijwe, U. S. Tewari and P. Vasudevan, "Friction and Wear Studies of a Short Glass-Fibre-Reinforced Polyetherimide Composites," *Wear*, Vol. 132, 1989, pp.247-264.

9. Parimal B. Mody, Tsu-Wei Chou, and Klaus Friedrich, "Effects of Testing Conditions and Microstructure on the Sliding Wear of Graphite Fibre/PEEK

Matrix Composite," *J. of Materials Science,* Vol. 23, No.11-12, 1988, pp. 4319-4330.

10. Zeng Hanmin, He Guoren and Yang Guicheng, "Friction and Wear of Poly(Phenylene Sulphide) and Its Carbon Fibre Composites: I. Unlubricated," *Wear,* Vol. 116, 1987, pp. 59-68.

11. Peggy, Cebe, Shirley Y. Chung, and Su-Don Hong, "Effect of Thermal History on Mechanical Property of PEEK below the Glass Transition Temperature," *J. of Applied Polymer Science,* Vol.33, 1987, pp. 487-503.

12. E. Hornbogen, "The Role of Fracture Toughness in the Wear of Materials," *Wear,* Vol. 33, 1975, pp. 251-259.

13. James M. Margolis, *"Engineering Thermoplastics Properties and Applications,"* Marcel Dekker, Inc., NY, 1985, pp. 283-314.

14. J. C. Hedrick, C. A. Arnold, M. A. Zumbrum, T. C. Ward, and J. E. McGrath, "Poly (Aryl Imide) Homo- and Polydimethylsiloxane Segmented Copolymer Blends: Influence of Chemical Structure on Miscibility and Physical Behavior," National SAMPE Symp. Exhib. Proc. Vol. 35, Book1, *35th International SAMPE Symposium and Exhibition - Advanced Materials; the challenge for the next decade Part1,* Anaheim, CA, April 2-5, 1990, pp.82-96.

15. J. E. Harris and L. M. Robeson, "Miscible Blends of Poly(aryl ether ketone) and Polyetherimide," *J. of Applied Polymer Science* Vol. 35, 1988, pp. 1877-1891.

16. General Electric Brochure (ULTEM), *Properties Guide,* GE Plastics, 1990.

17. A. Prasad and H. Marand, "Miscibility, Morphology, Crystallization and Melting Behavior of Poly(Ether-Ether-Ketone) (PEEK)/ Poly(Ether-Imide) (PEI)," paper submitted to *Polymer.*

18. A. Lustiger, F. S. Uralil, and G. M. Newaz, "Processing and Structural Optimization of PEEK," *Polymer Composites,* Vol. 11, no.1, Feb. 1990, pp. 65-75.

19. Margaret E. Talbott and George S. Springer, "The Effects of Crystallinity on the Mechanical Properties of PEEK Polymer and Graphite Fiber Reinforced PEEK," *J. of Composite Materials,* Vol.21, 1987, pp. 1056-1081.

20. P. T. Curtis, P. Davies, I. K. Partridge, and J. P. Sainty, "Cooling rate effects in PEEK and CF-PEEK," *Proceedings of the ICCM 6,* Vol. 4, Imperial College,

London 1987, pp.401-412.

21. Kyuichiro Tanaka and Seichi Ueda, "Effect of Spherulite Size on the Friction and Wear of Semicrystalline Polymers," *Proceedings of the JSLE International Tribology Conference,* Vol. 2, July 8-10, 1985, pp. 459-464.

22. H. Voss and K. Friedrich, "On the Wear Behavior of Short-Fibre-Reinforced PEEK Composites," *Wear,* Vol. 116, 1987, pp. 1-18.

23. Kyuichiro Tanaka, "Structure and Properties of Polymers Important to Their Wear Behavior," *Proceedings of the JSLE International Tribology Conference: Tribology in the 80's,* Vol. 1, 1983, pp.253-289.

24. Huy X. Nguyen and Hatsuo Ishida, "Poly(Aryl-Ether-Ether-Ketone) and its Advanced Composites: A Review," *Polymer Composites,* Vol. 8, no. 2, April 1987, pp. 57-73.

25. K. Friedrich, R. Walter, H. Voss and J. Karger-Kocsis, "Effect of SFR on the Fatigue Crack Propagation and Fracture of PEEK Composites," *Composites,* Vol. 17, no. 3, July 1986, pp.205-216.

26. M. Cirino, K. Friedrich, and R.B. Pipes, "Evaluation of Polymer Composites for Sliding and Abrasive Wear Applications," *Composites,* Vol. 19, no. 5, Sept. 1988, pp. 383-392.

27. O. Jacobs, K. Friedrich, G. Marom, K. Schulte and H. D. Wagner, "Fretting Wear Performance of Glass-, Carbon-, and Aramid-Fibre/Epoxy and PEEK Composites," *Wear,* Vol. 135, 1990, pp.207-216.

28. N. S. Eiss, Jr. and J. R. Potter III, "Fatigue Wear of Polymers," in L. H. Lee(ed.), *Polymer Wear and Its Control,* American Chemical Society, Washington D. C.,1985, pp.59-66.

29. J. W. Jones and N. S. Eiss, Jr., "Effect of Chemical Structure on the Friction and Wear of Polyimide Thin Films," in *Polymer Wear and Its Control,* American Chemical Society, 1985, pp. 135-148.

30. M. R. Chitsaz-Zadeh and N. S. Eiss, Jr., "Friction and Wear of Polyimide Thin Films," *Wear,* Vol. 110, 1986, pp. 359-368.

31. N. S. Eiss, Jr. and H. Czichos, "Tribological studies on Rubber-modified Epoxies: Influence of Material Properties and Operating Conditions," *Wear,*

Vol. 111, 1986 pp. 347-361.

32. Friedrich, K. *"Friction and Wear of Polymer Composites,"* Fortschritt-Berichte Der VDI Zeitschriften, Reihe 18, no. 15, 1985.

33. Briscoe, B. J., "Tribology of Polymers: state of an art." in *Physicochemical Aspects of Polymer Surfaces,* Vol. 1, ed. K. L. Mitttal, Plenum Publishing Co., NY, 1983, pp. 387-412.

34. B. Briscoe, "Wear of Polymer: an essay on fundamental aspects," *Tribology International,* Aug. 1981, pp.231-243.

35. J. Bijwe, U. S. Tewari, and P. Vassudevan, "Tribological Studies of Glass Reinforced Polyetherimide," *International Tribology Conference 1987,* Melbourne, Dec. 2-4, 1987.

36. J. Bijwe, C. M. Logani, and U. S. Tewari," Influence of fillers and Fiber Reinforcement on Abrasive Wear Resistance of Some Polymeric Composites," *89 Wear of Materials,* Vol. 1, ASME, 1989, pp. 89-97.

37. J. Bijwe, U. S. Tewari, and P. Vasuderan, "Friction and Wear Studies of an Internally Lubricated PEI composites," *J. of Synthetic Lubrication,* Vol.6, no. 3, 1989, pp. 179-202.

38. B. J. Briscoe, Lin Heng Yao, and T. A. Stolarski, "The Friction and Wear of PTFE-PEEK Composites: An initial appraised of the Optimum Composition," *Wear,* Vol. 108, 1986, pp. 357-374.

39. M. Cirino, K. Friedrich, and R. B. Pipes, "The Effect of Fiber Orientation on the Abrasive Wear Behavior of Polymer Composite Materials," *Wear,* Vol. 121, 1988, pp. 127-141.

40. Youngchul Lee and Roger S. Porter, "Crystallization of Poly(etheretherketone) (PEEK) in Carbon Fiber Composites," *Polymer Engineering and Science,* Vol. 26, No. 9, Mid-May 1986, pp. 633-639.

41. D. J. Blundell, D. R. Beckett, and P. H. Willcocks, "Routine Crystallinity Measurements of Polymers by DSC," *Polymer,* Vol. 22, May 1981, pp. 704-707.

42. D. C. Bassett, R. H. Olley, and I. A. M. Al Raheil, "On Crystallization Phenomena in PEEK," *Polymer,* Vol. 29, Oct. 1988, pp. 1745-1754.

43. "Standard Terminology Relating to Wear and Erosion," G40-90a, *Annual Book*

of ASTM standard, American Society for Testing and Materials, Philadelphia, PA, 1991.

44. G. M. Hamilton and L. E. Goodman, "The stress field created by a circular sliding contact," *J. of Applied Mechanics (Transactions of the ASME),* June 1966, pp. 371-376.

45. "Standard Test Method for Plane Strain Fracture Toughness of Metallic Materials," E399-83, Vol. 02.02, *Annual Book of ASTM standard, American Society for Testing and Materials,* Philadelphia, PA, 1990.

APPENDICES

A. Fracture Toughness Test

A compact specimen as shown in Fig. 40 was used for fracture toughness measurements under Mode I (tension) loading. The testing procedure is followed:

1. Zero the load on the Instron universal testing machine.
2. Select the scales on the X-Y recorder.
3. Make connections to the monitor load and extensometer displacement and position the origin.
4. Mount the specimen into the pin and clevis grips.
5. Zero the extensometer and mount it on the specimen.
6. Set the X-Y recorder to record.
7. Select the appropriate ramp rate for the crosshead; 2.54 mm/min (=0.1 in/min) was used.
8. Begin ramping.
9. After specimen completely fractures, stop ramping and remove the specimen.

Fracture toughness, K_c, is thickness dependent but becomes constant for thickness sufficient for plane strain. This constant toughness value is the plane strain fracture toughness, K_{Ic}, for Mode I (tension loading), which is a lower limiting value for K_c and is a material property. If the stress state upon the failure of the specimen is determined to be plane stress, the validity of linear elastic fracture mechanics (LEFM) has to be

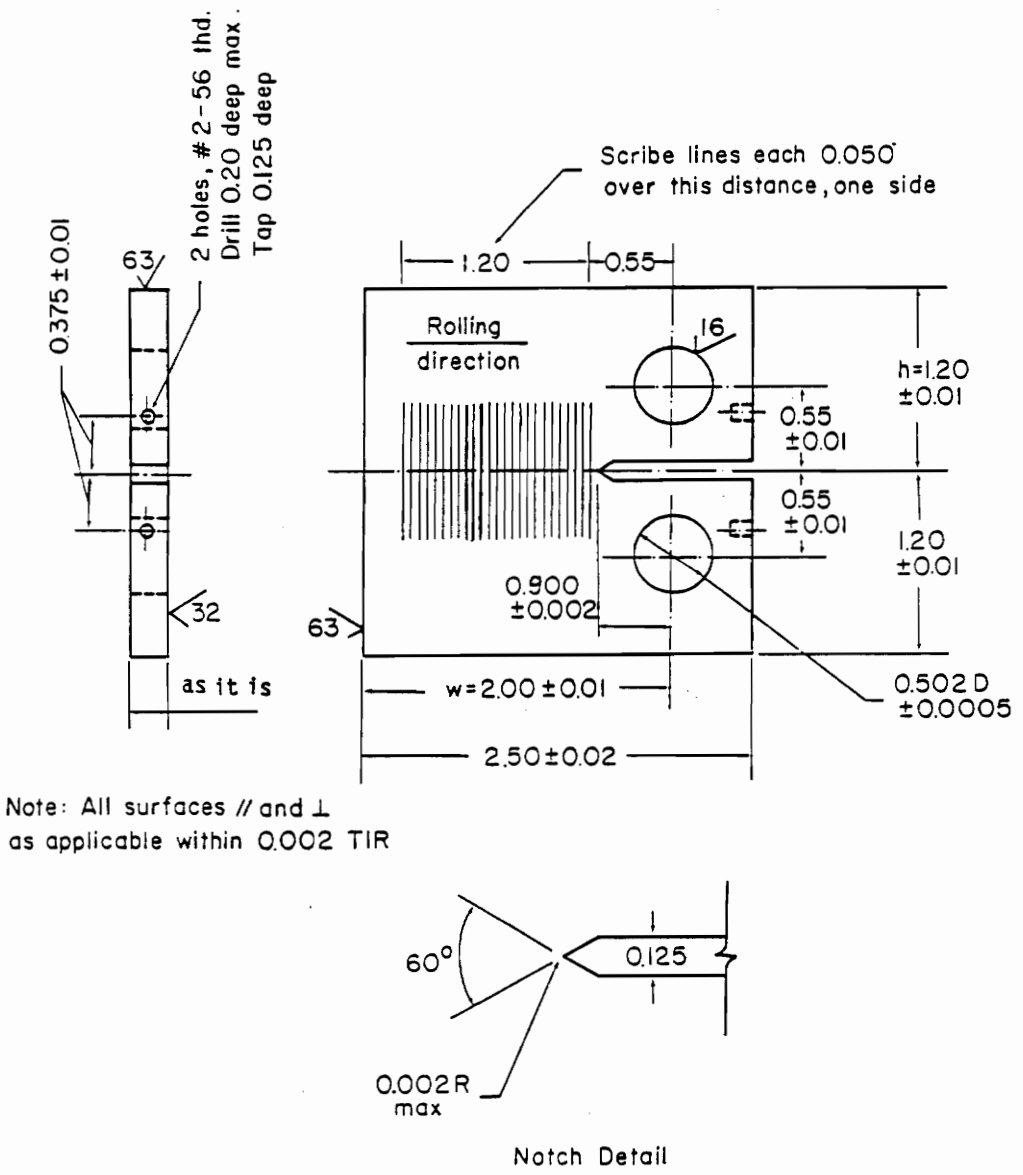

Figure 40. Dimensions of the compact specimen (inch)

made because the plastic zone around the notch may control the behavior of the crack. The procedure of determination of either plane strain or plane stress and validity of LEFM analysis in case of plane stress are followed:

$$\alpha = \frac{a_i}{w}$$

$$F_p = \frac{(2 + \alpha)}{(1 - \alpha)^{\frac{3}{2}}} \left(0.886 + 4.64\alpha - 13.32\alpha^2 + 14.72\alpha^3 - 5.6\alpha^4 \right) \qquad (\alpha \geq 0.2)$$

$$K_Q = F_p \frac{P_Q}{t\sqrt{w}}$$

Calculate the following values and check to see if the inequalities hold, then the stress state is plane strain.

$$2.5 \left(\frac{K_Q}{\sigma_0} \right)^2 < t,\ a_i,\ (w - a_i),\ and\ h$$

$$\frac{P_{max}}{P_Q} < 1.1$$

For plane stress, calculate the following values and check to see if the inequalities hold, then LEFM is valid. LEFM is always valid for plane strain.

$$4r_{0\sigma} < a_i,\ (w - a_i),\ and\ h$$

$$r_{0\sigma} = \frac{1}{\pi}\left(\frac{K_Q}{\sigma_0}\right)^2$$

where σ_0 = yield strength of specimen (for PEI specimen, σ_0 = 105 MPa or 15.2 ksi which is adopted from reference 16.)

h = half-height of specimen (3cm or 1.2 in.)

w = width of specimen (5cm or 2.0 in.)

a_i = crack length at the start of stable crack growth (2.3cm or 0.92 in.)

t = thickness of specimen (0.17cm or 0.068 in.)

P_{max} = maximum load on Fig. 41 (185 kg or 408.3 lbm)

P_Q = load corresponding to K_Q [45] (125 kg or 275 lbm)

α = dimensionless geometry factor (0.46)

F_p = dimensionless geometry factor (8.579)

K_Q = stress intensity (26.9 MPa$\sqrt{m}$ or 24.5 ksi$\sqrt{in}$)

$r_{0\sigma}$ = plane stress plastic zone size (2.1 cm or 0.827 in.).

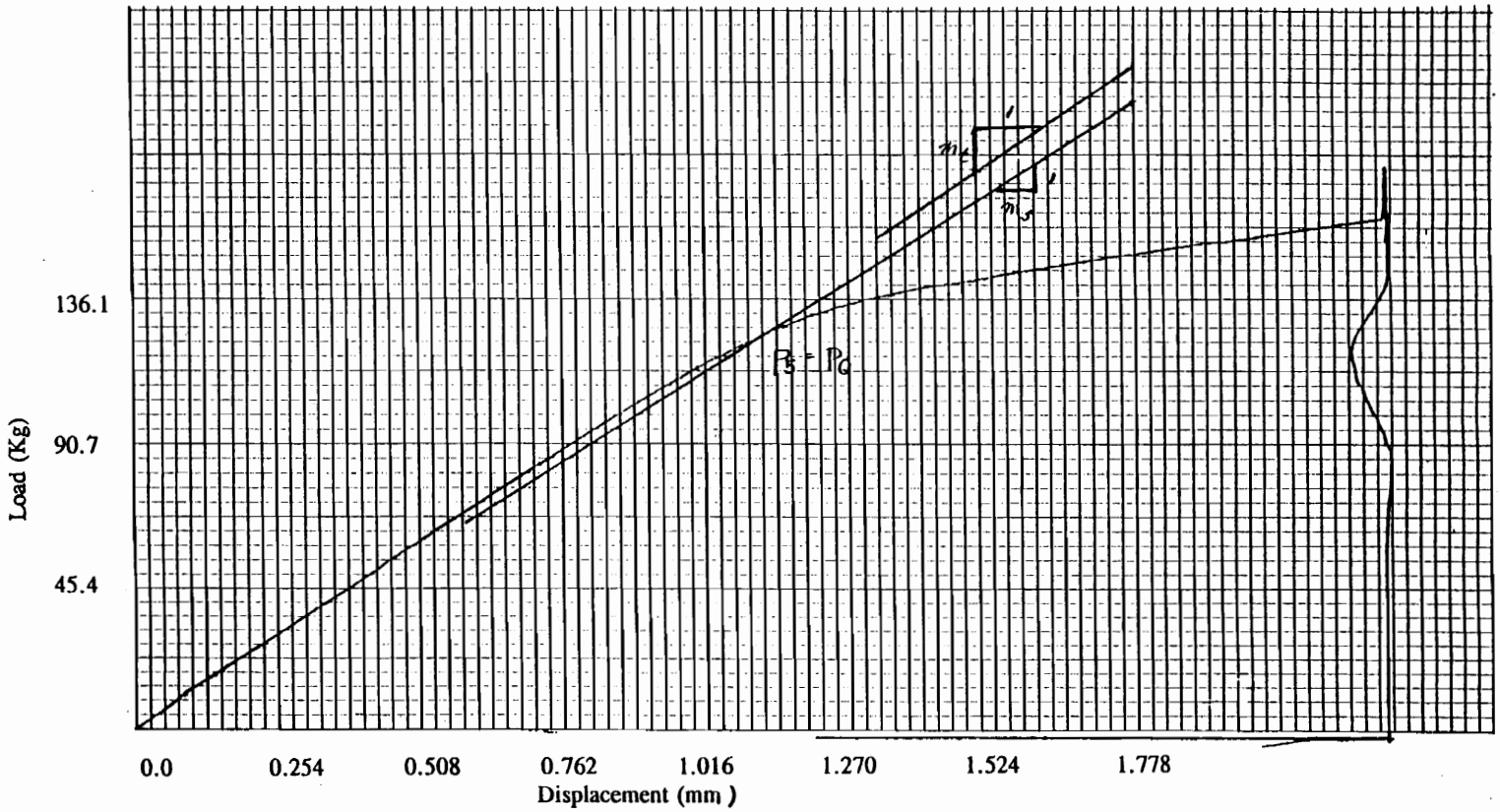

Figure 41. Load vs. Displacement of the fracture test of the untreated PEI

B. Tensile Test

Injection molded plaque of PEEK, PEI and their 50/50 blend were machined out into dog-bone specimens as shown in Fig. 5. The tensile test procedure is same as the one for fracture toughness test (Appendix A) except 0.5mm/min (0.02 in/min) cross-head speed was used instead of 2.54 (0.1 in/min). To obtain an accurate modulus, an extensometer (gage length = 12.7 mm or 0.5 in) was used initially. When the specimen showed a strain softening; at around 15% elongation measured by the extensometer, the elongation of the specimen was measured by the displacement of a cross-head of the Instron testing machine. While dismounting the extensometer from the specimen, the measurement of the elongation was stopped but the Instron was kept running. A load-elongation curve of the untreated PEEK specimen is shown in Fig. 42. In Fig. 42, the elongation measured by the extensometer is noted as "W/ EXTENSOMETER (%)" and used (%) scale for X-axis whereas the one recorded after detachment of the extensometer is marked as "W/o EXTENSOMETER (mm)" and used (mm) scale. Yield Strength (Y.S.), modulus (E), and displacement to break are listed in Table 15.

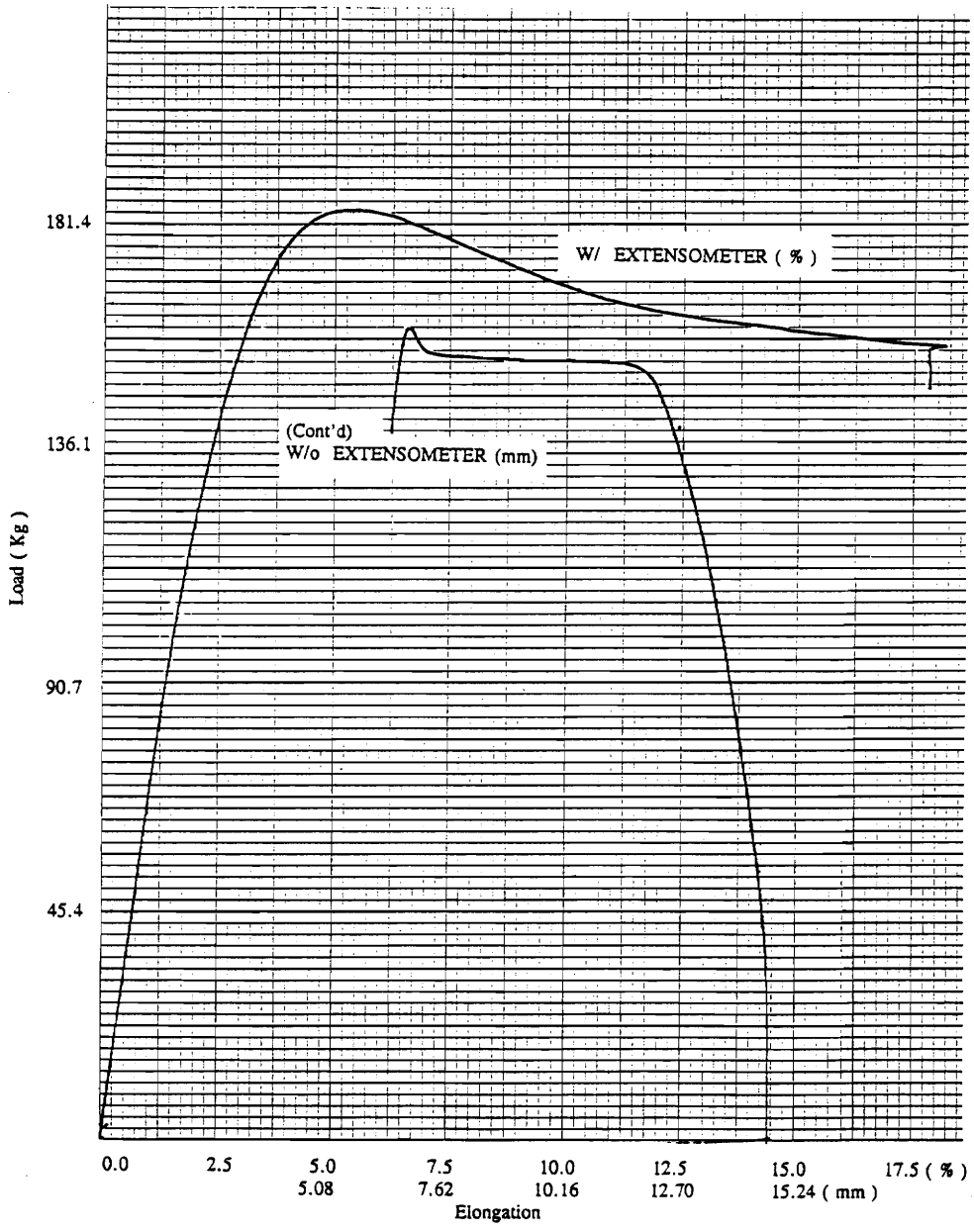

Figure 42. Load - elongation curve of the untreated PEEK

Table 15. Tensile test results

Composition	Sample Number	Y.S. (MPa)	E (MPa)	Displacement to break (mm)
PEEK	5	89.7	3315.0	15.2
	6	69.8	-	20.3
	9T	85.8	3468.0	40.6
	9B	82.9	3680.4	38.1
		(82.1±11.9)	(3487.8±372.2)	(28.6±17.5)
50/50	7T	80.0	2667.6	48.3
	7B	80.0	2700.0	38.1
		(80.0±0.0)	(2683.8±145.5)	(43.2± -)
PEI	6T	94.7	2614.5	7.6
	6B	95.4	2904.8	10.2
	10T	99.8	3105.4	7.6
	10B	99.7	2457.3	15.2
		(97.4±3.8)	(2770.5±399.8)	(10.2±4.9)

( ) Mean values and 95% confidence limits

C. Differential Scanning Calorimetry (DSC) Results

The glass transition temperature (T_g) and the percent of the PEEK crystallized relative to the PEEK content in the blend were obtained from the DSC traces shown in Fig. 43 - 49. The experimental DSC procedure was as follows:

1. Cut out small piece from the injection molded plaque, which weigh 6 to 13 mg, and place it into the aluminum pan.
2. Place sample and empty aluminum pans into the furnace or chamber.
3. Heat to 400 °C at a rate of 10 °C/min in nitrogen gas atmosphere (50ml/min).
4. Find an inflection point (T_g) from DSC trace before an exothermic peak and draw base lines to measure areas under the peaks.
5. According to Eq. 8 in Chapter 3.2, calculate the relative crystallinity of PEEK in the blend.

An example of calculation for the relative crystallinity (χ_c) of the 30% CFR 70/30 PEEK/PEI No. 13LT is followed:

from Fig. 49(a), $H_{endo} = 24.3$ mJ/mg

$H_{exo} = 10.7$ mJ/mg.

And $\Delta H_f = 130$ mJ/mg [19,40,42]

$\omega_{PEEK} = 0.49$.

Substitute above values into Eq. (8) and obtains

$$\chi_c = \frac{24.3 - 10.7}{130 \times 0.49} \times 100$$

$$\chi_c = 21.3.$$

Therefore the relative crystallinity of PEEK is 21.3%.

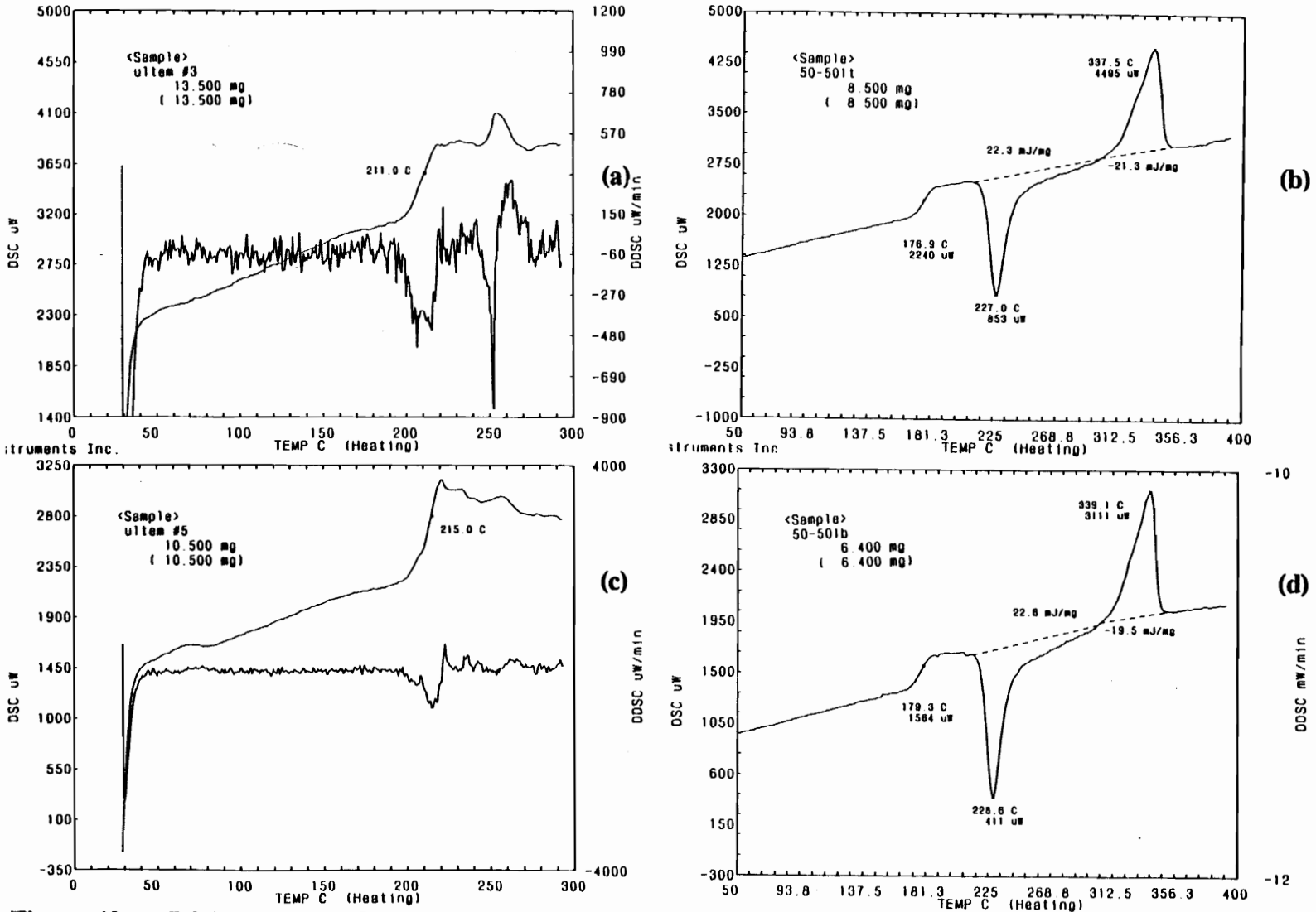

Figure 43. DSC traces for the untreated PEI and 50/50 blends: a)PEI 3 b)50/50 1T c)PEI 5 d)50/50 1B

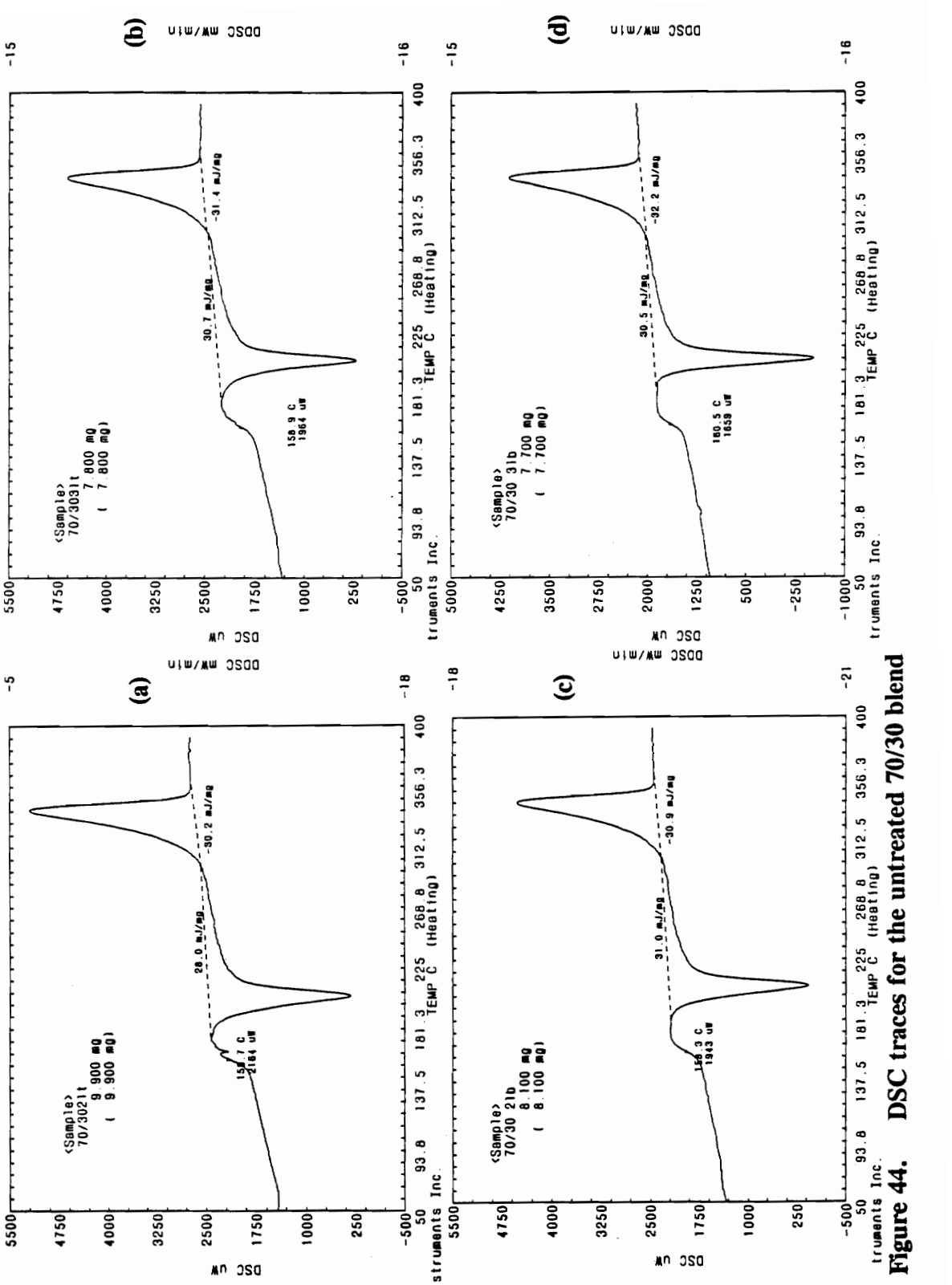

Figure 44. DSC traces for the untreated 70/30 blend

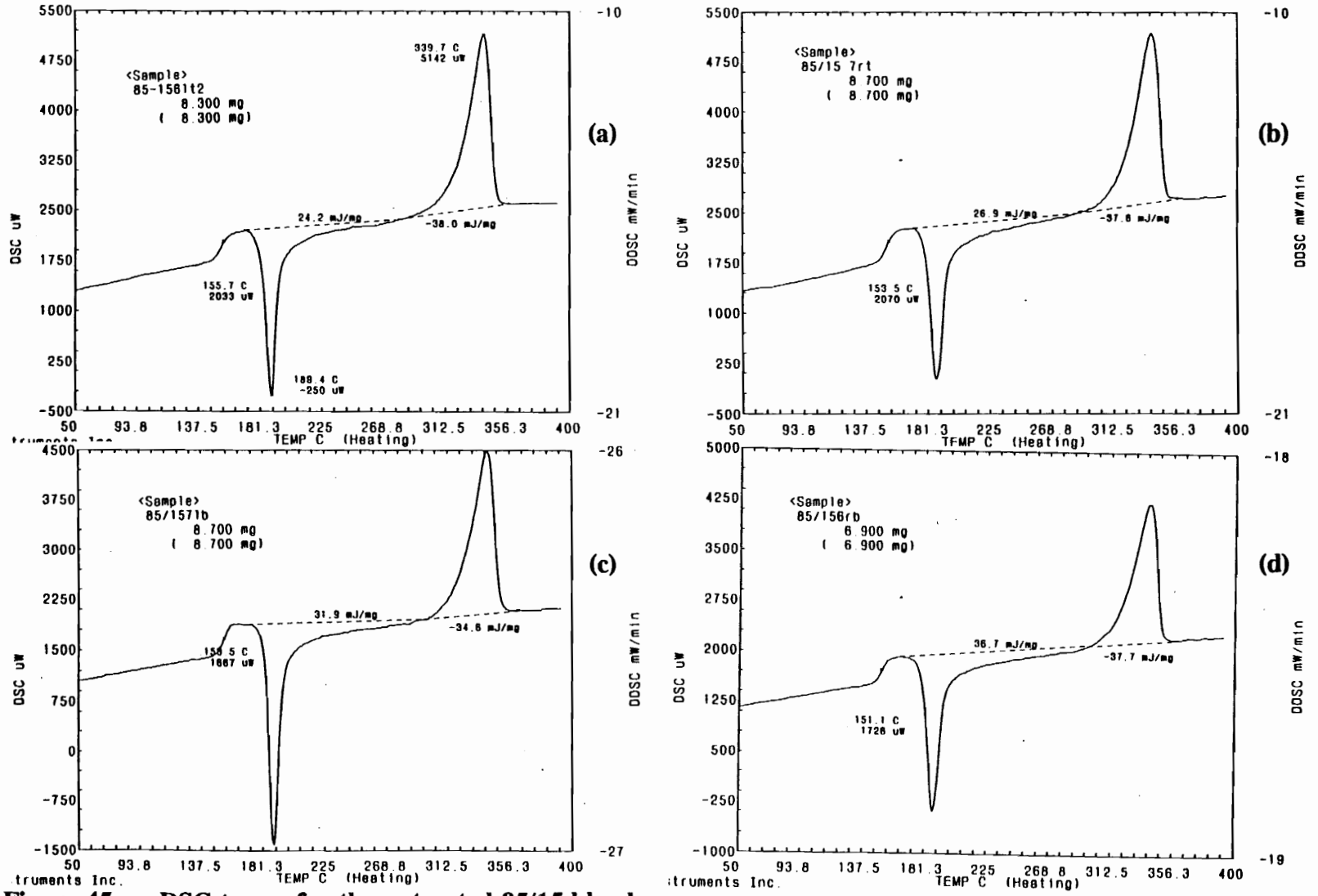

Figure 45. DSC traces for the untreated 85/15 blend

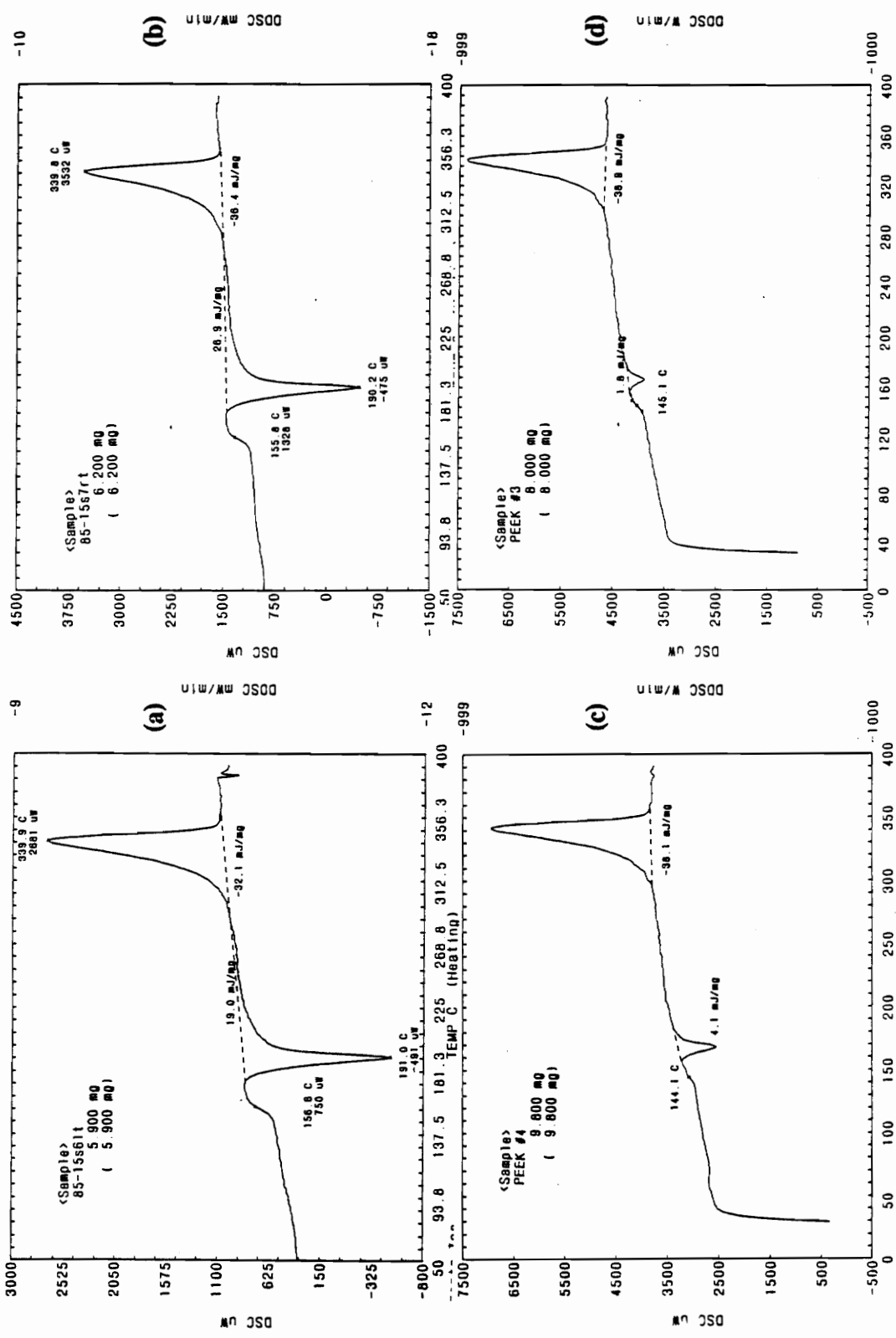

Figure 46. DSC traces for the untreated PEEK and 85/15 blends: a)85/15 S6LT b)85/15 S7RT (sample had collected from the surface of plaqe for 85/15) c)PEEK 4 d)PEEK 3

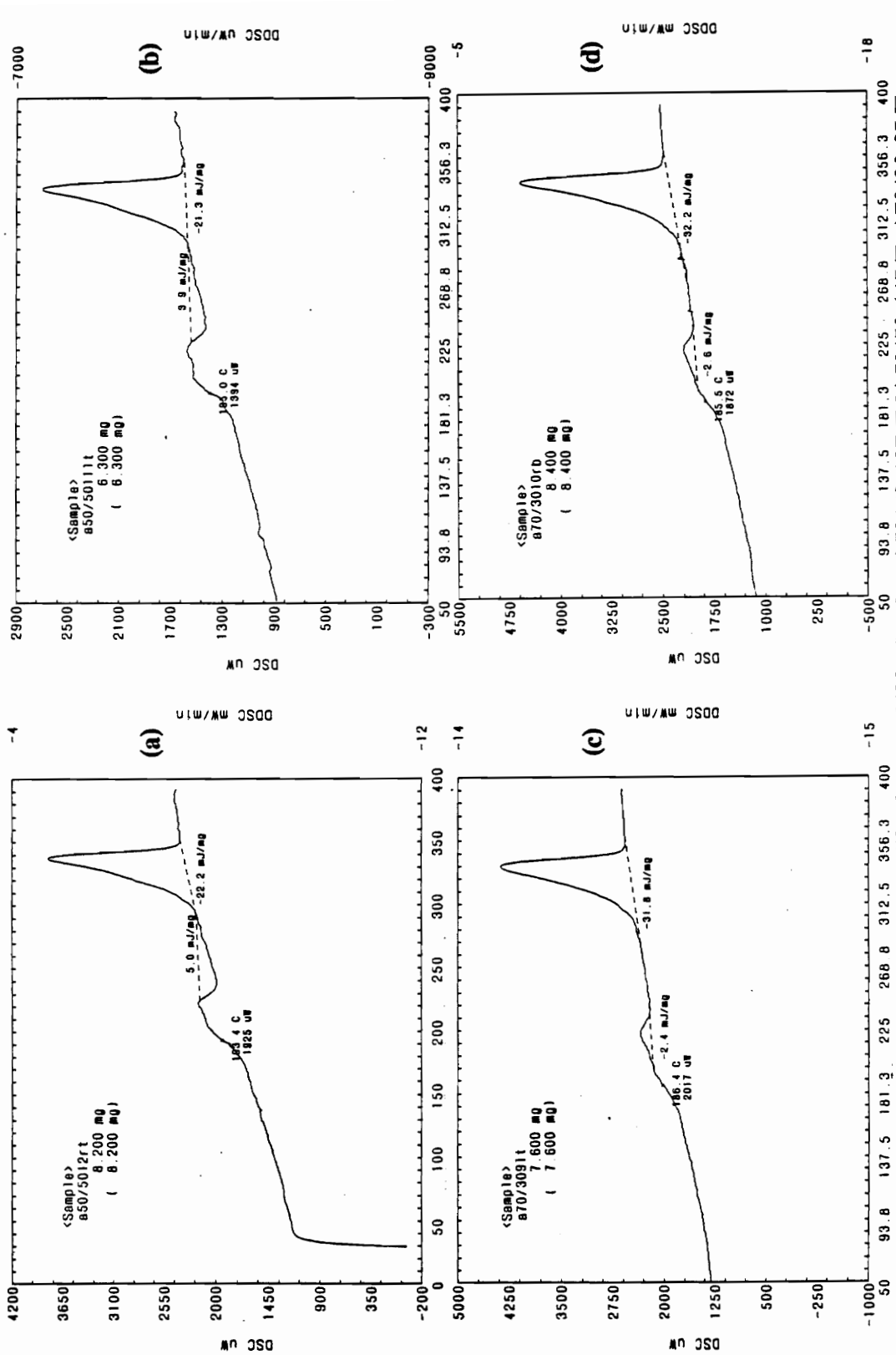

Figure 47. DSC traces for the annealed 50/50 and 70/30 blends: a)50/50 12RT b)50/50 11LT c)70/30 9LT d)70/30 10RB

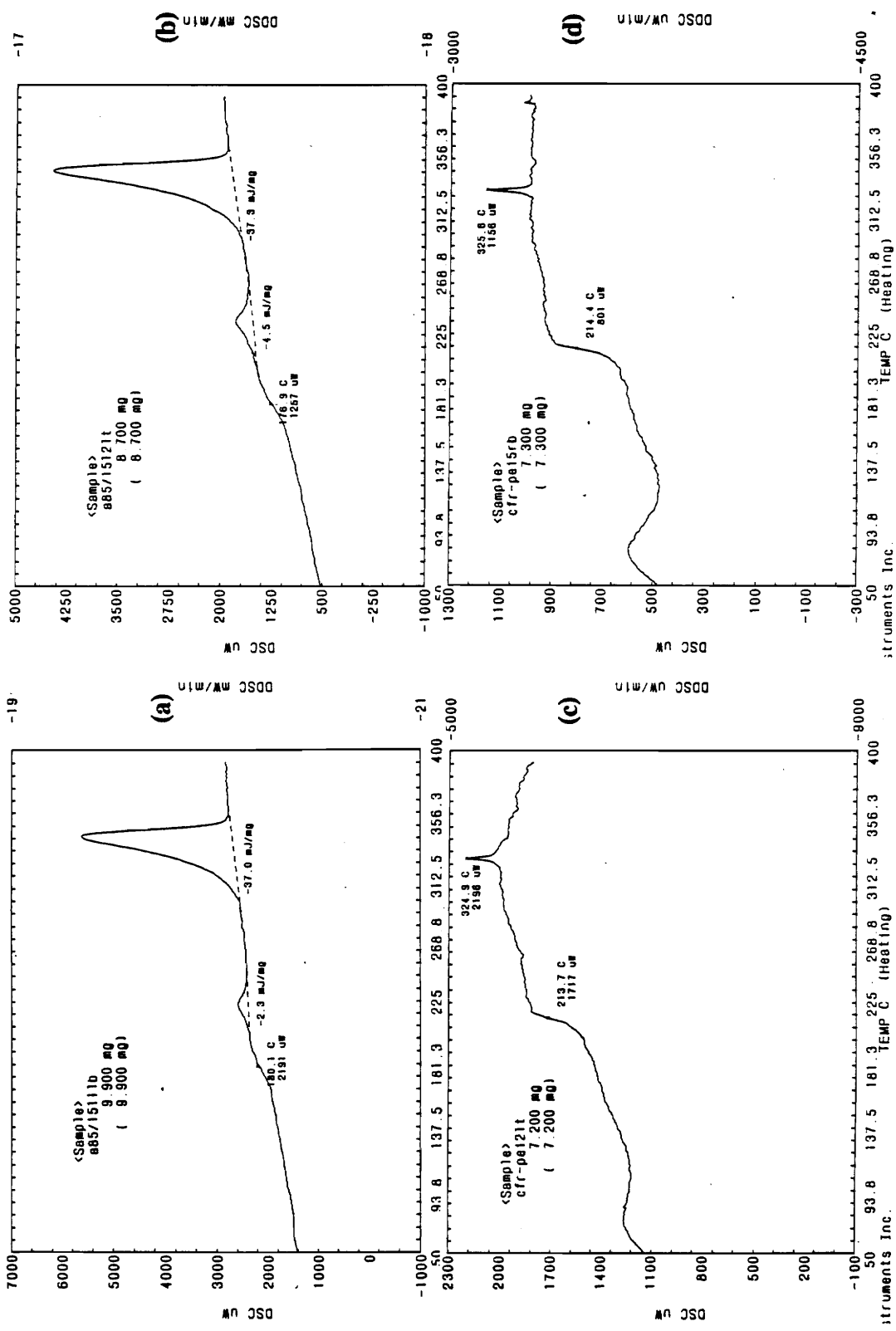

Figure 48. DSC traces for the annealed 85/15 (a & b) and CFR PEI(c & d)

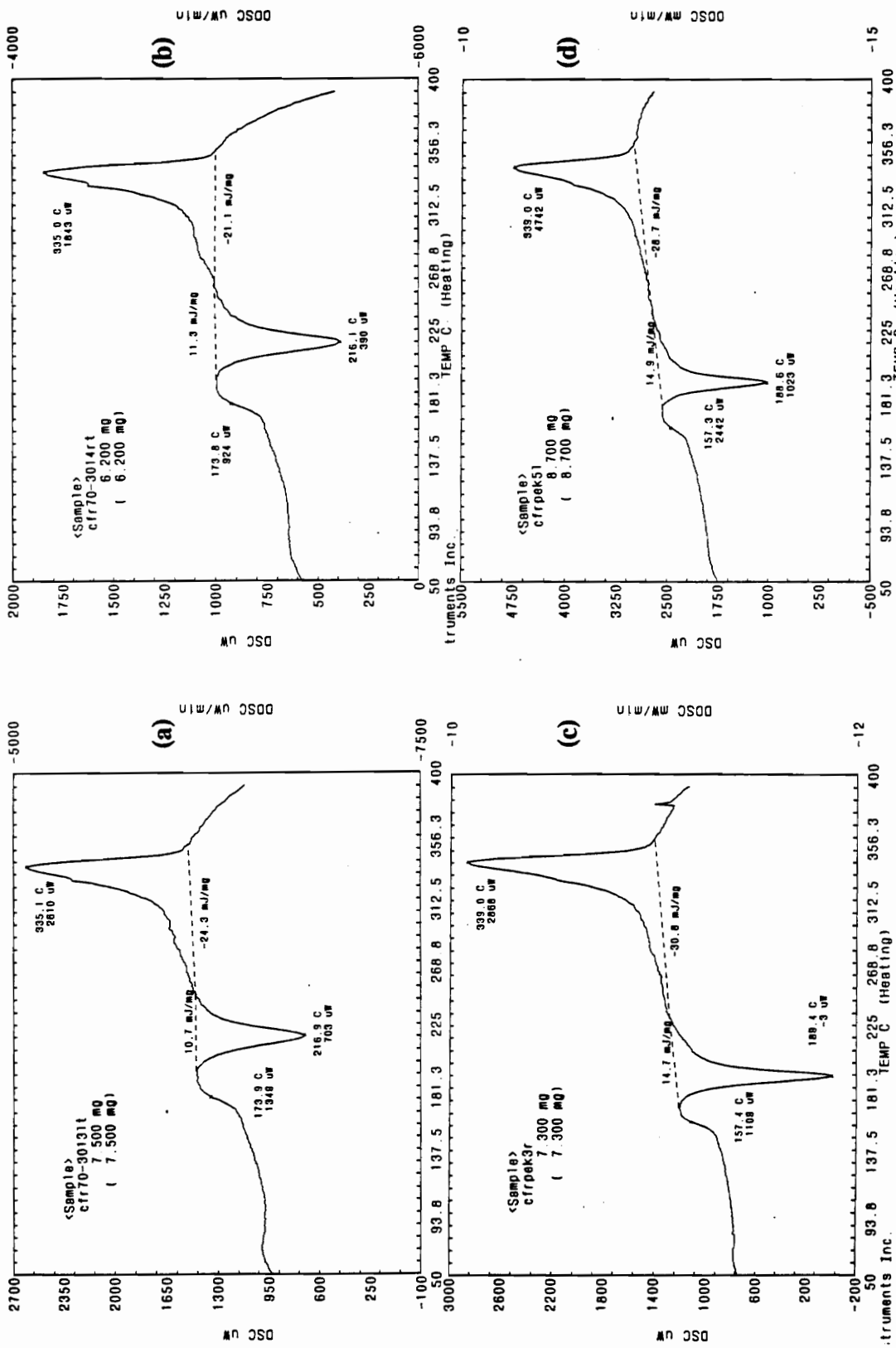

Figure 49. DSC traces for the CFR 70/30 (a & b) and PEEK (c & d)

D. Coefficient of Friction

In the following Tables 16 to 36, the coefficient of frictions at various number of cycles are listed. The steady state or kinetic coefficient of friction (μ_k) for each test is shown at the bottom of each table. "*" indicates the range of μ's which have averaged to obtain μ_k.

TABLE 16. Coefficient of friction : Untreated 100% PEEK

Test Conditions	5N-5cm/s		5N-15cm/s	
Specimens No.	5		4	
	Cycles	μ_k	Cycles	μ_k
	58	0.15	94	0.11
	95	0.17	847	0.11
	160	0.16	1775	0.11
	1273	0.14	2260	0.11
	1910	0.15	2744	0.11
	2355	0.15	3739	0.11
	2865	0.15		
	3151	0.14		
Average μ_k	0.15		0.11	

TABLE 17. Coefficient of friction : Untreated 50/50 (PEEK/PEI) @ 5N-5cm/s

Specimen No. 7		8		9	
Cycles	μ_k	Cycles	μ_k	Cycles	μ_k
5	0.18	18	0.20	9	0.18
153	0.18	71	0.26	59	0.19
459	0.22	189	0.27	168	0.25
* 589	0.24	* 372	0.30	* 354	0.28
1347	0.25	797	0.28	637	0.26
1683	0.24	1062	0.30	932	0.25
1989	0.25	1558	0.28	1221	0.27
2601	0.26	1947	0.29	1558	0.27
* 2901	0.25	2336	0.30	1829	0.27
		2832	0.31	3186	0.26
		3044	0.28	* 3398	0.25
		* 3505	0.31		
Average μ_k	0.25		0.29		0.26

TABLE 18. Coefficient of friction : Untreated 50/50 (PEEK/PEI) @ 5N-15cm/s

5		6		2RB	
Cycles	μ_k	Cycles	μ_k	Cycles	μ_k
57	0.11	76	0.14	10	0.17
688	0.23	497	0.14	100	0.25
936	0.23	1012	0.14	200	0.25
* 1490	0.26	2426	0.09	300	0.26
2979	0.28	3514	0.23	400	0.26
4125	0.32	* 4125	0.29	500	0.27
* 5271	0.29	4622	0.23	* 600	0.26
		5309	0.28	900	0.27
		6417	0.27	1200	0.27
		* 7563	0.26	1800	0.27
				2400	0.27
				2700	0.27
				3000	0.27
				* 3600	0.27
Average μ_k	0.29		0.27		0.27

TABLE 19. Coefficient of friction : Untreated 50/50 (PEEK/PEI) @ 15N-5cm/s

8		9		10	
Cycles	μ_k	Cycles	μ_k	Cycles	μ_k
5	0.09	5	0.06	4	0.10
46	0.11	92	0.13	122	0.23
268	0.25	328	0.24	* 458	0.25
* 566	0.27	* 588	0.26	825	0.25
734	0.27	794	0.27	1070	0.25
1204	0.27	1039	0.26	1436	0.27
1346	0.27	1345	0.26	1711	0.27
1693	0.26	1650	0.26	1986	0.27
1989	0.26	1986	0.27	* 2903	0.27
2433	0.26	2292	0.26		
2601	0.27	2567	0.27		
* 2938	0.26	* 2903	0.27		
Average μ_k	0.27		0.26		0.26

TABLE 20. Coefficient of friction : Untreated 50/50 (PEEK/PEI) @ 15N-15cm/s

2		3		4	
Cycles	μ_k	Cycles	μ_k	Cycles	μ_k
38	0.07	38	0.06	38	0.07
57	0.07	95	0.06	115	0.10
229	0.09	306	0.22	229	0.11
325	0.09	535	0.24	497	0.11
420	0.11	688	0.24	688	0.11
592	0.24	* 917	0.27	859	0.22
* 821	0.27	1375	0.27	1089	0.21
1089	0.24	1833	0.27	1261	0.24
1776	0.24	* 2292	0.30	* 1585	0.27
2292	0.28			2002	0.27
2636	0.29			2177	0.29
* 2979	0.29			2483	0.27
				2769	0.30
				* 2979	0.29
Average μ_k	0.27		0.28		0.28

TABLE 21. Coefficient of friction : Untreated 70/30 (PEEK/PEI) @ 5N-5cm/s

Cycles	3RB	2RB	1LB
10	0.23		
100	0.28	0.15	0.15
200	0.27	0.15	0.15
300	0.28	0.13	0.15
400	0.28	0.13	0.15
500	0.28	0.13	0.13
600	*0.25	*0.13	*0.11
900	0.25	0.13	0.13
1200	0.28	0.12	0.13
1500	0.26	0.13	0.13
1800	0.26	0.12	0.13
2100	*0.23	0.13	0.13
2400	0.13	0.13	0.13
2700	0.11	0.12	0.13
3000	0.13	*0.12	*0.13
Average μ_k	0.26	0.13	0.13

TABLE 22. Coefficient of friction : Untreated 70/30 (PEEK/PEI) @ 15N-5cm/s

Cycles	2RT	2RB
50	0.17	0.12
100	0.18	0.14
200	0.24	0.21
300	0.26	0.22
400	0.26	0.25
500	0.27	0.25
600	*0.27	*0.25
900	0.27	0.27
1200	0.27	0.27
1500	0.28	0.30
1800	0.29	0.30
2100	0.29	0.28
2400	0.29	0.29
2700	0.27	0.14
3000	0.27	0.20
3300	0.27	0.24
3600	*0.29	*0.27
Average μ_k	0.28	0.26

TABLE 23. Coefficient of friction : Untreated 70/30 (PEEK/PEI) @ 15N-15cm/s

Cycles	2RB	3RB	2RT	3RT
50			0.12	0.13
100	0.15	0.13	0.13	0.12
200	0.20	0.13	0.20	0.12
300	0.25	0.14	0.23	0.12
400	0.27	0.14	0.24	0.13
500	0.27	0.13	0.25	0.13
600	*0.28	*0.31	*0.27	0.13
900	0.29	0.32	0.30	*0.28
1200	0.29	0.32	0.30	0.31
1500	0.30	0.10	0.32	0.29
1800	0.29	0.10	0.32	0.30
2100	0.28	0.10	0.30	0.30
2400	0.29	0.10	0.30	0.30
2700	0.29	0.31	0.30	0.30
3000	0.29	0.33	0.30	0.31
3300	0.30	0.34	0.30	0.29
3600	*0.28	*0.34	*0.31	*0.29
Average μ_k	0.29	0.22	0.30	0.30

TABLE 24. Coefficient of friction : Untreated 85/15 (PEEK/PEI) @ 15N-5cm/s

Cycles	Bottom			Top	
	5RB	7RB	6LB	7LT	5RT
10	0.19	0.16	0.16	0.16	0.16
100	0.26	0.16	0.16	0.16	0.26
200	0.27	0.16	0.22	0.17	0.27
300	0.28	0.15	0.26	0.22	0.28
400	0.29	0.15	0.28	0.26	0.28
500	0.29	0.15	0.29	0.27	0.29
600	*0.29	*0.15	*0.29	*0.26	*0.29
900	0.28	0.14	0.30	0.27	0.29
1200	0.29	0.14	0.30	0.28	0.28
1500	0.28	0.14	0.29	0.26	0.28
1800	0.28	0.14	0.29	0.26	0.28
2100	0.28	0.13	0.29	0.27	0.27
2400	0.28	0.13	0.29	0.27	0.27
2700	0.28	0.13	0.28	0.27	0.26
3000	0.28	0.12	0.27	0.26	0.27
3300	0.27	0.12	0.28	0.26	0.26
3600	*0.27	*0.12	*0.29	*0.25	*0.27
Average μ_k	0.28	0.13	0.29	0.26	0.27

Bottom: specimens which were cut from the half of the plaque farthest to the manifold
Top : " " " closest "

TABLE 25. Coefficient of friction : Untreated 85/15 (PEEK/PEI) @ 15N-15cm/s

Cycles	Bottom		Top	
	7RB	5RB	7LT	5RT
10	0.15	0.24	0.17	0.14
100	0.16	0.22	0.16	0.17
200	0.16	0.24	0.15	0.29
300	0.16	0.19	0.15	0.30
400	0.16	0.27	0.14	0.29
500	0.16	0.27	0.14	0.30
600	0.16	*0.29	0.14	*0.30
900	0.13	0.26	*0.27	0.29
1200	0.13	0.28	0.28	0.30
1500	0.13	0.27	0.29	0.29
1800	0.13	0.28	0.29	0.30
2100	0.22	0.27	0.30	0.22
2400	*0.26	0.28	0.30	0.26
2700	0.26	0.26	0.27	0.26
3000	0.27	0.26	0.28	0.27
3300	0.26	0.27	0.28	0.27
3600	*0.27	*0.29	*0.28	*0.28
Average μ_k	0.26	0.27	0.28	0.28

Bottom: specimens which were cut from the half of the plaque farthest to the manifold
Top : " " " closest "

TABLE 26. Coefficient of friction : Untreated 100% PEI @ 5N-5cm/s

5		7		8	
Cycles	μ_k	Cycles	μ_k	Cycles	μ_k
32	0.26	7	0.16	12	0.25
*196	0.32	59	0.25	*248	0.27
319	0.32	177	0.25	540	0.27
574	0.28	354	0.25	936	0.27
878	0.30	*596	0.29	1139	0.28
1117	0.29	762	0.32	1452	0.27
1468	0.29	2338	0.32	1741	0.27
1851	0.29	2692	0.29	2054	0.26
2106	0.30	*3011	0.29	2375	0.25
2489	0.28			2621	0.26
2745	0.30			*3081	0.24
*3032	0.30				
Average μ_k	0.30	0.30		0.26	

TABLE 27. Coefficient of friction : Untreated 100% PEI @ 5N-15cm/s

1		2		3	
Cycles	μ_k	Cycles	μ_k	Cycles	μ_k
38	0.12	57	0.11	38	0.09
172	0.23	229	0.15	115	0.12
336	0.25	554	0.23	344	0.13
802	0.25	*688	0.25	*710	0.30
*1490	0.28	1261	0.26	917	0.25
2177	0.28	2177	0.26	1604	0.25
3094	0.28	2750	0.27	1948	0.28
*5539	0.28	4011	0.27	2330	0.27
		*6112	0.26	*6035	0.28
Average μ_k	0.28	0.26		0.27	

TABLE 28. Coefficient of friction : Untreated 100% PEI @ 15N-5cm/s

7		8		9	
Cycles	μ_k	Cycles	μ_k	Cycles	μ_k
5	0.13	5	0.08	10	0.16
46	0.27	31	0.09	100	0.21
*306	0.29	*183	0.25	200	0.29
550	0.29	458	0.25	300	0.28
764	0.32	1039	0.30	400	0.29
1070	0.32	1681	0.23	*600	0.29
1589	0.32	2688	0.28	900	0.30
2170	0.27	*3054	0.28	1500	0.30
*2903	0.31			1800	0.31
				2400	0.31
				2700	0.30
				*3000	0.30
Average μ_k	0.30	0.27		0.30	

TABLE 29. Coefficient of friction : Untreated 100% PEI @ 15N-15cm/s

Specimen No. 8			5A	10
Cycles	μ_k	Cycles	μ_k	μ_k
38	0.24	10	0.17	0.22
* 286	0.27	50	0.27	0.24
363	0.27	100	0.30	0.33
573	0.27	200	0.30	0.33
879	0.32	300	0.31	0.34
1031	0.28	400	0.31	0.34
* 1184	0.31	500	0.32	0.34
1375	*0.35	600	*0.32	*0.35
1489	0.36	900	0.32	0.34
1604	*0.37	1200	0.32	0.35
		1500	0.32	0.35
		1800	0.33	0.35
		2100	0.33	0.34
		2400	*0.33	0.35
		2700	0.36	0.35
		3000	0.37	*0.34
Average μ_k	0.36		0.32	0.35

TABLE 30. Coefficient of friction : Annealed 50/50 (PEEK/PEI) @ 5N-15cm/s & 15N-15cm/s

Cycles	5N-15cm/s			15N-15cm/s	
	11LB	11RC	12RC	12RC	11LB
10	0.18	0.21	0.19	0.12	0.17
100	0.17	0.23	0.17	0.23	0.23
200	0.21	0.25	0.22	0.27	0.25
300	0.21	0.23	0.21	0.27	0.29
400	0.21	0.26	0.21	0.28	0.31
500	0.23	0.24	0.22	0.30	0.30
600	*0.24	*0.27	*0.22	0.29	0.31
900	0.23	0.25	0.23	0.30	0.30
1200	0.25	0.24	0.23	*0.31	0.31
1500	0.24	0.23	0.23	0.31	0.31
1800	0.24	0.23	0.22	0.33	*0.32
2100	0.23	0.23	0.23	0.32	0.33
2400	0.23	0.22	0.23	0.31	0.34
2700	0.22	0.24	0.23	0.33	0.32
3000	*0.23	*0.24	*0.22	*0.32	*0.33
Average μ_k	0.23	0.24	0.23	0.32	0.33

TABLE 31. Coefficient of friction : Annealed 50/50 (PEEK/PEI) @ 15N-5cm/s

Cycles	12RC	11RC	13R
10	0.19	0.22	0.22
100	0.20	0.21	0.22
200	0.20	0.21	0.21
300	0.21	0.21	0.22
400	0.21	0.21	0.23
500	0.21	0.21	0.22
600	0.21	0.21	*0.23
900	0.22	0.21	0.21
1200	0.22	0.22	0.23
1500	0.21	*0.23	0.22
1800	0.22	0.22	0.23
2100	*0.24	0.23	0.22
2400	0.24	0.23	0.24
2700	0.24	0.23	0.23
3000	0.24	0.23	0.23
3300	0.25	0.24	0.24
3600	*0.25	*0.24	*0.24
Average μ_k	0.24	0.23	0.23

TABLE 32. Coefficient of friction : Annealed 70/30 (PEEK/PEI) @ 15N-5cm/s & 15N-15cm/s

Cycles	15N-5cm/s			15N-15cm/s		
	9RB	12RT	10LB	9RB	12RT	10RT
10	0.20	0.21	0.13	0.17	0.20	0.19
100	0.22	0.22	0.21	0.20	0.22	0.19
200	0.22	0.22	0.21	0.21	0.26	0.19
300	0.21	0.22	0.22	0.22	0.27	0.22
400	0.22	0.22	0.23	0.23	0.27	0.21
500	0.22	0.22	0.21	0.23	0.28	0.21
600	0.22	0.21	0.22	*0.24	*0.28	0.22
900	*0.24	0.23	*0.25	0.24	0.25	0.23
1200	0.24	0.23	0.24	0.25	0.25	0.23
1500	0.24	*0.25	0.25	0.25	0.25	0.22
1800	0.24	0.24	0.26	0.26	0.25	0.23
2100	0.24	0.23	0.24	0.25	0.26	*0.25
2400	0.25	0.24	0.24	0.25	0.26	0.24
2700	0.25	0.25	0.26	0.25	0.27	0.24
3000	0.25	0.26	0.27	*0.26	0.27	0.24
3300	0.24	0.24	0.24	0.15	0.26	0.24
3600	*0.24	*0.24	*0.27	0.21	*0.27	*0.24
Average μ_k	0.24	0.24	0.25	0.25	0.26	0.24

TABLE 33. Coefficient of friction : Annealed 85/15 (PEEK/PEI) @ 15N-5cm/s & 15N-15cm/s

Cyclrs	15N-5cm/s			15N-15cm/s	
	14RB	11RB	12RB	14RB	11RT
10	0.21	0.16	0.22	0.18	0.20
100	0.21	0.15	0.23	0.21	0.21
200	0.21	0.17	0.22	0.23	0.23
300	0.22	0.20	0.22	0.24	0.24
400	0.22	0.20	0.22	0.25	0.25
500	0.22	0.20	0.22	0.25	0.25
600	*0.21	0.22	0.22	*0.25	0.24
900	0.21	0.22	0.23	0.24	0.26
1200	0.22	0.21	*0.24	0.24	0.27
1500	0.21	0.22	0.22	0.25	*0.28
1800	0.21	*0.24	0.23	0.25	0.29
2100	0.21	0.24	0.22	0.24	0.28
2400	0.21	0.24	0.22	*0.24	0.29
2700	0.22	0.23	0.24	0.22	0.28
3000	0.23	0.23	0.23	0.22	*0.30
3300	0.22	0.25	0.24	0.22	0.25
3600	*0.22	*0.24	*0.24	0.20	0.25
Average μ_k	0.22	0.24	0.23	0.24	0.29

TABLE 34. Coefficient of friction : 30% CFR PEI @ 15N-5cm/s & 15N-15cm/s

Cycles	15N-5cm/s			15N-15cm/s		
	1LB	2RT	4LT	1LB	2RT	4LT
10	0.25	0.22	0.25	0.26	0.20	0.16
100	*0.29	0.28	*0.29	*0.29	0.27	*0.28
200	0.29	0.29	0.30	0.29	0.28	0.28
300	0.30	*0.30	0.29	0.29	*0.29	0.28
400	0.30	0.30	0.30	0.29	0.29	0.28
500	*0.30	0.30	0.30	*0.29	0.29	0.28
600	0.32	*0.30	*0.30	0.30	*0.29	*0.28
900	0.33	0.31	0.31	0.31	0.31	0.31
1200	0.34	0.32	0.32	0.33	0.32	0.32
1500	0.34	0.34	0.34	0.34	0.34	0.35
1800	0.34	0.34	0.35	0.35	0.35	0.35
2100	0.35	0.36	0.36	0.36	0.36	0.35
2400	0.36	0.36	0.37	0.37	0.37	0.36
2700	0.37	0.38	0.36	0.38	0.38	0.38
3000	0.37	0.39	0.36	0.38	0.38	0.38
3300	0.37	0.39	0.38	0.39	0.39	0.39
3600	0.37	0.39	0.38	0.39	0.40	0.39
Average μ_k	0.30	0.30	0.30	0.29	0.29	0.28

TABLE 35. Coefficient of friction : 30% CFR 70/30 (PEEK/PEI) @ 15N-5cm/s & 15N-15cm/s

Cycles	15N-5cm/s			15N-15cm/s		
	10LT	14LT	11LT	10LT	11LT	12LT
10	0.18	0.14	0.20	0.15	0.19	0.14
100	0.22	0.22	0.22	0.16	0.22	0.21
200	0.23	0.23	0.23	0.22	0.22	0.21
300	0.23	0.23	0.23	0.23	0.23	0.21
400	0.23	0.23	0.23	0.23	0.23	0.23
500	0.23	0.24	0.23	0.24	0.23	0.23
600	*0.23	*0.24	*0.24	*0.24	0.23	0.23
900	0.23	0.24	0.24	0.24	0.24	0.23
1200	0.23	0.24	0.24	0.24	0.24	0.23
1500	0.24	0.24	0.24	0.24	*0.25	*0.24
1800	0.24	0.24	0.24	0.25	0.24	0.24
2100	0.24	0.25	0.25	0.25	0.24	0.25
2400	0.24	0.25	0.25	0.25	0.24	0.25
2700	0.25	0.26	0.24	0.25	0.25	0.25
3000	0.25	0.25	0.24	*0.25	0.25	0.25
3300	0.26	0.26	0.26		0.26	0.25
3600	*0.26	*0.26	*0.26		*0.26	*0.25
Average μ_k	0.24	0.25	0.25	0.25	0.25	0.25

TABLE 36. Coefficient of friction : 30% CFR PEEK @ 15N-5cm/s & 15N-15cm/s

Cycles	15N-5cm/s			15N-15cm/s		
	2L	3L	4L	2L	3L	5R
10	0.18	0.20	0.16	0.19	0.18	0.15
100	0.21	0.22	0.21	0.21	0.23	0.20
200	0.21	0.23	0.23	0.22	0.23	0.20
300	0.22	0.23	0.23	0.22	0.23	0.21
400	0.22	0.23	0.23	0.22	0.23	0.21
500	0.22	0.23	0.24	0.22	0.23	0.21
600	0.22	0.23	*0.24	0.22	*0.23	*0.21
900	*0.24	0.24	0.24	*0.23	0.23	0.21
1200	0.24	0.24	0.24	0.23	0.23	0.21
1500	0.23	0.24	0.24	0.23	0.24	0.22
1800	0.24	*0.24	0.24	0.24	0.24	0.22
2100	0.24	0.23	0.25	0.24	0.23	0.22
2400	0.24	0.23	0.25	0.24	0.23	0.23
2700	0.24	0.24	0.25	0.24	0.25	0.23
3000	0.24	0.24	0.25	0.24	0.25	0.23
3300	0.24	0.24	0.25	0.24	0.26	0.24
3600	*0.24	*0.24	*0.26	*0.24	*0.27	*0.24
Average μ_k	0.24	0.24	0.25	0.24	0.24	0.22

E. Wear Rates

Cross-sectional area of wear track at each 600 cycle and wear rate for each test are listed in Table 37 to 45. A linear correlation (Eq. E1) on cross-sectional wear area versus number of cycles was performed and a correlation coefficient is expressed as the wear rate.

$$\underset{(10^{-6}\ mm^2)}{\textit{Wear Area}} = \underset{(10^{-6}mm^2/cycle)}{\textit{Wear Rate}} \times \textit{No. of Cycles} + \underset{(10^{-6}\ mm^2)}{\textit{Constant}} \qquad \text{(E1)}$$

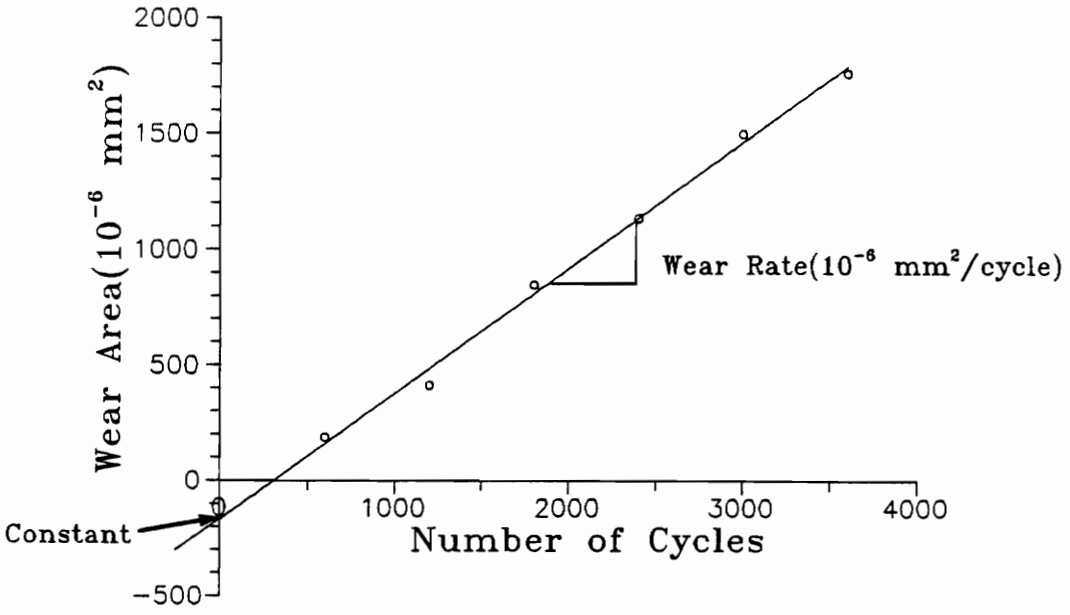

Figure 50. Schematic representation of the linear correlation on crossectional wear area versus number of cycles

TABLE 37. Wear areas (10^{-6} mm^2) for the Untreated 100% PEI @ 5N-5cm/s & 5N-15cm/s

Sample No.	5		7		8	
Load/Speed	Cycles	Area	Cycles	Area	Cycles	Area
5N-5cm/s	638	1295	605	1095	605	1395
	1284	2887	1065	2170	1065	2460
	1915	4337	1771	4040	1771	3988
	2553	5774	2485	5560	2485	5600
	3191	6570	3188	7475	3188	7425
	Wear Rate	2.107		2.452		2.310
	Constant	133		-403		-36
	r^2	0.988		0.999		0.999
Sample No.	1		2		3	
Load/Speed	Cycles	Area	Cycles	Area	Cycles	Area
5N-15cm/s	458	760	726	675	1031	920
	1375	3550	1406	3000	1833	2875
	2292	5210	2292	5240	2750	5425
	3438	7975	3438	7900	3896	7875
	5615	13300	6169	13850	6085	13075
	Wear Rate	2.386		2.369		2.397
	Constant	-130		-516		-1443
	r^2	0.998		0.995		0.999

Wear Rate (10^{-6} mm^2/cycle), Constant (10^{-6} mm^2)

TABLE 38. Wear areas (10^{-6} mm^2) for the Untreated 100% PEI @ 15N-5cm/s & 15N-15cm/s

Sample No.	7		8		9				
Load/Speed	Cycles	Area	Cycles	Area	Cycles	Area			
15N-5cm/s	611	5375	626	6000	600	6175			
	1222	9550	1222	9300	1200	12450			
	1833	14875	1833	15700	1800	18250			
	2445	20600	2443	21300	2400	23850			
	3056	25700	2932	25800	3000	28700			
	Wear Rate	8.457		8.830		9.408			
	Constant	-286		-392		950			
	r^2	0.998		0.992		0.998			
Sample No.	6		7		8			5A	10
Load/Speed	Cycles	Area	Cycles	Area	Cycles	Area	Cycles	Area	
15N-15cm/s	164	3700	229	5300	229	5875	600	31700	51150
	401	15750	477	10300	516	16100	1200	71900	99750
	630	31300	802	22600	917	40900	1800	105550	142100
	1031	66600	1261	62050	1261	63000	2400	135750	161270
	1375	100300			1719	113450	3000	164700	224100
	Wear Rate	80.940		55.490		71.275		54.975	67.903
	Constant	-14760		-13350		-18308		2965	13448
	r^2	0.988		0.926		0.926		0.995	0.979

Wear Rate (10^{-6} mm^2/cycle), Constant (10^{-6} mm^2)

TABLE 39. Wear areas (10^{-6} mm^2) for the Untreated 50/50 (PEEK/PEI) @ 5N-5cm/s & 5N-15cm/s

Sample No.	7		8		9	
Load/Speed	Cycles	Area	Cycles	Area	Cycles	Area
5N-5cm/s	612	385	708	425	920	540
	1224	699	1434	920	1575	910
	1837	1288	2124	1245	2195	1350
	2449	1588	2859	2040	2885	2135
	3061	2388	3618	2610	3540	2460
	Wear Rate	0.799		0.758		0.774
	Constant	-199		-182		-242
	r^2	0.974		0.986		0.984
Sample No.	5		6		2RB	
Load/Speed	Cycles	Area	Cycles	Area	Cycles	Area
5N-15cm/s	1146	800	3629	735	600	2888
	1875	2288	4716	2140	1200	4050
	3438	3525	5895	4400	1800	5923
	4584	4163	7074	6025	2400	7100
	5730	6363	8567	5520	3000	8075
					3600	8650
					4800	10075
	Wear Rate	1.080		1.074		1.733
	Constant	-750		-2656		2376
	r^2	0.995		0.849		0.959

Wear Rate (10^{-6} mm^2/cycle), Constant (10^{-6} mm^2)

TABLE 40. Wear areas (10^{-6} mm^2) for the Untreated 50/50 (PEEK/PEI) @ 15N-5cm/s & 15N-15cm/s

Sample No.	8		9		10	
Load/Speed	Cycles	Area	Cycles	Area	Cycles	Area
15N-5cm/s	612	1136	612	2000	612	2550
	1224	3300	1224	3875	1224	4710
	1833	4825	1833	5840	1833	5650
	2448	7350	2448	6950	2448	8500
	3060	8850	3060	9430	3060	10700
	Wear Rate	3.183		2.920		3.283
	Constant	-750		241		396
	r^2	0.995		0.990		0.981
Sample No.	2		3		4	
Load/Speed	Cycles	Area	Cycles	Area	Cycles	Area
15N-15cm/s	638	2810	344	2490	917	1885
	1031	12500	802	25300	1375	14900
	1375	23900	1146	31800	1833	46750
	1833	41900	1604	72200	2292	80400
	3094	153100	2521	141900	3094	151300
	Wear Rate	62.650		64.990		70.320
	Constant	-53033		-28676		-74722
	r^2	0.941		0.972		0.975

Wear Rate (10^{-6} mm^2/cycle), Constant (10^{-6} mm^2)

TABLE 41. Wear areas (10^{-6} mm^2) for the Untreated 70/30 and 85/15 (PEEK/PEI) @ 15N-5cm/s & 15N-15cm/s

		15N-5cm/s					15N-15cm/s			
70/30	Cycles	2RT	2RB	3RB	1RB		2RB	3RB	2RT	3RT
	600	675	625	38	75		1050	150	950	138
	1200	1750	14125	13	150		2288	1638	2225	4600
	1800	2513	2375	63	125		2600	3075	2525	6725
	2400	3350	3325	100	150		2625	2450	3550	6975
	3000	4100	3025	75	175		3975	3775	4525	7725
	3600	4825	4050	113	175		3975	3750	5150	7750
	Wear Rate	1.363	1.091	0.028	0.028		0.938	1.132	1.377	2.270
	Constant	5	178	7	82		781	94	262	883
	r^2	0.996	0.930	0.724	0.726		0.904	0.826	0.985	0.754
85/15	Cycles	7RB	6LB	5RB	7LT	5RT	7RB	5RB	7LT	5RT
	600	388	625	775	188	263	87	313	275	813
	1200	425	575	1263	500	900	188	763	750	938
	1800	500	938	1225	838	738	250	775	875	1088
	2400	600	1125	1213	1075	913	488	888	1325	1213
	3000	613	1450	1563	1313	1275	725	938	1700	1300
	3600	688	1438	1650	1563	1500	550	875	1750	1625
	Wear Rate	0.102	0.327	0.250	0.454	0.356	0.198	0.164	0.508	0.251
	Constant	319	338	755	-43	183	-35	413	45	635
	r^2	0.974	0.924	0.825	0.994	0.863	0.828	0.650	0.9656	0.96

Wear Rate (10^{-6} mm^2/cycle), Constant (10^{-6} mm^2)

TABLE 42. Wear areas (10^{-6} mm^2) for the Annealed 50/50 (PEEK/PEI) @ 5N-15cm/s, 15N-5cm/s & 15N-15cm/s

	5N-15cm/s			15N-5cm/s		
Cycles	11LB	11RC	12RC	12RC	11RC	13R
600	188	163	138	675	788	775
1200	413	425	325	1488	1225	1350
1800	850	638	738	1888	1763	1988
2400	1138	1025	838	2838	2350	3038
3000	1500	1213	1288	3463	2838	3750
3600	1763			4175	3588	4638
Wear Rate	0.558	0.450	0.468	1.160	0.925	1.312
Constant	-186	-118	-179	-17	149	-167
r^2	0.993	0.990	0.969	0.994	0.994	0.993

15N-15cm/s	Cycles	12RC	11LB	11RC	12LT
	600	9438	12850	23700	27600
	1200	16700	18200	39000	38400
	1800	26000	27950	40000	44350
	2400	30300	39700	41250	46250
	3000	36750	44750	43550	48250
	Wear Rate	11.370	14.216	6.991	8.191
	Constant	3370	3100	24915	26225
	r^2	0.987	0.982	0.705	0.870

Wear Rate (10^{-6} mm^2/cycle), Constant (10^{-6} mm^2)

TABLE 43. Wear areas (10^{-6} mm^2) for the Annealed 70/30 and 85/15 (PEEK/PEI) @ 15N-5cm/s & 15N-15cm/s

		15N-5cm/s			15N-15cm/s		
70\30	Cycles	9RB	12RT	10LB	9RB	12RT	10RT
	600	825	838	713	338	463	513
	1200	1300	1613	1225	588	838	638
	1800	1688	1375	1675	775	1113	850
	2400	1625	1775	1775	1013	1275	1075
	3000	1913	1863	1963	1063	1513	1325
	3600	2000	2475	2450	1113	1613	1500
	Wear Rate	0.364	0.444	0.523	0.263	0.377	0.344
	Constant	793	723	533	261	342	261
	r^2	0.884	0.843	0.954	0.932	0.966	0.993
85\15	Cycles	14RB	11RB	12RB	14RB	11RT	
	600	475	688	188	213	475	
	1200	675	788	263	350	913	
	1800	750	988	363	475	925	
	2400	838	963	525	550	1225	
	3000	1000	1213	588	700	1513	
	3600	1075	1175	550	825	1625	
	Wear Rate	0.193	0.175	0.140	0.199	0.373	
	Constant	396	600	118	100	328	
	r^2	0.979	0.906	0.902	0.995	0.960	

Wear Rate (10^{-6} mm^2/cycle), Constant (10^{-6} mm^2)

TABLE 44. Wear areas (10^{-6} mm^2) for the 30% CFR PEI and PEEK @ 15N-5cm/s & 15N-15cm/s

		15N-5cm/s			15N-15cm/s		
P E I	Cycles	1LB	2RT	4LT	1LB	2RT	4LT
	600	1975	1575	1325	2725	1200	1867
	1200	2875	2900	3100	5100	1800	4125
	1800	4375	3800	3700	6175	2925	4100
	2400	5225	4325	5150	7400	3700	4925
	3000	4975	5275	4975	8175	4875	6975
	3600	6175	5875	6275	8750	4450	6550
	Wear Rate	1.340	1.388	1.515	1.932	1.250	1.561
	Constant	1452	1043	905	2330	5333	1478
	r^2	0.913	0.9815	0.936	0.944	0.925	0.886
P E E K	Cycles	2L	3L	4L	2L	3L	5R
	600	800	713	950	1550	1725	800
	1200	1225	1088	1263	1800	1450	888
	1800	1575	1250	1225	2525	1700	1288
	2400	1725	1238	1363	2800	2225	1875
	3000	1675	1488	1363	2175	2300	2463
	3600	1738	1538	1638	3625	2525	2325
	Wear Rate	0.294	0.252	0.184	0.560	0.336	0.616
	Constant	838	688	913	1235	1280	313
	r^2	0.784	0.899	0.854	0.725	0.809	0.923

Wear Rate (10^{-6} mm^2/cycle), Constant (10^{-6} mm^2)

TABLE 45. Wear areas (10^{-6} mm^2) for the 30% CFR 70/30 (PEEK/PEI) @ 15N-5cm/s & 15N-15cm/s

	15N-5cm/s			15N-15cm/s		
Cycles	10LT	14LT	11LT	10LT	11LT	12LT
600	675	513	438	413	488	538
1200	763	700	575	625	713	838
1800	1013	600	850	738	550	1025
2400	988	863	1150	825	1075	1088
3000	1088	1163	1150	1350	988	1475
3600	1425	1425	1475		900	1500
Wear Rate	0.223	0.295	0.343	0.345	0.227	0.323
Constant	522	256	218	168	354	398
r^2	0.901	0.885	0.967	0.884	0.684	0.956

Wear Rate (10^{-6} mm^2/cycle), Constant (10^{-6} mm^2)

F. SAS

The two-way analysis of variance (ANOVA) had been performed to study the effect of load and/or speed on wear rates of the untreated PEI and 50/50 blend. A 0.05 level of significance was used to test the following hypothesis: (a) H_0^1 :there is no difference in the mean wear rates when different loads are used; (b) H_0^2 : there is no difference in the mean wear rates of the 2 different speeds; (c) H_0^3 : there is no interaction between the different loads and the different speeds. Results of ANOVA rejected all above hypotheses.

The Duncan's multiple-range tests were conducted to compare the wear rates of all samples run at each test condition (i.e., 5N-15cm/s, 15N-5cm/s, and 15N-15cm/s). Two-way ANOVA SAS programs and tables of input data and results followed by those of Duncan's tests are listed in the following pages. Each sample in Duncan's multiple-range tests was denoted numerably according to the following:

Sample No. 1 = Untreated 100% PEI

2 = Untreated 50/50 PEEK/PEI blend

3 = Untreated 70/30 PEEK/PEI blend

4 = Untreated 85/15(B) blend (sample from the farthest to the manifold)

5 = Untreated 85/15(T) blend (closest to the manifold)

6 = Annealed 50/50 blend

7 = Annealed 70/30 blend

8 = Annealed 85/15 blend

9 = 30% CFR PEI

10 = 30% CFR 70/30 PEEK/PEI blend

11 = 30% CFR PEEK.

Because of too much weight on a very large value of a sample compared to others during the pair-wise comparisons, Duncan's multiple range test sometimes grouped together small value samples even though their mean values were different. Therefore several subsequent multiple-range tests were performed after eliminating a group of large sample values.

2-Way ANOVA SAS output : Untreated 100% PEI

```
//PEI JOB XXXXX,SAS,CLASS=Q,JHY
1          SAS(R) LOG   OS SAS 5.18

NOTE: COPYRIGHT (C) 1984,1988 SAS INSTITUTE INC., CARY, N.C.  27512, U.S.A.
NOTE: THE JOB $$$$$Q17 HAS BEEN RUN UNDER RELEASE 5.18 OF SAS
      AT VIRGINIA TECH COMPUTING CENTER (01798001).
NOTE: CPUID    VERSION = 66  SERIAL = 120667  MODEL = 3084 .
      CPUID    VERSION = 66  SERIAL = 320667  MODEL = 3084 .
NOTE: NO OPTIONS SPECIFIED.

2229       OPTIONS LS=80;
2230       TITLE '2-WAY ANOVA UNTREATED 100%PEI';
2231       DATA;
2232       INPUT LOAD SPEED HEARRATE; LIST;
2233       CARDS;

RULE:      ----+----1----+----2----+----3----+----4----+----5----+----6----+----7
2232       5 5 2.107
2233       5 5 2.452
2234       5 5 2.310
2235       5 15 2.386
2236       5 15 2.369
2237       5 15 2.397
2238       15 5 8.457
2239       15 5 8.830
2240       15 5 9.408
2241       15 15 80.940
2242       15 15 55.490
2243       15 15 71.275
2244       15 15 54.975
2245       15 15 67.903
NOTE: DATA SET WORK.DATA18 HAS 14 OBSERVATIONS AND 3 VARIABLES. 1676 OBS/TRK.
NOTE: THE DATA STATEMENT USED 0.12 SECONDS AND 536K.

2248       PROC CHART;
2249       BLOCK LOAD / SUMVAR=HEARRATE GROUP=SPEED DISCRETE;
NOTE: THE PROCEDURE CHART USED 0.17 SECONDS AND 600K
      AND PRINTED PAGE 1.

2250       PROC ANOVA;
2251       CLASSES LOAD SPEED;
2252       MODEL HEARRATE = LOAD SPEED LOAD*SPEED;
2253       MEANS LOAD SPEED LOAD*SPEED / DUNCAN;
NOTE: THE PROCEDURE ANOVA USED 0.23 SECONDS AND 804K
```

BLOCK CHART OF HEARRATE SUMS

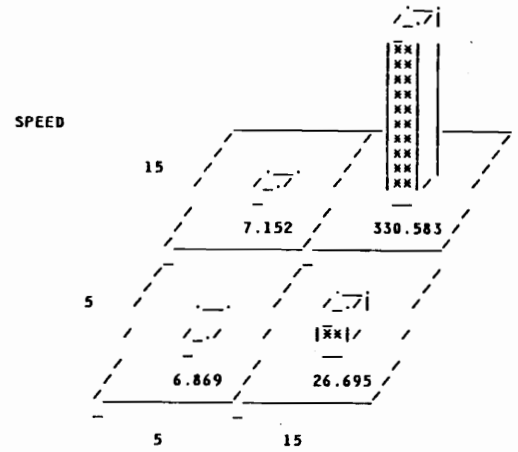

2-WAY ANOVA UNTREATED 100%PEI

ANALYSIS OF VARIANCE PROCEDURE

CLASS LEVEL INFORMATION

CLASS	LEVELS	VALUES
LOAD	2	5 15
SPEED	2	5 15

NUMBER OF OBSERVATIONS IN DATA SET = 14

2-WAY ANOVA UNTREATED 100%PEI

ANALYSIS OF VARIANCE PROCEDURE

DEPENDENT VARIABLE: HEARRATE

2-Way ANOVA SAS output : Untreated 100% PEI

ANALYSIS OF VARIANCE PROCEDURE

DEPENDENT VARIABLE: HEARRATE

PEI OUTPUT

SOURCE	DF	SUM OF SQUARES	MEAN SQUARE	F VALUE
MODEL	3	12279.98968868	4093.32989623	84.03
ERROR	10	487.11311653	48.71131165	PR > F
CORRECTED TOTAL	13	12767.10280521		0.0001

R-SQUARE	C.V.	ROOT MSE	HEARRATE MEAN
0.961846	26.3160	6.97934894	26.52135714

SOURCE	DF	ANOVA SS	F VALUE	PR > F
LOAD	1	6141.35751488	126.08	0.0001
SPEED	1	4598.51990834	94.40	0.0001
LOAD*SPEED	1	1540.11226546	31.62	0.0002

2-WAY ANOVA UNTREATED 100%PEI

ANALYSIS OF VARIANCE PROCEDURE

DUNCAN'S MULTIPLE RANGE TEST FOR VARIABLE: HEARRATE
NOTE: THIS TEST CONTROLS THE TYPE I COMPARISONWISE ERROR RATE, NOT THE EXPERIMENTWISE ERROR RATE

ALPHA=0.05 DF=10 MSE=48.7113

WARNING: CELL SIZES ARE NOT EQUAL.
HARMONIC MEAN OF CELL SIZES=6.85714

NUMBER OF MEANS 2
CRITICAL RANGE 8.38337

MEANS WITH THE SAME LETTER ARE NOT SIGNIFICANTLY DIFFERENT.

DUNCAN GROUPING	MEAN	N	LOAD
A	44.660	8	15
B	2.337	6	5

2-WAY ANOVA UNTREATED 100%PEI

ANALYSIS OF VARIANCE PROCEDURE

DUNCAN'S MULTIPLE RANGE TEST FOR VARIABLE: HEARRATE
NOTE: THIS TEST CONTROLS THE TYPE I COMPARISONWISE ERROR RATE, NOT THE EXPERIMENTWISE ERROR RATE

ALPHA=0.05 DF=10 MSE=48.7113

WARNING: CELL SIZES ARE NOT EQUAL.
HARMONIC MEAN OF CELL SIZES=6.85714

NUMBER OF MEANS 2
CRITICAL RANGE 8.38337

MEANS WITH THE SAME LETTER ARE NOT SIGNIFICANTLY DIFFERENT.

DUNCAN GROUPING	MEAN	N	SPEED
A	42.217	8	15
B	5.594	6	5

2-WAY ANOVA UNTREATED 100%PEI

ANALYSIS OF VARIANCE PROCEDURE

MEANS

LOAD	SPEED	N	HEARRATE
5	5	3	2.2896667
5	15	3	2.3840000
15	5	3	8.8983333
15	15	5	66.1166000

2-Way ANOVA SAS output : Untreated 50/50 PEEK/PEI blend

```
//U5050 JOB XXXXX,SAS,CLASS=Q,JHY
1          SAS(R) LOG   OS SAS 5.18

NOTE: COPYRIGHT (C) 1984,1988 SAS INSTITUTE INC., CARY, N.C.  27512, U.S.A.
NOTE: THE JOB $$$$$Q17 HAS BEEN RUN UNDER RELEASE 5.18 OF SAS
      AT VIRGINIA TECH COMPUTING CENTER (01798001).
NOTE: CPUID    VERSION = 66  SERIAL = 120667  MODEL = 3084 .
      CPUID    VERSION = 66  SERIAL = 320667  MODEL = 3084 .
NOTE: NO OPTIONS SPECIFIED.

2300       OPTIONS LS=80;
2301       TITLE '2-WAY ANOVA UNTREATED 50/50 PEI/PEEK';
2302       DATA;
2303       INPUT LOAD SPEED WEARRATE; LIST;
2304       CARDS;

RULE:      ----+----1----+----2----+----3----+----4----+----5----+----6----+----7
2305       5 5 0.799
2306       5 5 0.758
2307       5 5 0.774
2308       5 15 1.080
2309       5 15 1.074
2310       5 15 1.733
2311       15 5 3.183
2312       15 5 2.920
2313       15 5 3.283
2314       15 15 62.65
2315       15 15 64.99
2316       15 15 70.32
NOTE: DATA SET WORK.DATA21 HAS 12 OBSERVATIONS AND 3 VARIABLES. 1676 OBS/TRK.
NOTE: THE DATA STATEMENT USED 0.12 SECONDS AND 536K.

2317       PROC CHART;
2318       BLOCK LOAD / SUMVAR=WEARRATE GROUP=SPEED DISCRETE;
NOTE: THE PROCEDURE CHART USED 0.17 SECONDS AND 600K
      AND PRINTED PAGE 1.

2319       PROC ANOVA;
2320       CLASSES LOAD SPEED;
2321       MODEL WEARRATE = LOAD SPEED LOAD*SPEED;
2322       MEANS LOAD SPEED LOAD*SPEED / DUNCAN;
NOTE: THE PROCEDURE ANOVA USED 0.24 SECONDS AND 804K
      AND PRINTED PAGES 2 TO 6.
NOTE: SAS USED 804K MEMORY.
NOTE: SAS INSTITUTE INC.
      SAS CIRCLE
```

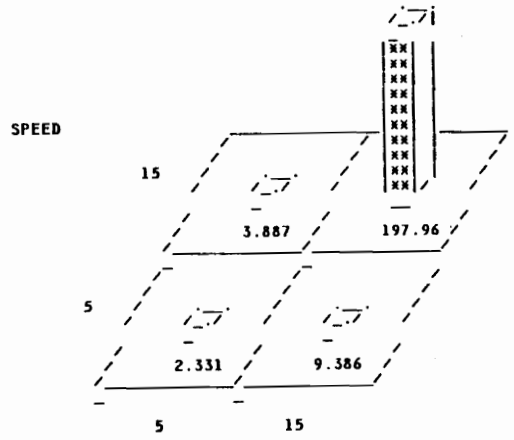

2-WAY ANOVA UNTREATED 50/50 PFI/PEEK

ANALYSIS OF VARIANCE PROCEDURE

CLASS LEVEL INFORMATION

CLASS	LEVELS	VALUES
LOAD	2	5 15
SPEED	2	5 15

NUMBER OF OBSERVATIONS IN DATA SET = 12
2-WAY ANOVA UNTREATED 50/50 PEI/PEEK

ANALYSIS OF VARIANCE PROCEDURE

DEPENDENT VARIABLE: WEARRATE

SOURCE	DF	SUM OF SQUARES	MEAN SQUARE	F VALUE
MODEL	3	9298.13513400	3099.37837800	793.12

2-Way ANOVA SAS output : Untreated 50/50 PEEK/PEI blend

ERROR	8	31.26254200	3.90781775	PR > F
CORRECTED TOTAL	11	9329.39767600		0.0001

R-SQUARE	C.V.	ROOT MSE	HEARRATE MEAN
0.996649	11.1076	1.97682011	17.79700000

SOURCE	DF	ANOVA SS	F VALUE	PR > F
LOAD	1	3371.03936533	862.64	0.0001
SPEED	1	3012.45140833	770.88	0.0001
LOAD*SPEED	1	2914.64436033	745.85	0.0001

2-WAY ANOVA UNTREATED 50/50 PEI/PEEK

ANALYSIS OF VARIANCE PROCEDURE

DUNCAN'S MULTIPLE RANGE TEST FOR VARIABLE: HEARRATE
NOTE: THIS TEST CONTROLS THE TYPE I COMPARISONWISE ERROR RATE, NOT THE EXPERIMENTWISE ERROR RATE

ALPHA=0.05 DF=8 MSE=3.90782

NUMBER OF MEANS 2
CRITICAL RANGE 2.62847

MEANS WITH THE SAME LETTER ARE NOT SIGNIFICANTLY DIFFERENT.

DUNCAN GROUPING	MEAN	N	LOAD
A	34.558	6	15
B	1.036	6	5

2-WAY ANOVA UNTREATED 50/50 PEI/PEEK

ANALYSIS OF VARIANCE PROCEDURE

DUNCAN'S MULTIPLE RANGE TEST FOR VARIABLE: HEARRATE
NOTE: THIS TEST CONTROLS THE TYPE I COMPARISONWISE ERROR RATE, NOT THE EXPERIMENTWISE ERROR RATE

ALPHA=0.05 DF=8 MSE=3.90782

NUMBER OF MEANS 2
CRITICAL RANGE 2.62847

MEANS WITH THE SAME LETTER ARE NOT SIGNIFICANTLY DIFFERENT.

DUNCAN GROUPING	MEAN	N	SPEED
A	33.641	6	15

OUTPUT

B	1.953	6	5

2-WAY ANOVA UNTREATED 50/50 PEI/PEEK

ANALYSIS OF VARIANCE PROCEDURE

MEANS

LOAD	SPEED	N	HEARRATE
5	5	3	0.7770000
5	15	3	1.2956667
15	5	3	3.1286667
15	15	3	65.9866667

Duncan's multiple range test : 5N - 15cm/s

```
//HSLL1 JOB XXXXX,SAS,CLASS=Q,JHY                                  JOB 8185
1          SAS(R) LOG    OS SAS 5.18          MVS/XA JOB $$$$$Q17 STEP FAKE     PR

NOTE: COPYRIGHT (C) 1984,1988 SAS INSTITUTE INC., CARY, N.C.  27512, U.S.A.
NOTE: THE JOB $$$$$Q17 HAS BEEN RUN UNDER RELEASE 5.18 OF SAS
      AT VIRGINIA TECH COMPUTING CENTER (01798001).
NOTE: CPUID    VERSION = 66  SERIAL = 120667  MODEL = 3084 .
      CPUID    VERSION = 66  SERIAL = 320667  MODEL = 3084 .
NOTE: NO OPTIONS SPECIFIED.

2085       OPTIONS LS=80;
2086       TITLE 'DUNCAN: @5N-15CM/S';
2087       DATA;
2088       INPUT SAMPLE WEARRATE; LIST;
2089       CARDS;

RULE:      ----+----1----+----2----+----3----+----4----+----5----+----6----+----7
2088       1 2.386
2089       1 2.369
2090       1 2.397
2091       2 1.080
2092       2 1.074
2093       2 1.733
2094       6 0.558
2095       6 0.450
2096       6 0.468
NOTE: DATA SET WORK.DATA13 HAS 9 OBSERVATIONS AND 2 VARIABLES. 2346 OBS/TRK.
NOTE: THE DATA STATEMENT USED 0.12 SECONDS AND 528K.

2099       PROC GLM;
2100       CLASSES SAMPLE;
2101       MODEL WEARRATE = SAMPLE;
2102       MEANS SAMPLE / DUNCAN;
NOTE: THE PROCEDURE GLM USED 0.23 SECONDS AND 804K
      AND PRINTED PAGES 1 TO 3.
NOTE: SAS USED 804K MEMORY.
NOTE: SAS INSTITUTE INC.
      SAS CIRCLE
      PO BOX 8000
      CARY, N.C. 27512-8000
PROCESSOR ENDED, COMPLETION CODE = S000, U0000
                CARDS     LINES    CPU SEC     EXCPS      KBS   PRIORITY     TOTAL
NUMBER OF          18        39          1       538     1950   PRIORITY        KB
CHARGES           .00       .00        .08       .00      .00        .06       .14
                                  DUNCAN: @5N-15CM/S

                          GENERAL LINEAR MODELS PROCEDURE

                             CLASS LEVEL INFORMATION

                           CLASS      LEVELS    VALUES

                           SAMPLE          3    1 2 6

                                                NUMBER OF OBSERVATIONS IN DATA SET = 9
                                                      DUNCAN: @5N-15CM/S

                                   GENERAL LINEAR MODELS PROCEDURE

DEPENDENT VARIABLE: WEARRATE

SOURCE                      DF      SUM OF SQUARES          MEAN SQUARE      F VALUE

MODEL                        2          5.41001356           2.70500678        55.20

ERROR                        6          0.29400267           0.04900044      PR > F

CORRECTED TOTAL              8          5.70401622                           0.0001

R-SQUARE              C.V.              ROOT MSE         WEARRATE MEAN

0.948457             15.9188            0.22136044            1.39055556

SOURCE                      DF           TYPE I SS   F VALUE    PR > F

SAMPLE                       2          5.41001356     55.20     0.0001

SOURCE                      DF         TYPE III SS   F VALUE    PR > F

SAMPLE                       2          5.41001356     55.20     0.0001
                                                      DUNCAN: @5N-15CM/S

                                   GENERAL LINEAR MODELS PROCEDURE

DUNCAN'S MULTIPLE RANGE TEST FOR VARIABLE: WEARRATE
NOTE: THIS TEST CONTROLS THE TYPE I COMPARISONWISE ERROR RATE,
      NOT THE EXPERIMENTWISE ERROR RATE

                                ALPHA=0.05  DF=6  MSE=.0490004

                             NUMBER OF MEANS          2          3
                             CRITICAL RANGE    0.442261   0.458386

          MEANS WITH THE SAME LETTER ARE NOT SIGNIFICANTLY DIFFERENT.

                DUNCAN    GROUPING              MEAN       N  SAMPLE

                                A              2.3840       3  1

                                B              1.2957       3  2

                                C              0.4920       3  6
```

Duncan's multiple range test : 15N - 5cm/s (Program)

```
//LSHL1 JOB XXXXX,SAS,CLASS=Q,JHY
1          SAS(R) LOG   OS SAS 5.18              MVS/XA JOB $$$$$Q1

NOTE: COPYRIGHT (C) 1984,1988 SAS INSTITUTE INC., CARY, N.C.  2
NOTE: THE JOB $$$$$Q17 HAS BEEN RUN UNDER RELEASE 5.18 OF SAS
      AT VIRGINIA TECH COMPUTING CENTER (01798001).
NOTE: CPUID    VERSION = 66  SERIAL = 120667  MODEL = 3084 .
      CPUID    VERSION = 66  SERIAL = 320667  MODEL = 3084 .
NOTE: NO OPTIONS SPECIFIED.

2103        OPTIONS LS=80;
2104        TITLE 'DUNCAN: @15N-5CM/S';
2105        DATA;
2106        INPUT SAMPLE WEARRATE; LIST;
2107        CARDS;

RULE:       ----+----1----+----2----+----3----+----4----+----5---
2106        1 8.457
2107        1 8.830
2108        1 9.408
2109        2 3.183
2110        2 2.920
2111        2 3.283
2112        3 1.363
2113        3 1.091
2114        4 0.102
2115        4 0.327
2116        4 0.250
2117        5 0.454
2118        5 0.356
2119        6 1.160
2120        6 0.925
2121        6 1.312
2122        7 0.364
2123        7 0.444
2124        7 0.523
2125        8 0.193
2126        8 0.175
2127        8 0.140
2128        9 1.340
2129        9 1.388
2130        9 1.515
2131        11 0.294
2132        11 0.252
2133        11 0.184
2134        10 0.223
2135        10 0.295
2136        10 0.343
NOTE: DATA SET WORK.DATA14 HAS 31 OBSERVATIONS AND 2 VARIABLES.
NOTE: THE DATA STATEMENT USED 0.12 SECONDS AND 528K.

2139        PROC GLM;
2140        CLASSES SAMPLE;
2141        MODEL WEARRATE = SAMPLE;
2142        MEANS SAMPLE / DUNCAN;
```

Duncan's multiple range test : 15N - 5cm/s (Output # 1)

GENERAL LINEAR MODELS PROCEDURE

CLASS LEVEL INFORMATION

CLASS	LEVELS	VALUES
SAMPLE	11	1 2 3 4 5 6 7 8 9 10 11

NUMBER OF OBSERVATIONS IN DATA SET = 31

DUNCAN: @15N-5CM/S 2

GENERAL LINEAR MODELS PROCEDURE

DEPENDENT VARIABLE: HEARRATE

SOURCE	DF	SUM OF SQUARES	MEAN SQUARE	F VALUE
MODEL	10	197.13549551	19.71354955	549.58
ERROR	20	0.71740133	0.03587007	PR > F
CORRECTED TOTAL	30	197.85289684		0.0001

R-SQUARE	C.V.	ROOT MSE	HEARRATE MEAN
0.996374	11.4910	0.18939395	1.64819355

SOURCE	DF	TYPE I SS	F VALUE	PR > F
SAMPLE	10	197.13549551	549.58	0.0001

SOURCE	DF	TYPE III SS	F VALUE	PR > F
SAMPLE	10	197.13549551	549.58	0.0001

DUNCAN: @15N-5CM/S 3

GENERAL LINEAR MODELS PROCEDURE

DUNCAN'S MULTIPLE RANGE TEST FOR VARIABLE: HEARRATE
NOTE: THIS TEST CONTROLS THE TYPE I COMPARISONWISE ERROR RATE,
NOT THE EXPERIMENTWISE ERROR RATE

ALPHA=0.05 DF=20 MSE=.0358701

WARNING: CELL SIZES ARE NOT EQUAL.
HARMONIC MEAN OF CELL SIZES=2.75

NUMBER OF MEANS	2	3	4	5	6
CRITICAL RANGE	0.336465	0.353343	0.365011	0.371837	0.377249

NUMBER OF MEANS	7	8	9	10	11
CRITICAL RANGE	0.381459	0.38475	0.38735	0.389428	0.391105

MEANS WITH THE SAME LETTER ARE NOT SIGNIFICANTLY DIFFERENT.

DUNCAN GROUPING	MEAN	N	SAMPLE
A	8.8983	3	1
B	3.1287	3	2
C C	1.4143	3	9
C C C	1.2270	2	3
C C	1.1323	3	6
D D	0.4437	3	7
D D D	0.4050	2	5
D D	0.2870	3	10
D D	0.2433	3	11
D D	0.2263	3	4
D	0.1693	3	8

Duncan's multiple range test : 15N - 5cm/s (Output # 2)

GENERAL LINEAR MODELS PROCEDURE

CLASS LEVEL INFORMATION

CLASS	LEVELS	VALUES
SAMPLE	9	3 4 5 6 7 8 9 10 11

NUMBER OF OBSERVATIONS IN DATA SET = 25

DUNCAN: @15N-5CM/S

GENERAL LINEAR MODELS PROCEDURE

DEPENDENT VARIABLE: HEARRATE

SOURCE	DF	SUM OF SQUARES	MEAN SQUARE	F VALUE
MODEL	8	5.42601624	0.67825203	57.76
ERROR	16	0.18788400	0.01174275	PR > F
CORRECTED TOTAL	24	5.61390024		0.0001

R-SQUARE	C.V.	ROOT MSE	HEARRATE MEAN
0.966532	18.0450	0.10836397	0.60052000

SOURCE	DF	TYPE I SS	F VALUE	PR > F
SAMPLE	8	5.42601624	57.76	0.0001

SOURCE	DF	TYPE III SS	F VALUE	PR > F
SAMPLE	8	5.42601624	57.76	0.0001

DUNCAN: @15N-5CM/S

GENERAL LINEAR MODELS PROCEDURE

DUNCAN'S MULTIPLE RANGE TEST FOR VARIABLE: HEARRATE
NOTE: THIS TEST CONTROLS THE TYPE I COMPARISONWISE ERROR RATE,
NOT THE EXPERIMENTWISE ERROR RATE

ALPHA=0.05 DF=16 MSE=.0117428

WARNING: CELL SIZES ARE NOT EQUAL.
HARMONIC MEAN OF CELL SIZES=2.7

NUMBER OF MEANS	2	3	4	5
CRITICAL RANGE	0.197377	0.207112	0.213812	0.217541

NUMBER OF MEANS	6	7	8	9
CRITICAL RANGE	0.220428	0.222626	0.224308	0.225608

MEANS WITH THE SAME LETTER ARE NOT SIGNIFICANTLY DIFFERENT.

DUNCAN GROUPING	MEAN	N	SAMPLE
A A	1.41433	3	9
B A	1.22700	2	3
B B	1.13233	3	6
C C	0.44367	3	7
C C C	0.40500	2	5
D C	0.28700	3	10
D C	0.24333	3	11
D C C	0.22633	3	4
D D	0.16933	3	8

Duncan's multiple range test : 15N - 5cm/s (Output # 3)

CLASS LEVEL INFORMATION

CLASS	LEVELS	VALUES
SAMPLE	6	4 5 7 8 10 11

NUMBER OF OBSERVATIONS IN DATA SET = 17
DUNCAN: @15N-5CM/S

GENERAL LINEAR MODELS PROCEDURE

DEPENDENT VARIABLE: WEARRATE

SOURCE	DF	SUM OF SQUARES	MEAN SQUARE	F VALUE
MODEL	5	0.15968522	0.03193704	6.00
ERROR	11	0.05850667	0.00531879	PR > F
CORRECTED TOTAL	16	0.21819188		0.0064

R-SQUARE	C.V.	ROOT MSE	WEARRATE MEAN
0.731857	25.2045	0.07293002	0.28935294

SOURCE	DF	TYPE I SS	F VALUE	PR > F
SAMPLE	5	0.15968522	6.00	0.0064

SOURCE	DF	TYPE III SS	F VALUE	PR > F
SAMPLE	5	0.15968522	6.00	0.0064

DUNCAN: @15N-5CM/S

GENERAL LINEAR MODELS PROCEDURE

DUNCAN'S MULTIPLE RANGE TEST FOR VARIABLE: WEARRATE
NOTE: THIS TEST CONTROLS THE TYPE I COMPARISONWISE ERROR RATE,
NOT THE EXPERIMENTWISE ERROR RATE

ALPHA=0.05 DF=11 MSE=.0053188

WARNING: CELL SIZES ARE NOT EQUAL.
HARMONIC MEAN OF CELL SIZES=2.76923

NUMBER OF MEANS	2	3	4	5	6
CRITICAL RANGE	0.136157	0.142525	0.14671	0.148868	0.150427

MEANS WITH THE SAME LETTER ARE NOT SIGNIFICANTLY DIFFERENT.

LSHL2 OUTPUT

MEANS WITH THE SAME LETTER ARE NOT SIGNIFICANTLY DIFFERENT.

DUNCAN GROUPING	MEAN	N	SAMPLE
A	0.44367	3	7
A			
B A	0.40500	2	5
B			
B C	0.28700	3	10
C			
C	0.24333	3	11
C			
C	0.22633	3	4
C			
C	0.16933	3	8

Duncan's multiple range test : 15N - 15cm/s (Program)

```
//HSHL1 JOB XXXXX,SAS,CLASS=Q,JHY
1          SAS(R) LOG   OS SAS 5.18            MVS/XA JOB $$$$$Q

NOTE: COPYRIGHT (C) 1984,1988 SAS INSTITUTE INC., CARY, N.C.
NOTE: THE JOB $$$$$Q17 HAS BEEN RUN UNDER RELEASE 5.18 OF SAS
      AT VIRGINIA TECH COMPUTING CENTER (01798001).
NOTE: CPUID    VERSION = 66  SERIAL = 120667  MODEL = 3084 .
      CPUID    VERSION = 66  SERIAL = 320667  MODEL = 3084 .
NOTE: NO OPTIONS SPECIFIED.

1952        OPTIONS LS=80;
1953        TITLE 'DUNCAN: @15N-15CM/S';
1954        DATA;
1955        INPUT SAMPLE WEARRATE; LIST;
1956        CARDS;

RULE:       ----+----1----+----2----+----3----+----4----+----5--
1955        1 80.940
1956        1 55.490
1957        1 71.275
1958        1 54.975
1959        1 67.903
1960        2 62.650
1961        2 64.990
1962        2 70.320
1963        3 0.938
1964        3 1.132
1965        3 1.377
1966        3 2.270
1967        4 0.198
1968        4 0.164
1969        5 0.508
1970        5 0.251
1971        6 11.370
1972        6 14.216
1973        6 6.991
1974        6 8.191
1975        7 0.263
1976        7 0.377
1977        7 0.344
1978        8 0.199
1979        8 0.373
1980        9 1.932
1981        9 1.250
1982        9 1.561
1983        10 0.345
1984        10 0.227
1985        10 0.323
1986        11 0.560
1987        11 0.336
1988        11 0.616
NOTE: DATA SET WORK.DATA9 HAS 34 OBSERVATIONS AND 2 VARIABLES.
NOTE: THE DATA STATEMENT USED 0.12 SECONDS AND 528K.

1991        PROC GLM;
```

Duncan's multiple range test : 15N - 15cm/s (Output # 1)

GENERAL LINEAR MODELS PROCEDURE

CLASS LEVEL INFORMATION

CLASS	LEVELS	VALUES
SAMPLE	11	1 2 3 4 5 6 7 8 9 10 11

NUMBER OF OBSERVATIONS IN DATA SET = 34
DUNCAN: @15N-15CM/S

GENERAL LINEAR MODELS PROCEDURE

DEPENDENT VARIABLE: HEARRATE

SOURCE	DF	SUM OF SQUARES	MEAN SQUARE	F VALUE
MODEL	10	25292.33854625	2529.23385462	105.63
ERROR	23	550.70834778	23.94384121	PR > F
CORRECTED TOTAL	33	25843.04689403		0.0001

R-SQUARE	C.V.	ROOT MSE	HEARRATE MEAN
0.978690	28.4464	4.89324445	17.20161765

SOURCE	DF	TYPE I SS	F VALUE	PR > F
SAMPLE	10	25292.33854625	105.63	0.0001

SOURCE	DF	TYPE III SS	F VALUE	PR > F
SAMPLE	10	25292.33854625	105.63	0.0001

DUNCAN: @15N-15CM/S

GENERAL LINEAR MODELS PROCEDURE

DUNCAN'S MULTIPLE RANGE TEST FOR VARIABLE: HEARRATE
NOTE: THIS TEST CONTROLS THE TYPE I COMPARISONWISE ERROR RATE,
NOT THE EXPERIMENTWISE ERROR RATE

ALPHA=0.05 DF=23 MSE=23.9438

WARNING: CELL SIZES ARE NOT EQUAL.
HARMONIC MEAN OF CELL SIZES=2.84483

NUMBER OF MEANS	2	3	4	5	6
CRITICAL RANGE	8.47824	8.90664	9.20222	9.38047	9.52341

NUMBER OF MEANS	7	8	9	10	11
CRITICAL RANGE	9.63571	9.72433	9.795	9.85202	9.89852

MEANS WITH THE SAME LETTER ARE NOT SIGNIFICANTLY DIFFERENT.

DUNCAN GROUPING	MEAN	N	SAMPLE
A	66.117	5	1
A			
A	65.987	3	2
B	10.192	4	6
B			
C B	1.581	3	9
C B			
C B	1.429	4	3
C			
C	0.504	3	11
C			
C	0.379	2	5
C			
C	0.328	3	7
C			
C	0.298	3	10
C			
C	0.286	2	8
C			
C	0.181	2	4

Duncan's multiple range test : 15N - 15cm/s (Output # 2)

GENERAL LINEAR MODELS PROCEDURE

CLASS LEVEL INFORMATION

CLASS	LEVELS	VALUES
SAMPLE	9	3 4 5 6 7 8 9 10 11

NUMBER OF OBSERVATIONS IN DATA SET = 26
DUNCAN: @15N-15CM/S

GENERAL LINEAR MODELS PROCEDURE

DEPENDENT VARIABLE: HEARRATE

SOURCE	DF	SUM OF SQUARES	MEAN SQUARE	F VALUE
MODEL	8	311.08299547	38.88537443	19.90
ERROR	17	33.21049992	1.95355882	PR > F
CORRECTED TOTAL	25	344.29349538		0.0001

R-SQUARE	C.V.	ROOT MSE	HEARRATE MEAN
0.903540	64.5336	1.39769768	2.16584615

SOURCE	DF	TYPE I SS	F VALUE	PR > F
SAMPLE	8	311.08299547	19.90	0.0001

SOURCE	DF	TYPE III SS	F VALUE	PR > F
SAMPLE	8	311.08299547	19.90	0.0001

DUNCAN: @15N-15CM/S

GENERAL LINEAR MODELS PROCEDURE

DUNCAN'S MULTIPLE RANGE TEST FOR VARIABLE: HEARRATE
NOTE: THIS TEST CONTROLS THE TYPE I COMPARISONWISE ERROR RATE,
NOT THE EXPERIMENTWISE ERROR RATE

HSHL1 OUTPUT

ALPHA=0.05 DF=17 MSE=1.95356

WARNING: CELL SIZES ARE NOT EQUAL.
HARMONIC MEAN OF CELL SIZES=2.7

NUMBER OF MEANS	2	3	4	5
CRITICAL RANGE	2.53391	2.65956	2.74624	2.79515

NUMBER OF MEANS	6	7	8	9
CRITICAL RANGE	2.83329	2.86252	2.88504	2.90257

MEANS WITH THE SAME LETTER ARE NOT SIGNIFICANTLY DIFFERENT.

DUNCAN GROUPING	MEAN	N	SAMPLE
A	10.192	4	6
B	1.581	3	9
B			
B	1.429	4	3
B			
B	0.504	3	11
B			
B	0.379	2	5
B			
B	0.328	3	7
B			
B	0.298	3	10
B			
B	0.286	2	8
B			
B	0.181	2	4

Duncan's multiple range test : 15N - 15cm/s (Output # 3)

GENERAL LINEAR MODELS PROCEDURE

CLASS LEVEL INFORMATION

CLASS	LEVELS	VALUES
SAMPLE	8	3 4 5 7 8 9 10 11

NUMBER OF OBSERVATIONS IN DATA SET = 22
DUNCAN: @15N-15CM/S

GENERAL LINEAR MODELS PROCEDURE

DEPENDENT VARIABLE: HEARRATE

SOURCE	DF	SUM OF SQUARES	MEAN SQUARE	F VALUE
MODEL	7	6.55612554	0.93658936	9.50
ERROR	14	1.37983792	0.09855985	PR > F
CORRECTED TOTAL	21	7.93596345		0.0002

R-SQUARE	C.V.	ROOT MSE	HEARRATE MEAN
0.826128	44.4334	0.31394243	0.70654545

SOURCE	DF	TYPE I SS	F VALUE	PR > F
SAMPLE	7	6.55612554	9.50	0.0002

SOURCE	DF	TYPE III SS	F VALUE	PR > F
SAMPLE	7	6.55612554	9.50	0.0002

DUNCAN: @15N-15CM/S

GENERAL LINEAR MODELS PROCEDURE

DUNCAN'S MULTIPLE RANGE TEST FOR VARIABLE: HEARRATE
NOTE: THIS TEST CONTROLS THE TYPE I COMPARISONWISE ERROR RATE,
NOT THE EXPERIMENTWISE ERROR RATE

ALPHA=0.05 DF=14 MSE=.0985599

WARNING: CELL SIZES ARE NOT EQUAL.
HARMONIC MEAN OF CELL SIZES=2.59459

HSHL3 OUTPUT

NUMBER OF MEANS	2	3	4	5
CRITICAL RANGE	0.590084	0.618769	0.638326	0.648901

NUMBER OF MEANS	6	7	8
CRITICAL RANGE	0.65693	0.662933	0.667442

MEANS WITH THE SAME LETTER ARE NOT SIGNIFICANTLY DIFFERENT.

DUNCAN GROUPING	MEAN	N	SAMPLE
A	1.5810	3	9
A			
A	1.4292	4	3
B	0.5040	3	11
B			
B	0.3795	2	5
B			
B	0.3280	3	7
B			
B	0.2983	3	10
B			
B	0.2860	2	8
B			
B	0.1810	2	4

Duncan's multiple range test : 15N - 15cm/s (Output # 4)

CLASS	LEVELS	VALUES
SAMPLE	6	4 5 7 8 10 11

NUMBER OF OBSERVATIONS IN DATA SET = 15
DUNCAN: @15N-15CM/S

GENERAL LINEAR MODELS PROCEDURE

DEPENDENT VARIABLE: HEARRATE

SOURCE	DF	SUM OF SQUARES	MEAN SQUARE	F VALUE
MODEL	5	0.14582577	0.02916515	2.44
ERROR	9	0.10740117	0.01193346	PR > F
CORRECTED TOTAL	14	0.25322693		0.1155

R-SQUARE	C.V.	ROOT MSE	HEARRATE MEAN
0.575870	32.2306	0.10924039	0.33893333

SOURCE	DF	TYPE I SS	F VALUE	PR > F
SAMPLE	5	0.14582577	2.44	0.1155

SOURCE	DF	TYPE III SS	F VALUE	PR > F
SAMPLE	5	0.14582577	2.44	0.1155

DUNCAN: @15N-15CM/S

GENERAL LINEAR MODELS PROCEDURE

DUNCAN'S MULTIPLE RANGE TEST FOR VARIABLE: HEARRATE
NOTE: THIS TEST CONTROLS THE TYPE I COMPARISONWISE ERROR RATE,
NOT THE EXPERIMENTWISE ERROR RATE

ALPHA=0.05 DF=9 MSE=.0119335

WARNING: CELL SIZES ARE NOT EQUAL.
HARMONIC MEAN OF CELL SIZES=2.4

NUMBER OF MEANS	2	3	4	5	6
CRITICAL RANGE	0.225223	0.23524	0.241438	0.244543	0.246637

MEANS WITH THE SAME LETTER ARE NOT SIGNIFICANTLY DIFFERENT.

DUNCAN GROUPING	MEAN	N	SAMPLE
A	0.50400	3	11
B A	0.37950	2	5
B A	0.32800	3	7
B A	0.29833	3	10
B A	0.28600	2	8
B	0.18100	2	4

4SHL3 OUTPUT

VITA

The author was born in Seoul, Korea on the very cold day, December 16,1965. He was used to graduating from schools in winter. But since February 1, 1983 when he immigrated in the U.S., his life has changed. He graduated from Susan E. Wagner High School on a sunny hot day in June of 1985. He studied Mechanical Engineering at Rensselaer Polytechnic Institute, in Troy, NY. He worked for New York Power Authority in 1988 through the cooperative education program. And the following year, another hot day of May, 1989 he received his Bachelor of Science degree in Mechanical Engineering. In the following June, the author began graduate studies toward a Master of Science degree in Mechanical Engineering at Virginia Polytechnic Institute and State University with the dream of graduating in winter. He found the science field which is the world's most densely populated with "?" and he is ?ing if he can graduate in summer of 1991. He wants to forget the dream he carried when he came to Virginia and wants to follow the trend and graduate in the hot summer. In the following September, he will pursue another degree, Master of Engineering Administration in Industrial and Systems Engineering at VPI & SU.

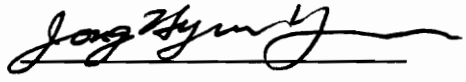

Jong Hyun Yoo